
Di-block copolymers as solid-state electrolytes for lithium ion batteries: novel and solvent-free production methods

Graduation thesis

26/10/2015

Master in Materials Science and Engineering

Faculty of Mechanical, Maritime and Material Engineering (3ME)

Delft University of Technology

Frieda M. Davey

The graduation project is a collaboration between TUDelft and DSM Geleen.

Di-block copolymers as solid-state electrolytes for lithium ion batteries: novel and solvent-free production methods

Graduation thesis

26/10/2015

Master in Materials Science and Engineering
Faculty of Mechanical, Maritime and Material Engineering (3ME)
Delft University of Technology

Graduating student:
Frieda Margarethe Davey
4319796

University supervisor:
Dr. Ir. M. Wagemaker

Company supervisor:
Dr. Ir. R.H.C. Janssen



Acknowledgments

There is one person without whom nothing of what follows in this work would have happened and that is Frans, the technician of the battery group where I spent the last nine months. He gave me endless support and advice that started from my sticky polymer melting experiments and continued to final data fitting. All the setups that needed to be thought of, designed and made are fruit of his enthusiasm and time. Because he is a handy lab worker with experience but also has solid theoretical background, he managed to help with practical experimental issues as well as ideas and smart reasoning. With good laughs and positive attitude, he managed to make sure that everything ran as smoothly as possible. And he managed to also make work fun, and that is equally important to me. So thank you Frans!

Many thanks go to my supervisor Marnix for proposing the contact with DSM and therefore initiating this project in the first place. Discussions with him about my work always ended up with an injection of positive attitude and renewed interest. His extremely positive and optimistic character have been a much appreciated counterbalance to my prudent (I call it realistic!) attitude. I really like his way of reasoning out of the box in simple and model-like ways: something to learn from.

Another key-figure of this experience has been Rob, my supervisor from DSM. I would like to thank him for allowing me to participate in some way in such a grand upcoming field that DSM is now entering. Although contact with him was limited to phone calls and not that many meetings in person (due to busy schedules and distance) took place, he always gave very useful input and guidance to the progress of my work.

I want to also thank Peter-Paul, a PhD from the battery group, because he has helped me with the ins and outs of the Autolab and of the electrochemical measurements in general. He definitely made my life a bit easier.

And a big thank you (and good luck!) to the ones that will actually *read* the rest of the document and not stop here! For the friends and dear ones who are mildly interested or want to pretend they know something about my work, but don't have so much time to spare: there is a summary of only two pages at the end of this document. I will already feel very honoured and surprised if you read that.

Viva!

Frieda

Abstract

Novel and solvent-free routes for producing solid-state electrolyte membranes for lithium ion batteries containing Li[N(CF₃SO₂)₂] (LiTFSI) and Arnitel[®] copolymers produced and provided by DSM are proposed and elaborated in this graduation project. Other lithium salts such as Li[B(C₂O₄)₂] (LiBOB) and LiCl have also been tested, but more research has been focused on LiTFSI. Arnitel materials with variable proportions of poly(ethylene oxide) (PEO) and polybutylene terephthalate (PBT) have been used. The presented solvent-free methods of incorporating the lithium salt are intended as an alternative to the solvent route, that involves the use of hazardous HFIP, previously investigated in internal DSM research. The methods proposed in this work are based on two different concepts: one involves melting the polymer and mixing in the lithium salt (referred to as melt-mixing), while the other two techniques make use of water as a medium to carry and incorporate the salt in the polymer chains. This has been performed on Arnitel pellets (method named water soaking) and on thin films of the same material (referred to as thin film soaking). The water can then be removed by complete drying. Samples produced through melt-mixing and water soaking have then undergone hot pressing and thus thin (150-200µm) free-standing electrolytes have successfully been prepared. DSC and electrochemical analysis such as impedance measurements between room temperature and approximately 65°C, cyclic voltammetry and lithium plating experiments are presented. The samples prepared during this research proved to have room temperature conductivity as high as 10⁻⁵ S/cm. Electrochemical stability seems instead to be an issue in the lower voltage, but this is ascribed to the inherent behaviour between the lithium electrolyte and seems to be independent of the production method used. Such electrochemical results are aligned with the internal DSM data on samples produced via the solvent route: it is therefore possible to consider the proposed production routes as feasible alternatives for cheaper, safer and more environmentally friendly methods to produce Arnitel-based solid-state electrolytes for lithium ion batteries.

Table of contents

1. Introduction.....	4
1.1 Context of the project.....	4
1.2 Lithium-ion batteries (LIBs).....	6
1.3 Solid-state polymeric electrolytes for LIBs: a literature review.....	8
1.3.1 Electrolyte requirements.....	8
1.3.2 Polymer matrix.....	9
1.3.3 Salts.....	11
1.3.4 Assembling a polymeric solid electrolyte.....	16
1.4 Research questions.....	18
2. Materials and methods.....	20
2.1 Chemicals and materials.....	20
2.2 Electrolyte sample preparation.....	22
2.2.1 Melt-mixing.....	22
2.2.2 Water soaking.....	25
2.2.3 Thin film soaking.....	27
2.2.4 Hot pressing.....	27
2.3 Differential scanning calorimetry (DSC).....	32
2.4 Electrochemical analysis.....	34
2.4.1 Conductivity measurements.....	34
2.4.2 Cyclic voltammetry.....	38
2.4.3 Discharge and electroplating experiments.....	39
3. Results and discussion.....	42
3.1 Electrolyte samples.....	42
3.1.1 Samples produced through melt-mixing.....	42
3.1.2 Samples produced through water soaking.....	45
3.1.3 Samples produced through thin film soaking.....	47
3.1.4 Hot pressed samples.....	47
3.2 DSC results.....	51

3.3 Electrochemical results	54
3.3.1 Conductivity	54
3.3.2 Stability window	66
3.3.3 Discharge experiments	70
4 Conclusions	75
5 Synopsis and outlook of the project	76
5.1 Summary	76
5.2 Future work and recommendations	78
Bibliography.....	82
Appendixes	85
Appendix A	86
Appendix B	87
Appendix C	88
Appendix D	90
Appendix E	103
Appendix F.....	105
Appendix G	108
Appendix H	114
Appendix I	117

1. Introduction

This introduction chapter is meant to provide the reader the means to understand the work that is presented in the report. The work is placed into its context in chapter 1.1 where the stakeholders are presented and the origin of the project is explained. A brief introduction to lithium ion batteries in general is offered in chapter 1.2, while the actual literature review is to be found in chapter 1.3. In this part the theoretical background of solid state polymeric electrolytes for lithium ion batteries is presented by explaining what requirements such systems should fulfil and by going in to more detail in the two main constituents of such electrolytes: the polymer matrix and the lithium salt. The last chapter (chapter 1.4) is instead dedicated to the research questions that were posed based on the knowledge acquired from the literature review. Therefore the goals of the project are indicated at the end of this section as to conclude the introduction and justify the work presented in the rest of the report.

1.1 Context of the project

This graduation research projects stems forth from a collaboration between DSM Geleen and TUDelft and finds its place in the field of solid polymeric electrolytes for lithium ion batteries. The interest for the topic arose from the specific interests and expertise of the two parties. On the one hand DSM is a worldwide producers of polymers for the most diverse applications, on the other side dr. Wagemaker (the TUDelft supervisor form this project) works in the field of rechargeable batteries and has accumulated expertise within the solid state lithium ion battery field. One of the tasks of the student was two combine the knowledge of both parties in order to learn the most from the two fields and to gain understanding on solid polymeric electrolytes based on DSM polymers. The project was proposed by dr. Rob Janssen (the DSM supervisor of the project) with the purpose of researching the potential of using DSM polymers for electrolytes, thus investigating the possibility of exploring and entering the lithium battery market and research field. However, since the energy storage field was an untrodden path for the company, it was necessary to rely on the knowledge of dr. Wagemaker for the battery-related issues. Interests met halfway, since for dr. Wagemaker the field of solid polymeric electrolytes was completely new, his focus rather being on inorganic crystalline electrolytes. As for the student, this was an occasion to learn from both worlds and combine the two fields of knowledge.

From an organizational standpoint, DSM, particularly dr. Rob Janssen, provided the DSM polymers of interest together with guidance and expertise in all the polymer related tasks. The student instead worked within the research group of dr. Wagemaker, located at the RID Reactor Institute Delft within TUDelft. Dr. Wagemaker provided supervision and experience in the lithium ion battery field and offered the research facilities.

Two are the DSM materials provided by the company and these are Arnitel® materials constituted by di-block copolymers. The difference between the two materials lies in the relative proportions of the two phases within the material. These Arnitel materials have been developed by DSM, who produces and sells them world-wide for the most diverse applications. Now the company is looking into the

possibility of using these materials, in combinations with adequate salts, to produce solid state polymeric electrolytes to be used in lithium ion batteries. As the research in this field is very new for DSM, this graduation project dealt with very basic and pioneering investigation where optimization was not the focus.

Some initial research had already been carried out by DSM and will be referred to as internal DSM data. These results have been considered as a starting point and will be presented briefly in this work. Also, such internal DSM data proved to be an important reference point for comparison of the results obtained throughout this graduation project.

The overall graduation project started on February 2nd 2015 and finds its conclusion on October 26th 2015 after a duration of nine months. The supervision role for the project is taken by Dr. Ir. Wagemaker for TUDelft and by dr. Janssen for DSM. The final outcome of the research will be judged by the graduation committee that is composed by the two supervisors, by Dr. Ir. Mol (associate professor at the 3ME faculty, TUDelft) and by Dr. Ir. Gonzalez Garcia (assistant professor at the 3ME faculty, TUDelft).

1.2 Lithium-ion batteries (LIBs)

In an historical moment that searches for renewable sources of energy as an alternative to fossil fuels, much scientific, economic and technological dedication is aimed at technologies that can produce energy from renewable sources. The two leading renewable energy technology are currently photovoltaics and wind turbines. Sun irradiation and movement of air masses are fluctuating sources due to weather conditions, latitude, geographical setting, alternating of day and night and so forth. With an ever increasing contribution of such energy sources to the local and global energy mix, the necessity for energy storage is of uprising importance. Therefore much, but not enough, research has been devoted to the development and improvement of rechargeable batteries as energy storage devices. The urge for development of the battery field has not only been created by fluctuating green energies, but has also been boosted by the gigantic boom of portable electronics such as computers and phones and by the developing electric vehicle industry. Batteries for these purposes should offer high energy density and are required to be lighter, cheap, longer lasting, fast to charge, durable and safe.

In the recent past lithium-ion batteries have outperformed other battery systems such as Pb-acid, Ni-Cd and others and have accounted for ~70% of the worldwide sales (1). In fig. 1 the performance of different battery systems are compared according to volumetric energy density and gravimetric energy density. The use of lithium salt as the electrolyte is justified by the fact that lithium is the lightest of metals and, when used as an anode in contact with lithium salt electrolytes, provides a wide electropositive potential window and thus allows for high energy density batteries. (2)

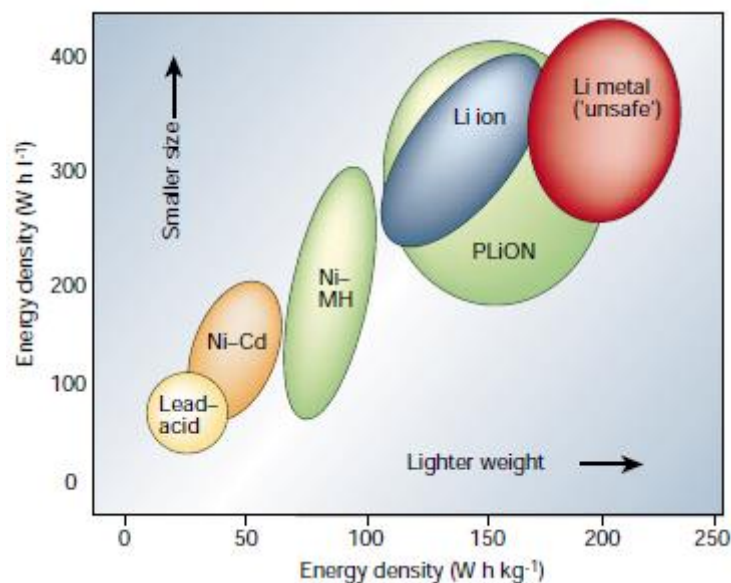


Figure 1 Comparison of different battery technologies in terms of energy volumetric density and specific density (2)

Lithium ion batteries (LIBs) are part of the rechargeable batteries family. The lithium ion is the charge carrier: it moves from the negative electrode to the positive electrode during discharge and does the inverse path during charging. Useful work is performed by the electron flow through a closed external circuit. The elements that constitute a LIB are the negative and positive electrode and the ionic electrolyte that allows for ionic movement as depicted in fig 2. The redox reaction takes place at the electrodes and the electrons are collected by the current collectors. The electrons are thus free

to move through the external circuit and reach the opposite electrode. Because reactions between the electrolyte and the electrode occur if the electrode potentials are outside the stability window of the electrolyte, a solid electrolyte interphase (SEI) may form at the interface of the two. This element will be briefly discussed also in chapter 1.3.

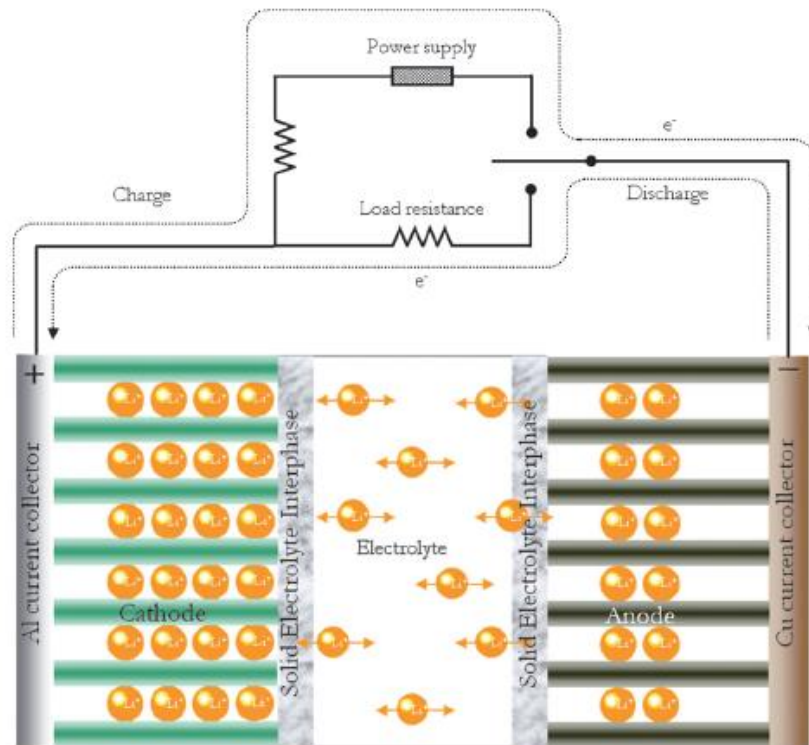


Figure 2 Working principle of a lithium ion battery (3)

This graduation project will focus on the electrolyte. The electrolyte can be in solid or liquid form: the former is the focus of this review and offers advantages over the latter as it eliminates the need for liquid electrolyte containment and leakage risk, while also improving safety and durability. The reduced containment or packaging needed also leads to an improvement in energy density. Out of the solid electrolytes, two classes of materials can be distinguished: inorganic crystalline materials and organic polymers. Solid state polymer electrolytes allow for flexible battery design, along with easier and cheaper processing, transparency, light weight and elasticity. (4) (5)

The purpose of this research project is to try to obtain a solid state polymeric electrolyte based on the material provided by DSM in combination with lithium salts. The polymer will act as a solid matrix in which the lithium ion of the salt is free to move and reach the two electrodes with the least hindrance possible.

1.3 Solid-state polymeric electrolytes for LIBs: a literature review

A solid polymeric electrolyte is fundamentally constituted by the polymeric matrix (chapter 1.3.2) and by the lithium salts (chapter 1.3.3). The lithium salts provide the lithium ion (the charge carrier), while the polymer is the host for this ionic movement. Much more complicated systems are to be found in literature and these involve the use of combination of different salts, ceramic nanoparticles or plasticizers. But all these possible tuning parameters were not considered throughout this research project as to no over complicate it. The purpose of this research was to investigate the possible feasibility of using Arnitel DSM polymers as electrolytes, not to optimize them. The effects of different salts and different polymer:salt ratios have been compared.

1.3.1 Electrolyte requirements

The purpose of the electrolyte in a lithium ion battery was introduced in the previous chapter: it must allow for transport of the lithium ion from one electrode to the other. Another function is to keep physically separated the electrodes as to avoid short-circuiting of the cell. Furthermore the electrons should not be able to go through the electrolyte, because if this were to happen fewer electrons would go through the external circuit and thus the power and the efficiency of the cell would be reduced. These and other requirements are listed below in a more quantitative manner (1).

- **Ionic conductivity** should be in the order of 10^{-4} S cm^{-1} at room temperature as to reach the performance levels of liquid electrolytes;
- **Ionic transference number**¹ is required to be as high as possible ($t_{ion} \sim 1$) because the polymer electrolyte should be a good ion conducting medium and an electronic separator. The larger the cationic transference number, the smaller the concentration polarization effect in the electrolyte due to the anion during charging and discharging and therefore the higher are the power density and the efficiency of the battery;
- **Chemical, thermal and electrochemical stabilities** should be high in order to avoid undesired electrode/electrolyte interface reactions, allow for wide temperature range of use and be adequate for a wide electrochemical stability domain;
- **Mechanical strength** should be sufficient to physically maintain the separation between the electrodes and guarantee the integrity of the entire device;
- **Electrode/electrolyte interaction** should be minimized to a stable and not highly resistive solid electrolyte interphase (SEI). Both phases should be protected by further decomposition and corrosion and the SEI should not prevent the passage of ions.

In a polymer-based electrolyte all the above mentioned properties strongly depend on the interactions between polymer and salt and the possible phases that can form depending on the concentration of the salt in the host polymer and temperature. An important polymer parameter

¹ The ionic transference number is the fraction of the total current carried in an electrolyte by a given ion. This ability to carry charge depends on the electrical mobility of the cation and the anion as expressed by $t_+ = D_+ / (D_+ + D_-)$ where D_+ and D_- are respectively the cationic and anionic diffusion coefficient. The transference number is indicative of the polarity of the material and therefore of the number of cycles the cell can endure (10).

that can be affected by the presence of the salt is the degree of crystallinity. The degree of crystallinity is the fraction of ordered molecules within the polymer. This relates to the ionic conduction that in turn depends strongly on the dynamics of the polymer chains. High chain mobility therefore results in high ionic conductivity but poor mechanical properties. This entails that crystalline polymers have low conductivity and are not suitable as electrolytes (6) (7). Fast ionic transport takes place in the amorphous electrolyte phases, in which conductivity can be two or three orders of magnitude higher than in the crystalline phase (5). Therefore the polymeric electrolyte should contain large and stable amorphous phases (low degree of crystallinity) and have low glass transition temperature in order to yield good flexibility of the polymer chains which are responsible for ionic transport.

1.3.2 Polymer matrix

The advantages of solid polymer electrolytes in LIBs are multiple. Safety is improved because the battery proves to be more tolerant to shock, vibration and mechanical deformation. The lack of liquid also entails that no rigid container is needed, thus removing the possibility of corrosion and explosion. Liquid electrolytes also have evaporation issues that increase the risk of flammability; solid state electrolytes are thus inherently safer. Furthermore the good compliance of polymers enables the electrolyte to conform to the electrode volume changes that occur during cycling. Solid polymer electrolytes also offer better shape flexibility and manufacturing integrity. (8)

The polymer matrix acts as a separator and as a host for the lithium ions. Although the physical, electrochemical and thermal properties of the electrolyte strongly depend on the interaction between salt and polymer, the polymer itself must be an adequate matrix for the conducting ions. It should act as a good solvent and therefore should have (5) (9):

- Atoms or groups of atoms with sufficient electron donor power to form coordinate bonds with the cations;
- Low barrier to bond rotation so the segmental motion of the polymer chains can promptly take place;
- Sufficient distance between the coordinating centres to allow for multiple intrapolymer ion bonds that appear to positively influence the ionic conductivity by allowing ionic hopping.

In the previous chapter it was pointed out how ionic conductivity and mechanical properties are typically not combined in one material: the higher the degree of crystallinity, the stronger the polymer but the lower is its conductivity and vice versa. A possible solution to this contradiction may be offered by di-block copolymers: conductivity and mechanical strength may be decoupled in block polymers. One polymer phase may be more amorphous and offer higher chain mobility, i.e. higher ionic conductivity, while the other polymeric phase may have a higher degree of crystallinity and contribute to the mechanical strength of the polymer. In these systems it is therefore possible to improve the mechanical properties without compromising the ionic conductivity. It must be kept in mind though that these properties may be strongly affected by the complexation of salts with the solvating copolymer blocks. A copolymer system becomes therefore more complex because the salt may react differently with the two phases. (10) (11) Encouraging results are to be found in the

literature of copolymers as electrolytes: Ghosh *et al.* (10) report a PEO-based copolymer with transference number as high as 0,9 with high LiBOB salt concentration.

The two polymeric materials received from DSM are indeed di-block copolymers composed of PEO and PBT. PEO is poly(ethylene oxide) with molecular formula $C_{2n}H_{4n+2}O_{n+1}$, while PBT is polybutylene terephthalate with molecular formula $(C_{12}H_{12}O_4)_n$. The molecular structure of the two are presented in figures 3 and 4. PEO is the rubbery and soft phase out of the two, while the hard blocks are of PBT. Together they make a thermo elastic copolymer with a peak melting temperature of about 220°C.

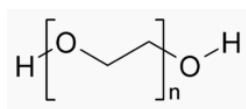


Figure 3 Molecular structure of PEO

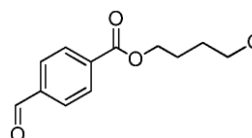


Figure 4 Molecular structure of PBT

The difference between the two polymers provided by DSM lies in the weight ratio of the two blocks (PEO and PBT) as shown in table 1. The polymer with 35wt% PEO will be referred to as PEO35, while the second material will be named PEO70.

Given name	PEO wt%	PEO Molecular weight
PEO35	35%	2000
PEO70	70%	4000

Table 1 Polymer material produced and provided by DSM for the research project

The two materials were provided in the form of cylindrical pellets of a few millimetres in length. They are obtained by extrusion and subsequent cutting into the final length.

No literature reference up to now has been found about PBT-containing copolymers used as electrolyte material. There is instead an outstanding quantity of research on PEO as polymer for solid state polymeric electrolyte material. PEO contains ether coordination sites for the dissociation of the lithium salt and has a flexible macromolecular backbone that allows for ion transport. The lithium ion can coordinate with oxygen atoms in a fixed ratio. These complexed ions move with the motion of a segment of polymer chain. (6) (8) The main advantages of PEO as a polymeric matrix for electrolytes are its good mechanical properties at room temperature, ease of fabrication of thin films, ability to ensure proper contact between the electrode and the electrolyte, high electron-donor power to form coordinated bonds with cations and low barriers to segmental motion of polymer chains (9).

PEO has been long used in very diverse fields such as cosmetics, pharmaceutical applications, paper and textile industry and so forth. In 1975 Wright (12) published his work, in which it was demonstrated how PEO is capable of ionic transport in solid phase. Already then a concept of its practical application as electrolytes in electrochemical devices was presented. However PEO has a very low melting temperature (depending on chain length) that makes it unusable for applications where the operating may reach temperatures up to 80°C as in batteries for electric vehicles.

Although much work has been already performed throughout the years on PEO, this research project has investigated an unknown field that is the use of a di-block copolymer of PEO and PBT, with the expectation that the presence of the PBT will positively influence the overall performance of the polymer as a matrix for the electrolyte, as the resulting copolymer has higher melting temperatures than pure PEO and the presence of the hard block may hinder the growth of lithium dendrites that compromise the cycle life of the cell.

1.3.3 Salts

The salts play a fundamental role in preparing the electrochemical cell as they are responsible for ionic transport within the organic electrolyte. While the polymer represents the physical host for the ions, acts as a separator between the two electrode and prevents electrons from going through, the polymer itself is not ionically conductive. Therefore it is the salt that carries the ionic charge between the two electrodes. The fundamental feature of ionic conduction in polymer electrolytes is the covalent bonding between the ionizing groups and the polymer backbone. The ionic conductivity takes place through ionic hopping mechanism: the electron donor polymer group solvates the salt cation and facilitates ionic separation. (5) (3) When choosing a salt it is also important to consider the effects of the anion, although it does not take part in the reactions during charge and discharge. In the working cell anions accumulate at the anode and are depleted at the cathode. This leads to a concentration polarization that strongly limits the performance of the cell, as the anion gradient adds to the overpotential of the cell by increasing the internal resistance. Furthermore the anions may move faster than the cations as their interaction with the polymeric matrix is weaker than that of the cation which are solvated by the oxygen atoms of the PEO matrix. If this is the case the ionic transference number decreases, that is the opposite of what is desired. (9) A maximum in conductivity seems to occur at concentrations around one lithium cation to eight ether oxygen atoms (7), but a clear explanation for this is not given. What is interesting is that bulky counterions can enhance the transference number without sacrificing the ionic mobility of the electrolyte. The bulky anion in fact is hindered in its movements and its mobility is therefore not very competitive with the mobility of the small lithium ion. This therefore enhances the transference number. Furthermore a big anion deforms the polymer matrix and partially inhibits the formation of orderly and crystalline phases. In this way the amorphous phase is present in a higher percentage and can allow for ionic conductivity. Thus the interest for inorganic salts with voluminous anions stems forth and a wide range of such salts is available. (10) (13) Besides the anion property, the amount of the lithium salt added to the polymer also effects the conductivity. In principle the more free cations are present, the higher is the ion conductivity. However the increasing amount of lithium may impair the motion performance of a segment of the polymer matrix due to the coordination between the cation and the oxygen atoms in the PEO chain. (7) (8).

The effect of adding a lithium salt is not only the one of supplying the polymer with charge carriers, that is the reason the salt is added in the first place. Interactions between the polymer host and the salt may lead to changes in the degree of crystallinity, glass transition temperature, melting temperature, etc. In fig. 5 the phase diagram of a commonly used salt, LiTFSI (that will be later discussed) in PEO is presented as an example. Unfortunately such phase diagrams are not available for all the lithium ion salts of interest; furthermore what the effect of the presence of the second

polymeric block, PBT, may be on the interaction with the salts needs to be yet completely investigated.

As for the polymer matrix, also the lithium salt needs to fulfil some requirements to be adequate for the electrolyte purpose. In order to mix the salt into the polymer matrix, different techniques are available as will be presented in the following chapter. Considering that in this project it has been decided to focus on melting the polymer (see chapter 1.3.4), the salts must be thermally stable above 212°C that is the melting temperature of the polymers provided by DSM. Another requirement is that the salts should have the highest electrochemical stability possible in order to be able to cope with the possible use of high voltage cathodes. It is therefore desirable that the chosen salts would be able to withstand voltages above 4V. Stability of the electrode/electrolyte interface must also be considered: an electrolyte interphase will form if the electrode potentials are outside the electrochemical stability window of the electrolyte. The electrolyte interphase should protect the electrode from further corrosion, but not hinder ionic transport to and from the electrode. If the interphase is highly resistive to lithium ions the power of the cell will be strongly reduced.

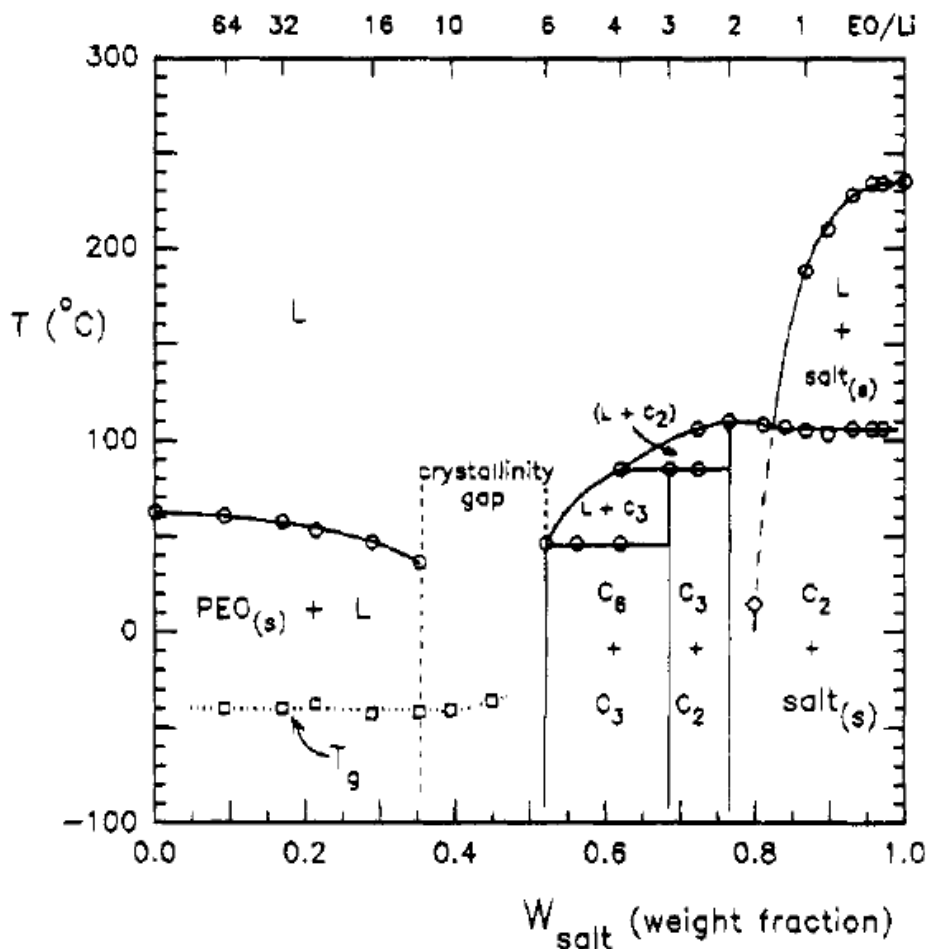


Figure 5 Phase diagram of LiTFSI in PEO (14)

After some initial literature study four salts were proposed that fit the aforementioned requirements. These are LiTFSI, LiBOB, LiODFB and LiFAP. Thermal and electrochemical stability data together with advantages and disadvantages of these salts are presented in the following tables.

LiTFSI

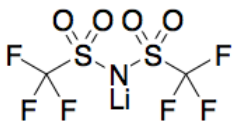
<i>Salt</i>	Li[N(CF ₃ SO ₂) ₂] Bis(trifluoromethanesulfonyl)imide
<i>Thermal stability</i>	T _m =236°C; T _{decomp} =360°C
<i>Molecule</i>	
<i>Electrochemical stability vs. Li⁺/Li</i>	4,5V in PEO ₂₂ LiTFSI
<i>Pros</i>	<ul style="list-style-type: none"> • Highly conducting; • Dissociates well in low dielectric constant solvents; • Increases viscosity (better ionic conductivity due to large anionic size); • Passivation film on carbonaceous anodes
<i>Cons</i>	<ul style="list-style-type: none"> • Strong corrosion of Al electrode

Table 2 Characteristic features of LiTFSI salt (3) (6) (15)

LiBOB

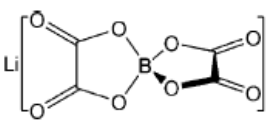
<i>Salt</i>	Li[B(C ₂ O ₄) ₂] Bis(oxalato)borate
<i>Thermal stability</i>	T=302°C
<i>Molecule</i>	
<i>Electrochemical stability vs. Li⁺/Li</i>	4,5V
<i>Pros</i>	<ul style="list-style-type: none"> • No risk of HF formation • Stable solid-electrolyte interface • High conductivity and good cycling behaviour • Environmentally benign • Excellent overcharge tolerance • Cheap
<i>Cons</i>	<ul style="list-style-type: none"> • Limited solubility in linear carbonates • Extremely sensitive to impurities • High viscosity and solid-electrolyte interface with high resistivity →reduced power of the cell

Table 3 Characteristic features of LiBOB salt (3) (16) (17)

LiODFB

<i>Salt</i>	Li[BF ₂ (CO ₂) ₂] Oxalyldifluoroborate
<i>Thermal stability</i>	T=240°C
<i>Molecule</i>	
<i>Electrochemical stability vs. Li⁺/Li</i>	>5V
<i>Pros</i>	<ul style="list-style-type: none"> • An improvement over LiBOB • Extremely soluble • Improved conductivity at low temperatures • Stable solid-electrolyte interface even at high temperature and high potentials • Excellent over-charge tolerance and cycling efficiency • Good for high potential cathodes
<i>Cons</i>	N.A.

Table 4 Characteristic features of LiODFB (3) (18) (19)

LiFAP

<i>Salt</i>	Li[PF ₃ (CF ₃ CF ₂) ₂] Tris(perfluoroethyl)trifluorophosphate
<i>Thermal stability</i>	T=220°C
<i>Molecule</i>	
<i>Electrochemical stability vs. Li⁺/Li</i>	5V
<i>Pros</i>	<ul style="list-style-type: none"> • Replacement of LiPF₆ • Excellent capacity retention
<i>Cons</i>	<ul style="list-style-type: none"> • High cost • Lower conductivity than LiPF₆

Table 5 Characteristic features of LiFAP (3) (20)

Finally, three salts have been chosen to be tested with the DSM materials: LiTFSI, LiBOB and LiCl.

LiTFSI was chosen because it is a routine salt used for PEO electrolytes and because DSM has already conducted some initial experiments with such salt. These experiments have been carried out using this as a lithium salt and proved to be very encouraging as the conductivity at room temperature was in the order of 10^{-5} S/cm (with a polymer to salt molar ratio of EO:Li⁺=20). Furthermore the only phase diagram found in literature is the LiTFSI in PEO (fig. 5), therefore this is the system of which most information is known. According to the phase diagram, intermediate crystalline compounds form at 52wt% composition of LiTFSI in PEO and at 68wt% where P(EO)₆LiTFSI and P(EO)₃LiTFSI are to be found respectively. The eutectic point is slightly below room temperature ($T_e=20^\circ\text{C}$) with 0,4wt% salt. Therefore at this composition a single phase is obtained if the temperature remains above 20°C , while if the composition is off-eutectic phase segregation occurs and crystallization occurs even at room temperature. (21) According to Armand *et al.* (14), there is a crystallinity gap for polymer:salt molar ratios between $6 < \text{EO}/\text{Li}^+ < 12$ as is to be seen in fig. 5. This concentration region may be interesting to investigate when deciding the concentrations of salt that will be tested. Different salt concentrations in the polymer are expected to yield different degrees of crystallinity and different ionic conductivity values. For example it is reported that the ionic conductivity in PEO/LiTFSI systems is ten times higher with a molar concentration of EO/Li⁺=20 compared to a molar concentration of EO/Li⁺=10 (22). Overall the EO/Li⁺=20 ratio seems to be the most common choice encountered during the literature study and is the concentration with which the DSM materials have been previously tested, as shown in the following table.

Polymer type	Polymer [g]	PEO weight percentage	Salt LiTFSI [g]	EO/Li ⁺ molar ratio
PEO35	3,5	0,35	0,335	20
PEO70	3,0	0,70	0,669	20

Table 6 Materials and quantities used in previous DSM experiments

In order to compare these salt concentrations with the phase diagram in fig. 5, the weight percentages are needed. These are respectively 21,47wt% and 24,16wt% for PEO35 and PEO70, therefore both are strongly hypoeutectic.

LiBOB was also chosen because it is a new and very promising salt, according to the available literature. As for the case of LiTFSI, most of the literature reports the use of a polymer to salt molar ratio of EO/Li⁺=20 (13) (23).

LiCl has also been chosen under recommendation from DSM. This salt is stable at high temperatures (300°C) and has already been used by DSM in similar polymeric matrices. Although the small anion present in this salt may seem a contradiction with the requirements explained above, it may offer the advantage of low weight. Thus higher weight ratios of salt to polymer may be achieved. Low conductivity values (10^{-7} S/cm) are reported for LiCl in PEO at room temperature, but these measurements were performed on a sample with EO/Li⁺ =50 (24). Results may be very different with

a much higher LiCl concentration. What also remains to be investigated is the effect of such a small anion on the transference number. Furthermore its opposite characteristics compared to LiTFSI offer the possibility of comparing the effects of a very big anion with a very small anion and may turn out to be of great interest. These two salts can therefore be seen as two extreme situations.

LiODFB and LiFAP were excluded because of the difficulty in retrieving them and because the lack of related literature makes these salts more difficult to work with.

1.3.4 Assembling a polymeric solid electrolyte

Polymeric electrolyte films are generally cast either by solution casting or by using a hot press. The two techniques are hereunder briefly described.

Solution cast method. This is the traditional and most common procedure for casting polymer electrolyte films. The polymer and the complexing salt are separately dissolved in a common solvent and then mixed and stirred together. The viscous slurry is poured into a Petri dish, the solvent is eliminated by slow evaporation and followed by vacuum drying and the electrolytic film is then ready. (1)

Hot press technique. This is a more recent technique first proposed by Gray *et al* (25), hereinafter adopted and modified by many groups. Dry powder of polymer and complexing salt are physically combined to an homogeneous mix that is then heated to around the melting temperature of the polymer while mixing is continued to ensure complete salt complexation. The slurry is then pressed and a uniform, free standing stable polymer electrolyte is obtained with a thickness in the micrometre range. This technique is advantageous as it is faster and cheaper than the previous one. Furthermore it allows for a completely dry and solution free procedure. (1) (26)

The initial experiments on Arnitel polymers carried out by DSM itself were based on the solution cast method. The solvent used was hexafluoro-2-propanol (HFIP) that is known to correctly dissolve LiTFSI and the PEO-PBT copolymers provided by DSM. The reason why it has been decided that the first experiments of this graduation project would be performed in a solvent free form is that HFIP is corrosive, strongly toxic, can cause severe irritation and therefore requires controlled and experienced use in adequate facilities. It is therefore of interest to DSM to investigate the possibility of obtaining electrolytic membranes in a safer and easier procedure. For this reason some initial literature research has been dedicated to hot pressing techniques, of which many variations exist.

Croce *et al.* (13) report soft milling of the dried components (PEO and LiBOB in EO/Li⁺=20 molar ratio) in polyethylene bottles and subsequent hot pressing of the powder mixture in aluminium molds at 80-100°C for 20-30 minutes with 3 tons of pressure. All the steps are performed in argon. Very homogeneous, semi-transparent membranes with thickness between 150 and 200 µm were obtained. Similar procedures were adopted by Sumathipala *et al.* (23), by Appetecchi *et al.* (26), by Shin *et al.* (22) and by Panero *et al.* (27) with other types of lithium salts and rigid homogeneous membranes with 50 to 300 µm in thickness were obtained.

A different approach in the way of using the hot press is instead reported by Abraham *et al.* (28): in this case melt mixing was performed, rather than powder ball milling, and the melt was then hot

pressed at 100°C. This method seemed to be an interesting starting point for the research that will be performed during this graduation project, as it eliminates the need for a solvent and does not require ball milling. The difficulty in performing ball milling (as reported in the aforementioned papers) with the polymeric material received from DSM is that it is in the form of pellets and ball milling would have to be performed in cryogenic conditions in order to have adequate brittleness for this type of procedure. Melt mixing would instead allow for a relatively simple procedure: the DSM materials can be melted ($T_m=212^\circ$) and the salt can be added (all the chosen salts have been purposely selected to be stable above this temperature – see previous chapter). Mixing and high temperatures are expected to lead to good dissolution and complete salt complexation. The melt could then be hot pressed.

The process of hot pressing also leads to improved ionic conductivity according to Zhou *et al.* (29), who noted a conductivity increase with the duration of the hot pressing, together with an increase of smoothness and transparency of the membrane. A decrease in the degree of crystallinity was also detected.

More in general, heat treatments may be considered as an option to decrease the degree of crystallinity in the polymer and enhance its ionic conductivity: quenching the electrolyte melt in liquid nitrogen has been reported to lead to such improvements (30).

The initially proposed methods to produce the electrolytic membrane will be discussed in chapter 2 and involve melt mixing and hot pressing, while the use of solvent was completely excluded. In the course of the project other methods were thought of and proposed. These are also explained in detail in chapter 2.

1.4 Research questions

The research questions that arose were determined in part by the literature review, in part by the requests of DSM. The general goal was to investigate the possibility of making solid state electrolytes for lithium ion batteries out of the Arnitel materials produced and provided by DSM. The research questions are already implicitly expressed in the previous chapters and can be summarized as follows:

1. What is/are the adequate lithium salt(s) to be combined with the Arnitel materials?
2. What polymer:salt ratio optimizes the electrolyte properties?
3. How to insert the lithium salt in the polymer to obtain a suitable electrolyte?
4. What are the electrochemical properties of the obtained electrolytes?

As previously explained, the Arnitel materials are not themselves lithium ion conductors, thus one or more salts must be chosen to be incorporated in order to achieve a material made up by a polymeric matrix in which the salt is inserted. The choice of the salt is also dependant on the proposed processing method for sample preparation; in the case of this work it was necessary for the salts to be thermally stable above the melting temperature of the polymers since melt-mixed was initially proposed. The three salts chosen for initial testing were LiTFSI, LiBOB and LiCl. Considering that two types of polymers were available, a matrix of six salt/polymer combination would be derived. Considering also the concentration variable, i.e. the EO:Li⁺ ratio, a third dimension would be added to such matrix of samples. From the first preliminary results a selection of the most promising combination of salt/polymer would follow as to dedicate more focus to the best samples. Much importance was given to investigating methods to incorporate the lithium salt in the polymer by means of a solvent-free route: for this reason it was chosen to try a melting procedure for which salt powders would be mixed in the molten polymer. This was the initial idea, but more alternatives were thought in the course of the project as will be explained in the section that follows. Hot pressing was thought of a technique to obtain thin and geometrically defined electrolyte free-standing membranes.

Once such samples would be prepared, electrochemical characterization would follow. It would be in fact necessary to determine whether the produced sample fitted the requirements needed to be considered as electrolyte material. Therefore the materials would be characterized in terms of ionic conductivity and voltage stability window. It is important to remark that at the start of the graduation project some internal research had already been performed by DSM. Electrolyte membranes composed of the Arnitel materials with LiTFSI had already been produced by the classical solvent route that involves the use of HFIP. These samples had already been characterized in terms of conductivity and electrochemical stability. Such internal DSM data therefore has been the reference point throughout the project as the focus was to produce equivalent (or better) performing electrolytes, but through a solvent-free route. Comparisons with data available in open literature were also made, but only the internal DSM data could yield such a close comparison, since the Arnitel copolymers are trademarked material.

Throughout the course of the graduation project another interest arose: it was in fact proposed to investigate whether such copolymer electrolytes could hinder the formation of lithium dendrites that form through the electrolyte while cycling the cell. The interest sparked from the fact that the Arnitel materials include a harder polymer phase (the PBT) that give the polymer very different mechanical properties from pure PEO. Dendrites seriously compromise the cycle life of polymeric cells and are at the moment one of the biggest limitations to such organic electrolytes. The toughness and improved hardness of DSM copolymer could therefore possibly stop or hinder the formation of dendrites. To this purpose it was initially proposed to use neutron depth scattering (NDP) to investigate lithium movement and accumulation during or after cycling inside the electrolyte. This entails that the samples should be satisfying enough from an electrochemical perspective to be considered for such type of investigation. Only some initial trials in this direction were actually performed and are left in the Appendixes as they do not constitute yet relevant results. The research about dendrite formation in the produced samples was finally left out of the graduation project and is rather recommended as future work.

2. Materials and methods

This chapter is dedicated to a description of the different procedures used to produce electrolyte starting from the co-polymers provided by DSM and of the methods employed to characterize the electrolyte membranes. After a brief description of the chemicals used throughout the project, chapter 2.2 is dedicated to the different routes to insert the lithium salt in the polymer and thus turn the system in to an electrolyte. Because this chapter encloses much of the creative and innovative work of the graduation project, it represents a central part of the report.

The remaining part of this Materials and Methods chapter is dedicated to introducing the different analysis performed on the produced electrolyte samples. Thermal characterization has been done through differential scanning calorimetry (chapter 2.3). Electrochemical analysis represent the core of the characterization of candidate electrolytes and is presented in chapter 2.4; this includes conductivity measurements, cyclic voltammetry and electroplating. All the chapters dedicated to analysis start with an introduction to the technique employed and then include a description of the setup, the settings and the measurement procedures as to allow for repeatability of the experiments.

2.1 Chemicals and materials

The chemicals used during the project are fundamentally lithium salts and Arnitel materials (co-polymers) from DSM; these are summarized in the tables below. Three lithium salts were purchased (LiTFSI, LiBOB and LiCl) and are all sensitive to moisture. Pure PEO with molecular weight of 4000 was also purchased for comparative reasons. The polymers from DSM have a very high water uptake and therefore must be very carefully dried.

Chemical	Form	Source
LiTFSI	Fine white powder	Sigma-Aldrich
LiBOB	Fine white powder	Sigma-Aldrich
LiCl	Fine white powder	Sigma-Aldrich
PEO MW4000	Platelets	Sigma-Aldrich

Table 7 Lithium salts and pure PEO purchased for the research project

As already introduced in chapter 1.3, the DSM materials are di-block copolymers composed of PEO and PBT. PEO is the abbreviation for poly(ethylene oxide) with molecular formula $C_{2n}H_{4n+2}O_{n+1}$, while PBT stands for polybutylene terephthalate with molecular formula $(C_{12}H_{12}O_4)_n$. The molecular structure of the two are presented in figures 3 and 4 in chapter 1.3. PEO is the rubbery and soft phase, while the hard blocks are of PBT. Together they make a thermoplastic copolymer with a peak melting temperature of about 220°C. The difference between the two polymers provided by DSM lies in the weight ratio of the two blocks (PEO and PBT) as shown in table 8. The polymer with 35wt% PEO will be referred to as PEO35, while the second material will be named PEO70.

Given name	Form	PEO wt%	PEO molecular weight	Source
PEO35	White pellets in cylindrical form	35%	2000	DSM
PEO70	White pellets in cylindrical form	70%	4000	DSM
PEO70	Thin translucent film of 15 μm in thickness	70%	4000	DSM

Table 8 Polymer material produced and provided by DSM for the research project

The two material were provided in the form of cylindrical pellets of a few millimetres in length. They are obtained by extrusion and subsequent cutting into the final length. The polymer PEO70 was also provided in the form of a thin film.

All salts and DSM materials (a part from the PEO70 thin film) were dried in the vacuum oven for a few days at 60 °C and then stored in a glovebox with argon environment and with moisture and oxygen levels below 1ppm. Once placed in the glovebox, the materials were left at rest before handling in order to guarantee a complete absence of water or oxygen.

The pure PEO could not be dried in the vacuum oven because at such temperature it is in the liquid phase. It was therefore carefully vacuumed in the antechamber of the glovebox and then left inside the box for 10 days to naturally release its water and oxygen impurities in the controlled environment.

2.2 Electrolyte sample preparation

Electrolyte samples were prepared through a variety of methods, all of which fulfilled the requirement of being solvent-free routes. The three methods proposed, implemented and described in this report represent novel ideas not mentioned in the literature reviewed by the student in the course of the graduation project. For this reason this chapter, together with the corresponding result chapter 3.1, assumes a very central role in this work and is written with much attention to detail.

The fundamental step in preparing electrolyte out of the polymer provided by DSM is the integration of the chosen lithium salts (LiTFSI, LiBOB and LiCl) in the polymeric matrix.

In order to exclude the need of solvent for this process, the first idea proposed was to melt the polymer and mix in the salt. This procedure is referred to as melt-mixing throughout the entire report and is described in detail in the following chapter.

Two other innovative and novel methods were also thought of, both being based on the very high water uptake of the co-polymers provided by DSM. The underlying principle is to take advantage of such uptake by preparing aqueous solutions of the lithium salts. The polymer can thus absorb the solution and thus the salt enters and diffuses through the polymeric matrix. By completely drying the sample in a water-free environment, the water can then be taken out and leave behind the polymer/salt system. In this way water is used as a transport medium for the lithium salt. This working principle was implemented in two different ways: in one case the polymer pellets were soaked in the aqueous salt-containing solution. After drying, the pellets were melted and thus samples similar to the ones obtained through melt-mixing were prepared. This method was named water-soaking and is described in detail in chapter 2.2.2. Both water soaked samples and melt-mixed samples then underwent hot pressing in order to obtain thin and geometrically defined electrolyte membranes.

The other alternative water-based route involved directly soaking of the Arnitel material in the form of thin films (15 μm), rather than the pellets. In this way no subsequent hot pressing procedure was needed to obtain thin membranes after drying the polymer. This direct procedure has been named thin film soaking and constitutes chapter 2.2.3.

The last chapter is instead dedicated to the hot pressing procedure necessary for the melt mixed and the water soaked samples. This step can be seen as the second phase of the preparation procedure of electrolytes through these two methods.

2.2.1 Melt-mixing

Melt-mixing was the first method thought of and performed. With such technique the polymer is heated above its melting temperature together with the salt. Once the system fluidises, mixing is performed in order to homogenise the system and allow for an even salt distribution throughout the polymeric molten matrix. Such salt/polymer mix can then be cooled down and allowed to solidify. The setup and the procedure are outlined in detail in the following pages, with descriptions not only of the final *modus operandi* but also briefly presenting some of the set-backs and difficulties initially encountered in order to justify the decisions taken.

Experimental setup

In order to get acquainted with the melting behaviour of the two polymers provided by DSM, some melting experiments were performed with no salt and in normal atmospheric environment. Initially a small quantity (a few grams) of polymer pellets were melted in a Petri dish using a heated plate as a heating element. The polymer melt revealed to be extremely dense and viscous and soon turned to dark brown colours. Such change of colour can most likely be ascribed to an oxidation process, since this first test was performed in air. What was important to notice from a practical point of view was that, once solidified, the polymer was impossible to detach from the glass surface of the Petri dish. The same results was obtained when the melting was carried out in an oven, rather than on a heating dish.

The next melting tests were then performed in the glovebox after drying all the components in the vacuum oven for 24 hours. Due to the complete lack of oxygen and water contamination it was possible to melt the polymer pellets with no darkening and evident sign of oxidation. Again the melting was performed on a Petri dish place on a heated plate. But the problem of the polymer sticking to the glass was encountered again and it was impossible to get the molten or solidified polymer out of glass containers.

It was therefore clear that another container material was needed that would not allow for such severe sticking. A carbon-glass jar was then used, but this choice did not prove successful either in avoiding the sticking.

The next container material that was thought of was PTFE (Teflon). PTFE containers were not available at the labs and a normal small Teflon pan (kitchenware) was too big to fit through the anti-chamber of the glovebox. Furthermore the surface of such a pan should be smaller than that of the heating plate (diameter of 15 cm) as to guarantee homogeneous heat distribution.

What was then used was Teflon foil, available in any house-hold store. A piece of such foil was cut out and placed directly on the heating plate. A few grams of polymer pellets were place on the Teflon foil. Once melted and re-solidified, the polymer peeled off very easily from the foil and left no residues on it. Thus it was understood that PTFE is the material to be used for the melt-mixing technique, as it allows for a stick-free process and can endure the temperatures required for the melting of such polymers. PTFE Petri dishes, jars, mixing rods and spatulas were promptly ordered, but due to long delivery time, all samples have been prepared simply on Teflon foil and mixed with a PTFE rod. Thus, the experimental setup used for the melt-mixing procedure consisted of a heating plate, a scale, Teflon foil, a PTFE little rod for mixing and a small metal disk of a few hundred grams used as a small weight to obtain flat solidified polymer disks.

Procedure

After performing different melting experiments in presence of one of the salts, the following procedure was set and all samples have been made exactly in the same way as to allow for repeatability and comparability. Again it is important to stress that all materials were completely dried in the vacuum oven and then placed in the glovebox where the experiments took place.

The samples prepared are listed in the following table. Some reference material of pure polymer, with no salt added, was also prepared in the same way and is listed at the end of the table. For the calculations of the required mass to obtain the desired EO:Li⁺ ratio mass calculations please see Appendix A.

Polymer	Salt	EO:Li⁺	Polymer mass [g]	Salt mass [mg]
PEO35	LiTFSI	20	2,19	250
PEO70	LiTFSI	20	2,19	500
PEO35	LiTFSI	10	2,19	500
PEO70	LiTFSI	10	2,19	1000
PEO35	LiBOB	20	2,16	167
PEO70	LiBOB	20	2,16	333
PEO35	LiCl	20	2,38	40
PEO70	LiCl	20	2,38	80
PEO	LiTFSI	20	3,07	1000
PEO35			~2,5	
PEO70			~2,5	

Table 9 Summary of all samples prepared through melt-mixing

One sample of pure PEO with the same molecular weight as the PEO in the Arnitel materials (MW 4000) was prepared with LiTFSI to allow for comparison between DSM material and the equivalent PEO system. It was in fact deemed interesting to evaluate the effect of the PBT hard block, all other variables remaining the same, in terms of sample mechanical and electrochemical properties.

The reason for choosing a EO:Li⁺=20 ratio for all salts has been already explained and is linked to the frequency with which such concentration is reported in literature and also to the known internal DSM data. The reason for choosing also a EO:Li⁺=10 for LiTFSi derives from the considerations on the phase diagram of PEO and LiTFSI presented in the previous chapter. It was in fact indicated that for such concentration the crystallinity should be reduced due to a crystallinity gap in the phase diagram. What follows is the detailed description of the melt-mixing method.

Step 1: A square piece (approximately 10cm x 10cm) of Teflon foil is placed on the heating plate, that is placed in the glovebox at room temperature.

Step 2: The required masses of polymer and salt are accurately weighed on the scale and transferred to the Teflon foil on the heated plate.

Step 3: The temperature of the heating plate is set to 250°C². When the polymer starts softening it is mixed with the Teflon rod in order to distribute the salt evenly. Due to the high viscosity of such melts mixing is not performed so easily, but can be achieved.

Step 4: After leaving the mixture at rest on the heating plate for about a minute, it is stirred again.

Step 5: A second piece of Teflon foil is placed on top of the mix and a heated metal disk is placed on top of the foil/melt/foil stacking. This small weight of a few hundreds grams evens out the surface of the molten polymer and allows for a flat disk of material when solidified. The viscosity of the melt is such in fact, that it does not flow to a flat smooth surface.

Step 6: The heated disk is removed and the foil/melt/foil is removed from the heating plate and placed on a metal plate as to allow for fast cooling and creating almost a quenching condition.

Step 7: Once the polymer+salt mix is solidified, the two Teflon foils are easily peeled off and a thin (<1mm, more is discussed in the results chapter) disk of electrolytic material is obtained as can be seen in chapter 3.1.

2.2.2 Water soaking

The term water soaking is here used to describe a different procedure for inserting the salt in the polymers. The idea stems forth from the ability of such polymers to absorb water. According to the data sheets of the two polymers provided by DSM, the water uptake of PEO35 is 33%, while PEO70 reveals a 132% value of water uptake. PEO is well known to absorb and swell in presence of water, so it is reasonable to find a higher water uptake for the polymer with a higher content of PEO. The idea was to make a solution of salt and water and then soak the polymer pellets in such a solution until complete swelling and absorption of the solution. The water therefore would behave as medium to carry the salt within the polymer chains. Subsequent drying would allow to eliminate the water and ideally leave only the salt distributed in the polymer pellets. Since the PEO70 shows a much higher water uptake experiments of this type were only performed using such polymer.

Experimental setup

One of the attractive features of such method, is its ease. Seal tight small jars are needed to prepare the water based salt solution and later soak the pellets without the risk of loss of water due to evaporation. Demineralized water was used and the polymer pellets and salts were previously dried in the vacuum oven and stored in the glovebox. A heating plate in the glove box was also needed to melt the polymer+salt system after drying in order to obtain disks of material as in the melt-mixing. The detailed procedure is explained in the following paragraph.

² Although the melting temperature of the two polymers is lower than 250°C, it must be considered that the set temperature of the heating plate is not the temperature that the sample reaches due to heat losses. At lower set temperatures in fact the polymer pellets are not completely molten.

Procedure

Water soaking experiments were only performed with PEO70 due to its higher water absorption. Samples of each salt were prepared respecting the EO:Li⁺=20 ratio. Thus three samples have been prepared with this method. In table 10 the masses of salt, polymer pellets and demineralized water used for the preparation of the sample are indicated. The fact that the water mass is not precisely the same arises from the difficulty of measuring such small quantities: during the measurement in fact the mass quickly changes due to evaporation. In any case high precision was not needed because the effort was not focused on obtaining a replicable molarity of the solution, but rather having the correct quantity of water that would allow for the pellets to be completely submerged, but also avoid surplus water that would not be absorbed by the pellets. If such experiment needs to be repeated, it can be done more accurately and with consideration on the molarity of the solution.

What follows are the detailed experimental steps, some of which do not take place in the glovebox due to the use of water. These will be pointed out for sake of clarity.

	LiTFSI sample	LiBOB sample	LiCl sample
Salt mass	250 mg	167 mg	40 mg
Water mass	1,56 g	1,40 g	1,65 g
PEO70 pellets mass	1,09 g	1,08 g	1,19 g

Table 10 Masses of chemicals used for the water soaking process

Step 1: The polymer pellets and the salt are accurately weighed in the glovebox and placed in two separate air-tight small screw-top jars. In this way the material can be safely brought outside the glovebox.

Step 2: The required quantity of demineralized water is quickly added to the jar containing the salt. It is then immediately closed as to avoid evaporation and shaken to allow for a perfectly transparent solution.

Step 3: The polymer pellets are then added to the jar with the salt solution and again the tap is immediately screwed on tight. The quantity of solution and the geometry of the jar are such that the pellets are completely covered by the water solution.

Step 4: The sealed jar containing the polymer pellets soaked in the salt water-based solution are left for 24 hours to allow for complete absorption. The water immediately starts becoming turbid and the pellets immediately start swelling.

Step 5: Once the 24 hours have passed no more water is to be seen and the pellets are swollen. The jar is then opened and dried in the vacuum oven for 24 hours.

Step 6: After drying the material is moved to the glovebox where complete removal of oxygen and water traces is guaranteed. In the glovebox the pellets are again weighed in order to determine if all the salt has entered the pellets.

Step 7: The pellets (polymer+salt) are placed on Teflon foil and heated on the heating plate (set to 250°C) until they completely melt. As in the melt-mixing procedure, a heated metal disk is placed above in order to flatten out the melt and obtain a thinner disk.

Step 8: The heated metal disk is removed and the melt sandwiched between the Teflon foil is put to cool on a metal plate in order to achieve a fast cooling rate and thus some kind of quenching, just as in the melt-mixing procedure.

2.2.3 Thin film soaking

This chapter is dedicated to the description of an alternative route to producing thin electrolyte samples without the need for melt-mixing or hot pressing. It is a technique that has been thought of to take advantage of the availability of PEO70 thin films from DSM and involves no melting, but rather uses the water uptake capability of such polymer, similarly to the samples prepared from polymer pellets soaked in a water based solution. The further simplification of this procedure is that it requires no hot pressing as the sample already has the correct geometry.

This method consists in placing in a 5x5cm² container a piece of PEO70 thin film of 15µm (provided by DSM already in this form) on Cu foil (both films with the same area as the container) and dropping on the system an aqueous solution of LiTFSI. The quantities used were 21mg and 11mg of salt in 3mL of distilled water respectively for sample TF1 and TF2. The system is given several hours for the solution to swell the polymer and allow for diffusion of the Li salt in the thin polymer film. The remaining liquid is dried out by placing the system in a vacuum chamber and can then be safely stored in the water- and oxygen-free environment of the glove box. In order to maintain a smooth contact between the two layers and avoid the polymer from shrivelling, a hollow stainless steel cylinder is vertically placed on the system as a weight.

While drying the thin polymer film containing the salt adheres to the copper foil, which will constitute the current collector for any kind of electrochemical measurement. To ensure an even better adherence and to avoid any risk of delamination, the two-layer system can be heated in the glove-box to 200°C on a heating plate and then left to naturally cool.

The samples obtained through such procedure are reported in chapter 3.1.3, while the measured conductivity is presented and discussed in chapter 3.3.1.

2.2.4 Hot pressing

Hot pressing was performed in two different setups because ideation and development of an improved system required time. Therefore the first samples were hot pressed in a conventional cylindrical die set, while hot pressing was later improved and performed in a custom-made system that was designed and produced specifically for this project. The two methods are here blow described separately.

Hot pressing in a conventional cylindrical die set

In order to hot press the salt-containing polymer previously prepared, either through melt-mixing or through water soaking, and obtain a thin disk of electrolytic material, a cylindrical die set was used. Such a device was surrounded by a heating element in order to combine pressure and temperature for processing. In this way it was possible to apply a controlled pressure on the sample using a hand press and allow for temperature control. Due to the polymer's and salt's sensitivity to air, the whole procedure was carried out in the glove box with water and oxygen contents below the ppm limit. The hot press is shown in fig. 6 while the exploded view of the die set is illustrated in fig. 7.

The die set shown in fig. 7 is made up of two stainless steel cylinders of 12,7 mm of diameter. A small disk of the salt-containing polymer is placed in between two PTFE disks (in order to avoid sticking of polymer to the stainless steel surfaces) and such stack is placed between the two cylinders as shown in fig. 7. When inserted in the cavity of the die, pressure can be applied through the press and temperature can be increased thanks to the heating element wrapped around the system and connected to a temperature controller.

Small disks of salt containing polymer were cut out from the previously prepared samples (either through melt-mixing or water soaking, see chapters 2.2.1 and 2.2.2 respectively) using 6 or 7 mm punches in order to obtain pieces with a mass of about 20 mg.

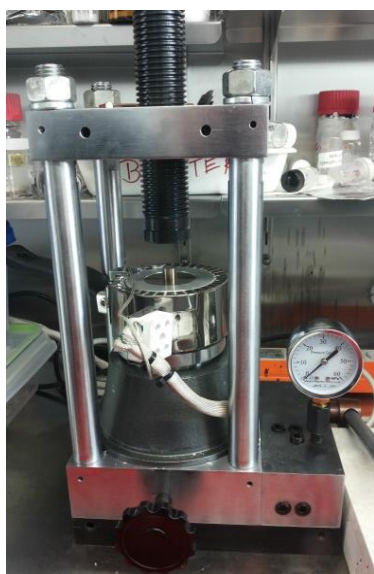


Figure 6 Hot press setup in the glovebox. The heating element around the die set can be seen.

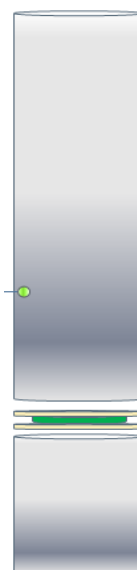


Figure 7 Exploded view of the hot pressing setup that includes the cylindrical die set and the sample (in green) between two PTFE disks (in yellow).

The hot pressing conditions that were found to yield good samples were a set temperature of 150°C and 3,2 tons of applied pressure on the system. With such parameters it was possible to soften the material sufficiently to flatten it out to a thin disk, but avoid overflow of material that can occur if pressure or temperature are excessive, leading to loss of material and sticking of the die set parts.

Temperature and pressure are immediately released as soon as the system reaches 150°C and the whole system is allowed to cool naturally.

Sample name	Composition	Preparation method (prior to hot pressing)
HP1	PEO 70 + LiTFSI EO:Li ⁺ =20	Melt-mixing
HP2	PEO 70 + LiTFSI EO:Li ⁺ =20	Melt-mixing
HP3	PEO 70 + LiTFSI EO:Li ⁺ =10	Melt-mixing
HP4	PEO 70 + LiTFSI EO:Li ⁺ =20	Water soaked
HP5	PEO 70 + LiBOB EO:Li ⁺ =20	Melt-mixing
HP6	PEO 70 + LiCl EO:Li ⁺ =20	Melt-mixing

Table 11 Sample series HP prepared through hot pressing in cylindrical die set

With this procedure six samples containing PEO70 were prepared as summarized in table 11. Samples containing LiTFSI were prepared with both a EO:Li⁺ ratio of 20 and 10 as described previously, while the ones containing LiBOB and LiCl are only in the EO:Li⁺ ratio of 20. The LiTFSI-containing series also includes a water soaked sample (HP4).

Hot pressing in custom made press-cells

The hot pressing method described in the previous chapter proved to be initially satisfactory but also revealed some drawbacks such as irregular sample surface and not controlled thickness. Furthermore the sample needed to be moved to a cell for electrochemical measurements, where adequate electric contact was not ideal. For this reason a customized system was designed that would allow for hot pressing of the sample and impedance measurements to be done all in the same setup and in a more replicable manner. Because of its double function the device is later referred to as press-cell.

Fig. 8 shows a drawing of the system once closed, while fig. 9 is a picture of the open press-cell. The press-cell is made up of three pieces: two stainless steel identical parts and a separator in Peek. The stainless steel parts have a central raised disk where the electrolyte material is pressed and that constitute the electrode surfaces of the device. They also present two holes (fig. 8) required to insert the connectors for any kind of electrochemical measurement. The peek ring is meant as a separator to guarantee a known and precise thickness of the sample (that is the distance between the

electrodes) while pressing. The volume left between such separator and the central electrodes is meant for possible overflow of excessive electrolyte material placed between the electrodes.

Different press-cells were initially produced as to evaluate what was the ideal combination of electrode size and separator thickness. Two different electrode areas of 1cm^2 and 2cm^2 were made together with separators that would yield a spacing between the electrodes (and therefore the final sample thickness) of $200\mu\text{m}$ and $500\mu\text{m}$. Thus, four different combinations were possible. The combination of big area and thin electrolyte has been chosen after different trials, therefore all sample produced in such cells have a surface of 2cm^2 and a thickness of approximately $200\mu\text{m}$.



Figure 8 Drawing of the closed press-cell. The holes for connection to any measuring device are visible.



Figure 9 Picture of the open press-cell. The metal electrodes are in stainless steel, the white separator is in Peek.

The hot pressing using the press-cells takes place in the glove box with the following procedure: a disk of salt containing polymer is cut out from the previously prepared samples with a 16mm punch and placed on the electrode area of one of the two stainless steel parts. In this way the entire electrode area is covered. The peek separator is placed and the top stainless steel closes the press-cell. Such system is then placed in the hot press and pressed at 200°C with 1 ton of applied pressure. The reason for choosing different temperature and pressure conditions compared to the pressing described for the cylindrical die set is the presence of the peek separator: its Young's modulus is 3,6 GPa and therefore it is advisable to choose a lower pressure as to avoid any significant deformation of the plastic and thus guarantee the precision in the sample thickness. In order to counterbalance the lower applied pressure, a higher processing temperature guarantees sufficient deformability of the polymeric sample. Once the system reaches the set temperature of 200°C , the press-cell is allowed to cool naturally.

The table that follows summarizes the samples from the PC series prepared in the press-cell. Since at the moment of performing these experiments the conductivity results from the HP series were already known it was chosen to only produce LiTFSI-containing samples. The reasons for this choice will appear clear from chapter 3.3. Samples PC1 and PC2 were made to check whether the different cells (different surface area and thickness) yielded the same conductivity results, in order to be able to affirm that result were independent of the system used. These samples were used also to determine a fixed procedure to perform impedance measurements in this new setup.

Sample name	Composition	Preparation method (prior to hot pressing)	Press-cell used (Area/Thickness)
PC1	PEO 70 + LiTFSI E0:Li ⁺ =20	Melt-mixing	1cm ² /200μm
PC2	PEO 70 + LiTFSI E0:Li ⁺ =20	Melt-mixing	2cm ² /500μm
PC3	PEO 70 + LiTFSI E0:Li ⁺ =20	Melt-mixing	2cm ² /200μm
PC4	PEO 70 + LiTFSI E0:Li ⁺ =20	Water soaking	2cm ² /200μm
PC5	PEO 70 + LiTFSI E0:Li ⁺ =10	Melt-mix	2cm ² /200μm
PC6	PEO 35 + LiTFSI E0:Li ⁺ =20	Melt-mixing	2cm ² /200μm

Table 12 Sample series PC prepared through hot pressing in the press-cells

2.3 Differential scanning calorimetry (DSC)

Differential scanning calorimetry is a thermo-analytical technique which allows to detect thermal transitions. The sample and a reference are simultaneously heated up in parallel in order for the two to be maintained at the same temperature. The difference in amount of heat required to increase the temperature of the sample and the reference is measured as a function of temperature. When the sample undergoes a physical transformation as a phase transition, more or less heat will need to flow in order for the sample and the reference to maintain the same temperature. The measured difference in heat flow can be negative or positive depending on whether the process is exothermic or endothermic. Melting is an example of endothermic phase transition, while crystallization is exothermic.

The result of a DSC experiment is a plot of heat flux versus temperature. A positive peak indicates endothermic reactions, a negative peak is instead symptom of an exothermic reaction.

DSC was the first analysis performed on the materials produced through melt-mixing and water soaking (as described in chapters 2.2.1 and 2.2.2). To this purpose a small piece (see table below for DSC sample masses) of each sample was cut out of the polymer+salt disks and sealed in aluminium cups. This procedure and the punching of the DSC cups were performed in the glovebox to guarantee no water or oxygen contamination. The measuring procedure was identical for all samples and included only a controlled heating step up to 275°C. This temperature was chosen in order to slightly surpass the processing temperature that was 250°C. Any higher temperature was not deemed relevant for the purpose of a candidate electrolyte for lithium ion batteries.

Sample	Composition	EO:Li⁺	Method	Sample mass [mg]
1	PEO35+LiTFSI	20	Melt-mix	18,1
2	PEO70+LiTFSI	20	Melt-mix	5,8
3	PEO35+LiTFSI	10	Melt-mix	12,1
4	PEO70+LiTFSI	10	Melt-mix	5,7
5	PEO35+LiBOB	20	Melt-mix	6,9
6	PEO70+LiBOB	20	Melt-mix	7,5
7	PEO35+LiCl	20	Melt-mix	7,2
8	PEO70+LiCl	20	Melt-mix	9,2
9	PEO35		Melt	11,4
10	PEO70		Melt	12,0
11	PEO70+LiTFSI	20	Water soaking	3,3
12	PEO70+LiBOB	20	Water soaking	4,0
13	PEO70+LiCl	20	Water soaking	2,3

Table 13 Summary of DSC samples and main remarks

The program that was run consisted of three steps:

1. Hold at 25°C for 2 minutes
2. Heat to 275°C at 10°C/min
3. Hold at 275°C for 2 minutes

Natural cooling followed in all cases and no data was recorded for the cooling process. It was not possible to perform any measurement below room temperature because the device used does not offer a cooling system to record DSC plots at lower temperatures.

Before starting the measurements, blank samples were tested in order to be able to subtract the background signal. Such blank DSC cups were also sealed in the glovebox, as to contain argon like all the other cups.

2.4 Electrochemical analysis

In order to characterize a candidate electrolyte for a lithium-ion battery it is necessary to perform a series of electrochemical analysis. As already introduced in chapter 1.3.1, there are some fundamental requirements that an electrolyte should meet. In the first place it is of vital importance for the ions to be able to move as freely as possible from one electrode to the other during charging and discharging, thus the conductivity of the electrolyte should be measured. This is performed through impedance spectroscopy and is explained in detail in chapter 2.4.1.

Furthermore the electrolyte should be stable in a voltage window that is as wide as possible in order to enable the use of high voltage cathode materials and thus obtain higher power from the battery. Cyclic voltammetry is the technique to evaluate the stability of the electrolyte, as explained in chapter 2.4.2.

As stated above, it is of central importance for the electrolyte to be able to conduct ions. This entails that the conductivity due to ions and to electrons must be distinguished. When performing impedance spectroscopy, in fact, it is only possible to measure the conductivity of the sample, this being the sum of the ionic and electronic conductivity. To prove whether the conductivity derives indeed from the movement of lithium ions rather of electrons it is necessary to be able to electrochemically plate lithium. Such experiment are described in chapter 2.4.3.

If a candidate electrolyte proves to have good conductivity, be stable for a wide voltage range and be an ionic conductor, it may be said that it meets the basic and fundamental requirements for a successful electrolyte.

The detailed setups for such analysis and the related theoretical background are described in the following dedicated chapters.

2.4.1 Conductivity measurements

Conductivity measurements were performed by measuring the resistance of the samples. In order to measure the resistance it is necessary to do electrochemical impedance spectroscopy. Impedance is the opposition to the flow of alternating current in a system that includes a resistor (an energy dissipater) and a capacitor (an energy storage element). If the system is purely resistive the impedance is simply the resistance. With impedance spectroscopy it is possible to measure the impedance of the system over a range of frequencies; in this way the frequency response to the system is detected.

Such measurements generally involve applying an alternating potential to the electrochemical cell and measuring the current through the cell. In a pseudo-linear system (condition that is achieved by applying small excitation signals), the current response to a sinusoidal potential $V_t = V_0 \sin(\omega t)$ will be a sinusoid at the same frequency but shifted in phase $I_t = I_0 \sin(\omega t + \phi)$, where V_0 and I_0 are respectively the amplitudes of the potential and the current, ω is the frequency and ϕ is the shift in phase.

The impedance, being defined as the ability of the circuit to resist the flow of electrical current, can be expressed therefore as

$$Z = \frac{E}{I} = Z_0 \cdot \frac{\sin(\omega t)}{\sin(\omega t + \phi)} \quad \text{Equation 1}$$

where Z_0 is the ratio between the voltage and current amplitudes.

Using Euler's relationship it is therefore possible to express the impedance as a complex number:

$$Z = Z_0 \cdot (\cos \phi + j \sin \phi) \quad \text{Equation 2}$$

The real and imaginary part of the impedance are plotted respectively in the X-axis and the Y-axis of a Nyquist plot. In such a plot each point is the impedance at a specific frequency. The data collected can be fitted with the use of equivalent circuit models in order to gain the numerical values of elements of the system such as resistance, capacity, inductance, etc. For the research carried out during this project only the resistance was required and therefore only the real part of the impedance was needed. Therefore the intersection of the Nyquist plot with the X-axis yields the R value, i.e. the resistance of the system.

The resistance of the sample is proportional to its resistivity and thickness and inversely proportional to the active area, as shown in eq. 3 where R is the resistance, ρ is the resistivity, l the thickness of the sample and A the area.

$$R = \rho \cdot \frac{l}{A} \quad \text{Equation 3}$$

The active area is the area of the smallest electrode, as this defines the region of the electrolyte that is actually participating to the conduction of ions. See fig. 10 that shows the case where the one of the electrode has the smallest area.

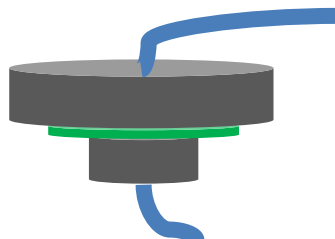


Figure 10 Schematic representation of two electrodes (in grey) with different surface areas together with the polymeric electrolyte placed in between (in green). Electric connection to the Autolab is shown in a simplified way as two cables (in blue).

The conductivity, being defined as the inverse of the resistivity, can be calculated therefore through eq. 4, where σ is the conductivity.

$$\sigma = \frac{1}{\rho} = \frac{l}{R \cdot A} \quad \text{Equation 4}$$

The active area A is known, as is the thickness of the electrolyte; through impedance measurements the resistance is measured. More details regarding the extrapolation of the R value can be found in the in the result chapter and in the appendixes. Once these three parameters are known the conductivity is calculated according to eq. 4.

Ionic conductivity depends on the mobility of the ions and is therefore a thermally activated process. This entails that conductivity increases with temperature, therefore it is necessary to perform such impedance measurements in a selected temperature range. The collected conductivity data is then plotted in an Arrhenius plot, where the logarithm of the conductivity is displayed as a function of the inverse of temperature. Such plots summarize concisely the temperature dependence of the conductivity of the electrolyte and yield all the necessary information regarding the electrolyte from a conductivity perspective. When considering an electrolyte for a possible battery, it is important to know the conductivity within the temperature range at which the battery would be used. If electric vehicles are taken as an example such operational temperatures range from below freezing temperature to about 70°C. The reason for which no conductivity data was measured below room temperature during this project was the lack of an appropriate cooling device for such experiments. The setup used for impedance measurements is described in the following paragraphs.

Impedance measurement setup

From chapter 2.2 it must be recalled that a variety of samples was made, therefore more than one setup was needed to perform conductivity measurements. Due to the fact that the press-cell required development of the concept and time for actual production, the first measurements were performed in another system, previously referred to as blocking cell. This is a cell that is closed by screwing the two parts together: in this way the electrolytic sample can be placed between the two stainless steel electrodes and while screwing on the two parts an internal spring guarantees sufficient force to enable good contact between the interfaces (see fig. 11). The two connectors on the extremities of the blocking cell allow for cable connection to the Autolab, the devices used for measuring impedance throughout the course of such experiments. All the samples from the HP series and the soaked thin film (series TF) were measured using such a measuring setup. These were chronologically the first samples made and measurements in the blocking cell were only performed at room temperature as to make a first screening of the samples and to make a selection of the compositions to test in a range of temperatures.



Fig. 11 Blocking cell used for impedance measurements of sample series HP and TF.

Once the press-cells were available, samples (Series PC) were produced using this improved system and from that point on all impedance measurements were performed directly in the press-cells. To guarantee an air tight system even outside the glovebox, the press cell was wrapped with Kapton tape. The experiments described in chapter 3.3.1 made evident the strong dependence between the pressure on the press-cell and the contact quality between the electrolyte/electrode interfaces: this allowed to define a fixed procedure for impedance measurements in order to standardize experiments and allow for reproducible, consistent and comparable results. The press-cell that was from this point on used had an electrode area of 2 cm^2 and a sample thickness of approximately 200 microns and the system was kept under 1,5 tons of pressure while performing the conductivity measurements. Such pressure was achieved by using a hand press. Due to the need of such press it was not possible to simply insert the sample in an oven to perform temperature dependant impedance measurements. For this reason a heating system was devised that would wrap around the press-cell and allow for uniform heating of the sample while simultaneously applying the required pressure. The system is shown in the figure below for clarity. With such setup it was possible to simultaneously apply heat and the adequate pressure for good contact.



Fig. 12 Hand press combined with heating device used for impedance measurements in the press-cells (PC series). The press-cell is inserted in the heating block and connected to the Autolab.

In this way Arrhenius plots could be obtained: these display the conductivity as a function of temperature and represent a substantial part of electrochemical testing of electrolytes.

Impedance measurements were performed on an Autolab impedance spectrometer from Metrohm Autolab in a frequency range between 100Hz and 1MHz at temperature between ambient temperature and approximately 65°C with current in the range of 1 mA. The software used for data fitting was Nova 1.11, the software provided together with the Autolab device.

The temperature of the press-cell was brought to approximately 65°C, temperature at which the first measurement was taken. The thermostat was then gradually lowered to allow for repetition of the measurement at different temperature steps until room temperature was reached. At each temperature step the system was allowed to rest in order to reach thermal equilibrium. The temperature was measured by using a thermocouple in contact with the outer walls of the press-cell immediately before and after the measurement. The average of the two was taken as the temperature at which the conductivity measurement was performed. As may be expected the difference between the initial and final temperature was null when the system was close to room temperature, as in this condition the driving force for natural cooling is very low.

The results of the described conductivity measurements are presented and discussed in chapter 3.3.1.

2.4.2 Cyclic voltammetry

Cyclic voltammetry (from this point on referred to as CV) is a potentiodynamic electrochemical measurement during which the potential of the working electrode is linearly ramped up or down versus time at a certain scan rate expressed as V/s. Such cycles of ramps in potential between two voltage limits may be repeated multiple times while the current at the working electrode is plotted versus the applied voltage: this yields the cyclic voltammogram plot. Peaks in the plotted current denote that reactions are taking place for the specific voltage applied. Oxidative processes appear as positive peaks, while reductive processes are indicated by negative currents. With such measurements it is possible to determine the voltage window within which the electrolyte is electrochemically stable, i.e. the voltage range that exhibits a flat current profile.

Solid electrolyte interphases (SEI) may form and this will also be detected as degradation peaks. The SEI should protect the electrode from further corrosion, but not hinder ionic transport to and from the electrode. Knowing the upper and lower allowed voltages enables to choose adequate electrodes to be matched with the electrolyte. It is desirable for the stability window to be as wide as possible in order to be able to use cathodes with a high voltage and anodes with a low voltage: in this way the power of the cell can be maximized.

At voltages lower than 0V vs. Li^+/Li a reversible cathodic process is expected, corresponding to lithium plating on the working electrode. The equivalent opposite is expected at voltages slightly higher than 0V vs. Li^+/Li on the return scan, corresponding to lithium stripping from the working electrode; this is a reversible oxidative process. The presence of these two peaks is of high

importance as it proves the ability of the electrolyte to effectively swap lithium ions from one electrode to the other.

Cyclic voltammetry experiments were performed on samples PC3, PC4, PC5 and PC6 as these were the samples deemed most relevant after the impedance measurements (more details on such choice are given in chapter 3.3.1). Measurements took place in KF cells, the cells standardly used within the research group. These can be seen in the figures below. The two stainless steel electrodes form the body of the cell. One of the two includes a spring behind the flat electrode surface. Such spring allows to create pressure and improved contact between the different interfaces. The black tensioning chain wraps around the cell and clamps it tight by applying pressure on the spring behind the smaller electrode. The O-ring guarantees an air tight environment even when outside of the glovebox. The cells were assembled in the water- and oxygen-free environment of the glovebox by placing the electrolyte disk on the bigger electrode and stacking a small disk of lithium metal on top of it. The lithium disk was cut out of a metal sheet by using a 10 mm punch. Delicate scraping with plastic tweezers was needed to reveal very shiny surfaces on both sides of the disk. Once the stack was gently pressed together, the cell was closed with the other electrode (the one containing the spring) and clamped together with the tensioning chain.



Fig. 13 Open KF cell



Fig. 14 Closed KF cell

Thus the CV measurement system involved a “0-Volt” cell with lithium metal as the reference electrode and stainless steel as working electrode. The cells were taken out of the glovebox just before measurements and connected to the Autolab.

CV scans were performed in a voltage window between $-0,5V$ and $+5V$ at a scan rate of 5 mV/s with a step potential of 1 mV for two complete cycles of discharge/charge at room temperature. Such measurements were repeated with the same settings but only for one cycle also at 45°C . Reasons for measurements at such temperature will be justified by the electroplating results presented in chapter 3.3.3. Temperature control was obtained by placing the cell in an oven at the set temperature. Sufficient time was given for the centre of the cell to reach thermal equilibrium with the environment. The obtained CV plots are presented in chapter 3.3.2.

2.4.3 Discharge and electroplating experiments

Electroplating experiments were intended to prove the ability of the prepared electrolyte disks to effectively conduct lithium ions. The idea behind such experiments is to run a discharge current and verify whether the voltage of the cell reaches $0V$ and remains at a stable null voltage plateau. If this

happens it can be deduced that the lithium ions were effectively able to reach the cathode and initiate nucleation. At this point a Li/Li cell forms due to electroplating and this is why the measured voltage should be null.

Although the idea behind such an experiment is very simple, the actual implementation proved to be very challenging. What follows is a brief description of the failed setups that were used and is meant to give grounds to the choice for the final testing setup and method described in the last paragraph of the current chapter.

Measurements consisted in discharging the cell previously used for CV scans (no alterations made on the cell). Initially the intention was to perform such experiment using the Maccor S4000, but this was not possible neither in potentiostatic or galvanostatic mode as the current going through the system was too low for the device to deal with. Initially this may be surprising considering the very high conductivity of the samples even at room temperature (please see conductivity results in chapter 3.3.1), but it must be kept in mind that in the KF cells the contact is not nearly as good as in the press cells kept under 1,5 tons of pressure. Therefore evidently the resistance of the system in the KF cells was too high to run a high enough current for the Maccor to detect. The first solution that was thought of was to place the cell in an oven and perform the experiments at 50°C in order to obtain improved conductivity. This trial though failed like the previous ones as the interface resistance was still the bottleneck for ion conduction.

In theory it would have been possible to perform the electroplating experiments in the press-cells and apply again a high pressure to guarantee optimal contact, as previously done for impedance measurements. This was not as straightforward, as it is necessary for such experiments to have a lithium anode and lithium foil is too thick to fit in the press-cell: the spacer in the press-cell is in fact designed to yield a polymer disk of the same thickness during hot pressing and thus adding the a lithium disk leads to a too thick stack. In this configuration the press-cell cannot guarantee an air-tight seal and be brought out of the glovebox to be connected to the Autolab. A route to go around such a problem was thought of: the idea was to substitute the thick lithium foil with a electrodeposited lithium layer in order to have a thinner lithium anode and thus be able to close the press-cell adequately. Such thin lithium anode was produced as follows.

In a KF cell a 15mm lithium disk was placed and covered with a wider disk of Solupor separator. Four drops of liquid electrolyte (1,0 M lithium hexafluorophosphate solution in ethylene carbonate and dymethyl carbonate 50/50 purchased from Sigma-Aldrich) were placed on top and the stack was completed with a disk of copper foil. Two KF cells were prepared and then connected to the Maccor for discharge: one was run with 0,02 mA and one with 0,1 mA as to compare the effect of two different discharge currents. The lithium was in this way allowed to travel through the separator and plate on the Cu foil. Once the plating was over, the KF cell was brought back in to the glovebox and the Cu foil with thin deposited Li was removed and in theory ready to be used as an anode in the press-cell together with the polymer electrolytes.

However the process described above did not yield satisfying enough lithium anodes as they proved to be quite porous and not shiny. Therefore it was still not possible to use the press-cells for the measurements and the procedure would have required much further improvement. The next solution that was thought of was to revert to the KF cells but perform the measurements on the Autolab rather than on the Maccor: the Autolab is in fact a much more sensitive device and can deal with very low currents.

Final setup and procedure

Therefore electroplating experiments were finally performed on the same samples as those used for CV and are therefore samples PC3, PC4, PC5 and PC6. A discharge current of 10^{-5} A was run for 5 minutes and a rest step of 5 minutes followed. Such experiments were performed in the same way at different temperatures ranging from 25°C to 55°C by keeping the sample in an oven at the desired temperature. The reason for repeating the experiments at increasing temperature will be discussed together with the results shown in chapter 3.3.3.

3. Results and discussion

The results presented in this broad chapter range from the intermediate steps of the procedures in making the electrolyte (chapter 3.1), to DSC results (chapter 3.2) and electrochemical results (chapter 3.3).

3.1 Electrolyte samples

In this section the results from the intermediate steps in producing the polymeric electrolyte through different routes are shown. Observations and remarks are also presented. The first two chapters deal with the melt-mixing procedure and the water soaking respectively. The samples obtained through thin film soaking are instead treated in chapter 3.1.3. In the case of the melt-mixed and water soaked samples, hot pressing followed and yielded the final samples: these are discussed in chapter 3.1.4, where results deriving from the use of the traditional cylindrical die set are given in addition to the ones produced in the custom made press-cells. Overall much importance is given to practical details, considerations and remarks as to facilitate possible further work by other hands.

3.1.1 Samples produced through melt-mixing

What follows is a small collection of pictures (fig. 15) of the salt+polymer disks obtained with the melt-mixing procedure described in chapter 2.2.1.

The pure PEO sample is not shown as the sample obtained was in gel form and did not meet the requirement of being a solid-state free-standing electrolyte. This sample was therefore discarded and not further considered during the rest of the project.

The thickness of the samples was not measured in view of the hot pressing procedure that was later performed and that yielded anyways a controlled micrometre thickness. It may be estimated that the thicker samples of figure 15 were about 1 mm in thickness, while the thinner ones reached thicknesses in the micrometre range, with some areas as thin as to be transparent.

The most noticeable feature of the collection of sample is that the ones containing PEO35 are much thicker and more rigid. While stirring the melts, such samples proved to much more viscous than the ones containing PEO70 and the molten material was not flowing easily. This also entails that when the heated metal disk was placed on top of the molten material, the pressure was not enough to make the material flow sufficiently to flatten out, as instead the PEO70-containing samples did. Considering that the two polymers are di-block copolymers with different proportion of soft block (PEO) and hard block (PBT), such difference in viscosity and sample thickness can be ascribed to the lower content of soft block in the PEO35 (35wt% of PEO in PEO35 compared to 70wt% of PEO in PEO70). Many bubbles seem to form during the mixing and are then trapped during solidification leading to visible bubbles or holes in the samples. This is mostly visible in the thinner samples.

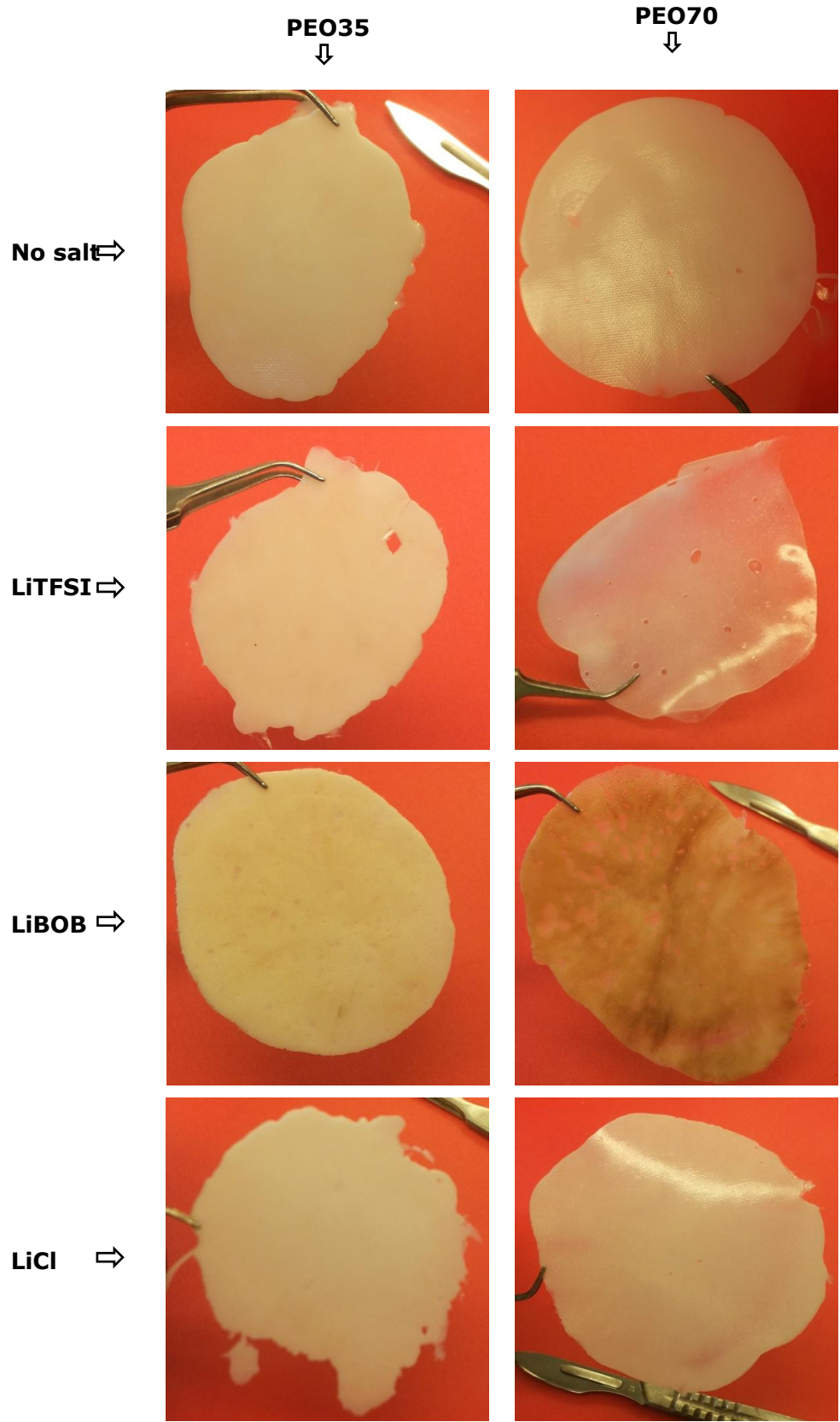


Figure 15 Matrix of samples prepared through melt-mixing. The salt and the type of polymer are indicated respectively to the left and on the top of the figure.

Another important feature is the different colour of the samples containing LiBOB. Shortly after the melting starts the sample starts to change from white to yellowish and easily turns to brown. Also small bubbles form while in the molten state and the sample puffs up. Any oxidation process due to oxygen may be excluded since the procedure takes place in an oxygen free environment, but such symptoms may be ascribed to some kind of chemical reaction that is yet unknown. According to the literature review LiBOB is stable to 302°C, so no decomposition should take place. Also such a behaviour does not emerge in other experiments reported in literature that perform melt mixing or hot pressing with LiBOB. But such experimental work is always performed with pure PEO, therefore melting takes place at a much lower temperature and this makes such examples not really comparable with what has been done with the DSM polymers. Moreover the LiBOB containing samples also yielded interesting DSC measurements, so more thought to this phenomenon will be given in chapter 3.2.

What is important to obtain in such a process is a good degree of homogeneity: the salt should be evenly distributed within the polymeric matrix. While stirring different behaviours of salt dispersion were noticed. Apart from the aforementioned difficulty in stirring the PEO35 samples due to their extreme viscosity, also the different salts behave differently in contact with the molten polymer.

LiTFSI appeared to mix quite easily and the disks of polymer+salt material do not show any inhomogeneity visible to the naked eye if observed against a strong light. Although LiTFSI is reported to be stable up to 360°C, its melting temperature is reported to be 236°C, therefore below the temperature set on the heating plate. If LiTFSI indeed melts during the melt-mixing procedure, this could improve the miscibility of the salt and the polymer.

LiBOB integration in the polymeric matrix proved to be harder because the melt was more viscous and would not easily flow when stirred, especially when PEO35 was used. Furthermore the peculiar look and colour of the sample do not allow to easily conclude anything regarding the homogeneity of the mix.

LiCl showed yet another behaviour: while mixing, the salt seemed to evenly stick to the molten polymer, but did not seem to be incorporated easily. Quite some mixing and “folding” of the melt was needed to disperse the salt. Once cooled the disk containing PEO35 seemed quite homogeneous, while in the sample with PEO70 (more thin and transparent) homogeneously dispersed little white dots were to be seen when observing the sample against a strong light. With the naked eye it is hard to determine if these are just small bubbles (due to trapped argon while mixing and solidifying, this is visible also in other samples) or if such dots are actually small salt crystals. In some cases sharp edges or angles can be seen in such dots, and this would confirm that they are crystal grains because a bubble would show no angle. But observing such small details with a naked eye is very challenging, so it is hard to come to a conclusion. It would be thus useful to have an optical microscope available, but this not easily done within a glovebox.

A general remark is that guaranteeing good mixing and homogeneity is not easy in such a setup due to the high viscosity and the stickiness of the melt. The following step of hot pressing allows for a better distribution of the salt within the polymeric matrix, but it may be thought to use a kneader in the future. Small kneaders are available and would be adequate to be used within the glovebox, as are also small extruders. If the melt-mixing procedure yields any kind of interesting result, such apparatus may be considered in the future for improved results.

3.1.2 Samples produced through water soaking

The final disks (fig. 16) were very similar looking to the ones obtained by melt-mixing.

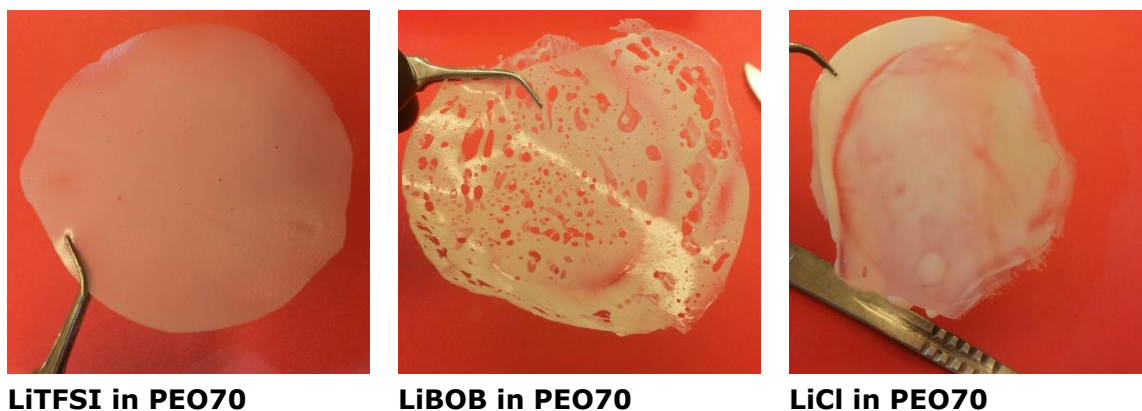


Figure 16 Samples prepared through water soaking.

The LiBOB-containing sample is indeed a bit darker, just as had happened with the melt-mixing but the phenomenon is in this case less evident because the material was heated for less time since mixing was not necessary.

Remarks

The procedure of water soaking is remarkably easy to perform and avoids the difficulties that arise in trying to mix the very viscous melt. The final heating step not only allows for a thin disk of material, but also for some additional temperature enhanced diffusion time. The salt that entered the pellets should therefore be quite well distributed.

What was interesting to notice is that after drying the pellets in the vacuum oven some were partially stuck to the base of the glass jar. Furthermore small residues were visible, thus indicating that not all the salt managed to enter the pellets. This can be seen clearly in figure 17.

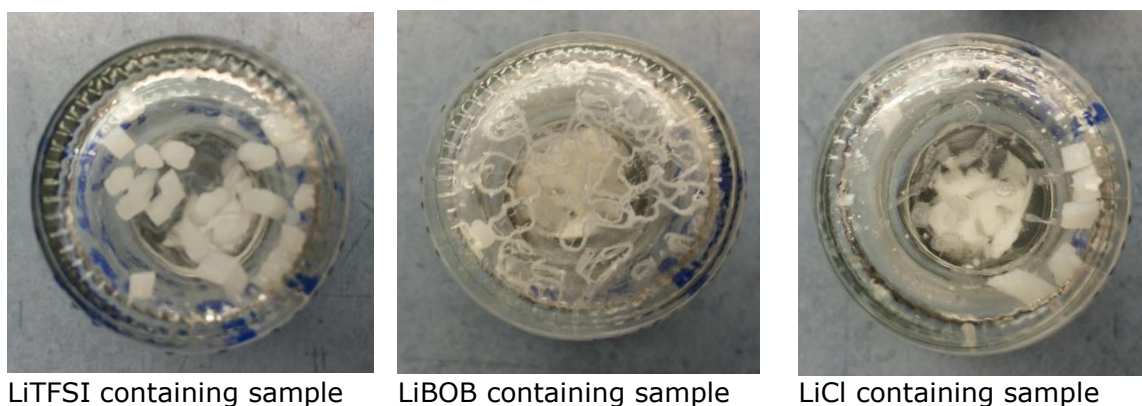


Figure 17 Deposits on the jar bottom after drying the soaked pellets. Some pellets are still encrusted, but removable by tapping the jar.

In order to know how much salt actually was absorbed in the polymer pellets, a mass comparison was measured. The mass of salt and of polymer initially weighed in the glovebox were compared with the weight of the pellets before melting (thus water free in both cases because dried and stored in the glovebox). There is no reason to think that the mass of the polymer would have changed, so the mass loss is only ascribed to the partial loss of salt. Such mass data is showed in table 14 and indicates that the mass loss is quite small compared to the considered masses of salt and polymer.

		LiTFSI sample	LiBOB sample	LiCl sample
Masses before water soaking	Salt	250 mg	167 mg	40 mg
	Polymer	1,09 g	1,08 g	1,19 g
	Total sum	1,340 g	1,247 g	1,230 g
Masses after water soaking and drying	Total	1,332 g	1,230 g	1,229 g
	Polymer	1,09 g	1,08 g	1,19 g
	Salt	242 mg	150 mg	39 mg
Salt mass loss		3,2%	10,2%	2,5%

Table 14 Mass balance of salt and polymer pellets before and after soaking

It may therefore be concluded by such mass balance that most of the salt has been inserted into the polymer pellets, although its diffusion through the polymeric chains is unknown.

Furthermore it may be noted that the highest salt loss occurs in the case of LiBOB. This seems to be also evident from the fig. 17. This could be related to the fact that the solution of LiBOB was the most concentrated (see table 10) out of the three: this may have modified the absorption capability of the solution into the polymer pellets. Such loss of salt must be kept in mind in the future when performing any type of measurement, as the final EO:Li⁺ is less than 20. If the water soaking method will be repeated in the course of the project an improved and more controlled procedure should be thought of. The quantity of water could be kept fixed or the molarity of the solution could be the fixed parameter. What is also important is to guarantee the complete soaking of the pellets, but at the same time there should not be excessive solution as the PEO70 has a water uptake of 132%, so any excess of solution would surely lead to an incomplete absorption of the salt. For this reason the shape and geometry of the container used for such soaking must also be kept in mind.

If future measurements reveal that such method to incorporate the salt in the polymer works, it may be certainly considered to increase the salt concentration and evaluate its effect.

From a broader perspective, a very relevant and fundamental issue must be considered when preparing samples with such a method: lithium salts in water may react and new chemical bonds may form. It will therefore be interesting in the future to determine what compounds have actually been incorporated in the polymeric matrix. To this purpose infrared spectroscopy (IR) or Raman spectroscopy could be used for example. In this initial phase it was deemed better to try such water dissolution of the salt, leaving further investigation for when the first electrochemical results will be available.

3.1.3 Samples produced through thin film soaking

Samples produced through thin film soaking on copper foil had simply the appearance of thin copper foil, with the polymer thin film not being in anyway visible as it is transparent and well adherent when dried on the metal foil.

This method proved to be an extremely easy and direct way to produce in only one step a polymer thin film containing the Li salt and guarantees a good contact with one of the electrodes (Cu in this case). With the hot pressing methods described previously it would not be possible to obtain such thin electrolytes. On the other hand, with this procedure it is not possible to exactly be aware of the salt concentration in the polymer, because the evaporation of the liquid may leave areas with higher salt concentration. If it is assumed that the salt is evenly incorporated in the polymer throughout the entire surface polymer surface, a EO:Li⁺ of approximately 12 and 20 is found for sample TF1 and TF2 respectively, but the assumption of uniform salt distribution is strongly debatable. Please refer to Appendix B for description of such estimation.

While the aqueous solution dries, the polymer film tends to create creases and small bubbles between the metal foil and the polymer film tend to form. It proves therefore challenging to obtain a wide satisfactory sample area. If this method will be considered in the future, a system for keeping the polymer film taut over the copper foil just be devised. Out of the entire sample surface only a small region was sufficiently smooth to be used. This region was cut out and then underwent impedance measurements. The conductivity of the samples prepared in such manner was measured as described in chapter 2.4.1.

3.1.4 Hot pressed samples

Samples that underwent hot pressing form two separate sample series as described in chapter 2.2.4: the first samples, part of the HP series, were hot pressed in the cylindrical die set between PTFE disks, while the samples belonging to the PC series were produced by performing the hot pressing procedure in the custom-made press-cells. As the procedure and the results differ, they are presented separately, following the chronological order of sample production.

HP series

The samples prepared through the hot pressing procedure in the conventional cylindrical die-set appear to be slightly translucent and whitish in color. No inhomogeneity in color was to be seen. As can be seen in the figure below, free standing thin electrolyte membranes were thus successfully produced by means of a solvent-free route (fig. 18).

The samples proved to be satisfactory for the first trials, but presented irregular surfaces and thicknesses. Furthermore, as the figure below shows, the sample do not have a well-defined geometry or neat edges. These effects are to be ascribed to the PTFE disks that at such temperature and pressure also are very flexible and cannot guarantee a smooth and perfectly flat surface.



Fig. 18 One of the samples obtained by hot pressing in the cylindrical die set

Initially a micrometer was not available, therefore the thickness was estimated knowing the density of the material and the mass of the sample. Such calculations are shown in Appendix C, while table 15 summarizes the resulting thickness values.

Sample name	Composition	Preparation method (prior to hot pressing)	Estimated thickness [μm]
HP1	PEO 70 + LiTFSI E0:Li ⁺ =20	Melt-mixing	128
HP2	PEO 70 + LiTFSI E0:Li ⁺ =20	Melt-mixing	184
HP3	PEO 70 + LiTFSI E0:Li ⁺ =10	Melt-mixing	179
HP4	PEO 70 + LiTFSI E0:Li ⁺ =20	Water soaked	101
HP5	PEO 70 + LiBOB E0:Li ⁺ =20	Melt-mixing	82
HP6	PEO 70 + LiCl E0:Li ⁺ =20	Melt-mixing	184

Table 15 Samples prepared through hot pressing in cylindrical die set (series HP)

PC series

The samples prepared through the hot pressing procedure in the custom-made press-cells also appear slightly whitish and translucent, similarly to the HP series. The drastic improvement in these sample is the well-defined geometry and the extremely smooth surfaces.

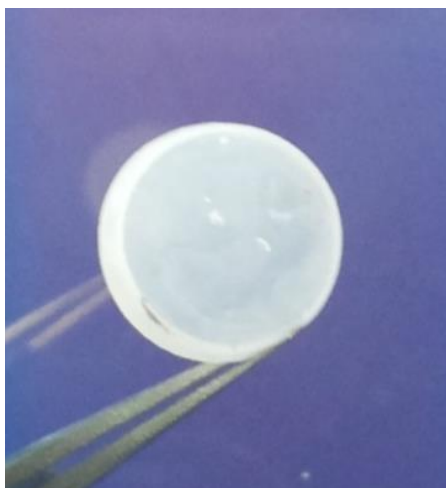


Figure 19 One of the samples obtained by hot pressing in the press-cell

Furthermore the production of these electrolyte disks proved to be much more straightforward than series HP because no PTFE foil was needed. Once the pressing system cooled down sufficiently, the press-cell could be opened and the electrolyte films proved to be very well adhered to the electrodes, but it was possible to peel it off without compromising their integrity.

The edges perpendicular to the plane of the membrane (visible in the figure above) are due to the accumulation of polymer in the spill-over zone of the press-cell due to applied pressure that squeezes out the excess polymer from the electrode area. These edges constitute no problem for the impedance measurements as such analysis takes place in the press-cell itself, but were later cut away with a surgeon knife for all further analysis as to obtain a sample with no protuberances.

The Peek spacers used in the press-cells were of approximately known thickness as explained in chapter 2.2.4, but the precise thickness of the obtained electrolyte membranes was later measured with a micrometre. It is in fact important to know such dimension as precisely as possible not only to characterize the membrane geometrically, but also to calculate the conductivity of the sample based on the impedance results. An overview of the measured thicknesses is shown in the table below.

Sample name	Composition	Preparation method (prior to hot pressing)	Measured thickness [μm]
PC1	PEO 70 + LiTFSI E0:Li ⁺ =20	Melt-mixing	200 μm
PC2	PEO 70 + LiTFSI E0:Li ⁺ =20	Melt-mixing	500 μm
PC3	PEO 70 + LiTFSI E0:Li ⁺ =20	Melt-mixing	202 μm
PC4	PEO 70 + LiTFSI E0:Li ⁺ =20	Water soaking	195 μm
PC5	PEO 70 + LiTFSI E0:Li ⁺ =10	Melt-mixing	168 μm
PC6	PEO 35 + LiTFSI E0:Li ⁺ =20	Melt-mixing	155 μm

Table 16 Samples prepared through hot pressing in the custom-made press-cells (series PC)

3.2 DSC results

The first analysis performed on the samples, both produced by melt-mixing and by water soaking, was differential scanning calorimetry (DSC) according to the settings described in chapter 2.3. The resulting thermal spectra are presented in the following chapters together with considerations and remarks. A comparison between the DSC plots of all samples is shown in fig. 20, while a summary table with the most important remarks can be found in the following page.

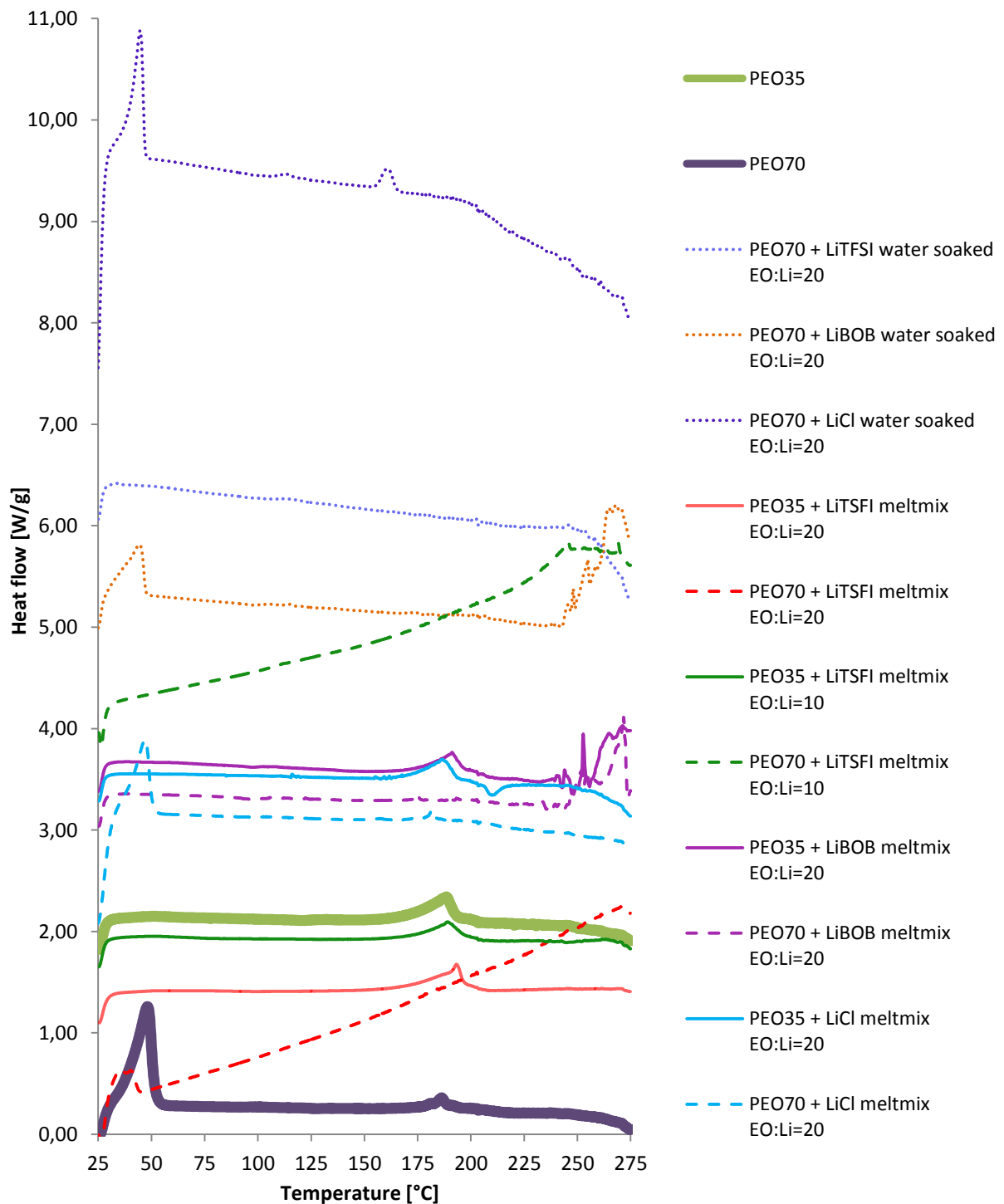


Figure 20 Comparison between the DSC plots of all analysed samples

In order to make the many plots more readable, the water soaked samples have been assigned a small-dashed line, the pure polymer samples are indicated with a thick marker and the samples that differ only in type of polymer (but not in salt or in EO:Li⁺ ratio) are marked in the same colour but the PEO70-containing sample is indicated with a broad dashed line. For separate graphs of each sample and exact peak positions please see Appendix D. This summary is meant as a concise comparison of all results.

Sample	Composition [polymer+salt] [EO:Li⁺/method]	Sample mass [mg]	Remarks on DSC cup	Remarks on measurement data
1	PEO35 + LiTFSI 20 / Melt-mixed	18,1		- Asymmetric peak at 193°C
2	PEO70 + LiTFSI 20 / Melt-mixed	5,8		- Diagonal slope - Small peak at low temperatures
3	PEO35 + LiTFSI 10 / Melt-mixed	12,1		- Peak at 189°C, less asymmetric than sample 1
4	PEO70 + LiTFSI 10 / Melt-mixed	5,7		- Dip above 25°C: recrystallization? - Diagonal slope
5	PEO35 + LiBOB 20 / Melt-mixed	6,9	Inflated	- Asymmetric peak at 191°C; - Discontinuous plot above 230°C
6	PEO70 + LiBOB 20 / Melt-mixed	7,5	Inflated	- Small peak at 175°C; - Small peaks at lower temperatures; - Discontinuous plot above 230°C
7	PEO35 + LiCl 20 / Melt-mixed	7,2		- Asymmetric peak at 186°C; - Recrystallization peak at 210°C
8	PEO70 + LiCl 20 / Melt-mixed	9,2		- Big peak at 47°C with shoulder; - Small peak at 181°C
9	PEO35 Melt	11,4		- Peak at 189°C, less asymmetric than sample 1; - Bumps at lower temperatures
10	PEO70 Melt	12,0		- Big peak at 48°C; - Smaller peak at 186°C with small shoulder
11	PEO70 + LiTFSI 20 / Water soaked	3,3		- Diagonal slope - Small bump at 125°C
12	PEO70 + LiBOB 20 / Water soaked	4,0	Inflated	- Big peak at 44°C with shoulder; - Discontinuous plot above 220°C
13	PEO70 + LiCl 20 / Water soaked	2,3		- Big peak at 44°C with shoulder - Small peak at 160°C

Table 17 Summary of DSC samples and main remarks

The collected data allows for some basic remarks and considerations to be made:

- Pure polymers, melt-mixed samples and water dissolved samples show all different spectra. The asymmetric peak at around 40-50°C seems to be due to PEO70, but does not appear in all the PEO70-based samples.
- LiBOB-containing samples clearly show some kind of reaction happening above 220°C and the DSC cups drastically increased in volume. Also during melting such samples showed some kind of reaction (bubbling, puffing up, change of colour; see chapter 3.1.4)
- Recrystallization happens in an evident manner only in one case that is sample 7.
- Diagonal slopes (samples 2, 4, 11) are of not clear interpretation, but the lack of peaks may indicate that no phase transitions are taking place.
- When a melting peak is visible, it seems always to appear between 175°C and 193°C, independently from the polymer or the salt used.
- The pure PEO35 and PEO70 samples show a peak at a similar temperature, respectively 189°C and 186°C. This is surprising because the melting temperature reported in the data sheet of the polymer PEO70 is 211°C, but this is not observed in the DSC measurements reported in this document.
- Asymmetric peaks may be related to simultaneous melting and recrystallization. This is possible in a di-block copolymer, and even more in presence of a third phase (the salt). Such asymmetric peaks are also found in the DSC plots of the pure material sent by DSM.
- A comparison between the PEO70+LiTFSI samples with EO:Li⁺ ratio of 10 and 20 (respectively the dotted green and red plots in fig. 20) allows to conclude that indeed no peak at low temperature is to be seen at the eutectic composition, as expected from the phase diagram presented in the literature overview.

What appears again evident, as was already pointed out in the previous chapter, is that LiBOB-containing samples seem to react in some way due to heating (please see the “Remarks” paragraph in chapter 2.2.1). Judging from the DSC results, reactions start occurring above ~230°C. Chemical investigation would therefore be needed to find out what reactions take place between the LiBOB and the PEO or the PBT at such temperature. This issue was considered out of the scope of the project and was therefore not investigated further.

From a quantitative data interpretation perspective it must be kept in mind that such DSC graphs plot the specific heat flow, therefore the heat flow divided by the mass of the sample in the DSC cup. Such mass is the sum of the polymer and the salt content. When analysing the peaks, it must be kept in mind that the peak height has no absolute meaning, as its value has been divided by the total sample mass, although the peak itself could be caused by only one of the phases. Therefore the most relevant and significant data is the position of the peaks rather than their relative or absolute height.

3.3 Electrochemical results

Electrochemical results are presented in this chapter and represent a central part of the work done during the course of the project. The results that follow answer the question whether the different combination of polymers and lithium salts and the different concentrations used lead to an ionically conductive system, adequate to be employed as solid state electrolyte for lithium batteries. Furthermore the stability window for some of the most relevant samples is presented. This allows to understand what electrode would be adequate to be used in combination with the obtained electrolyte and thus the maximum capacity of a hypothetical battery. The chapter is divided in to different sub-chapters, each one being dedicated to different types of electrochemical results.

3.3.1 Conductivity

Conductivity measurements were performed on a wide range of samples, in different setups and in different testing conditions (see chapter 2.4.1). For this reason the chapter is divided in different parts that group measurements performed with analogous procedures in order to allow for comparability of the results. What follows is presented in chronological order as to allow the reader to follow the development of the different systems and to accompany the reader through the choices that were taken throughout the project.

The first impedance measurements were performed on the HP series in the blocking cell at room temperature. The experiments allowed to make a selection of the best performing salt/polymer combinations.

The thin film electrolytes (TF series) were also tested in the blocking cell and these results represent the second part of the chapter. Next, measurements in the press-cells were conducted as soon as these were available. Only LiTFSI-containing samples were produced and tested for the PC series as this salt yielded the best room temperature conductivity from the blocking cell experiments. The use of the press-cells for conductivity measurements posed immediately the problem of adequate interface contact between the electrolyte and the electrodes. For this purpose the conductivity dependence on the applied pressure on the cell (and therefore the better contact) was investigated and is reported in a dedicated section of this chapter. Finally, once a standard procedure was settled for conductivity measurements in the press-cells, a series of measurements on LiTFSI-containing samples was performed as a function of temperature. Thus Arrhenius plots were obtained and are presented in the last part of this chapter.

Impedance in blocking cell – salt species and concentration effects in HP series

In this chapter a comparison between samples containing different salt species and concentrations is presented. The conductivity of the samples has been measured in the blocking cell as described in the dedicated chapter at room temperature. Fig. 21 shows the Nyquist plots obtained with such measurements, while table 18 contains the conductivity values calculated as previously described (see chapter 2.4.1).

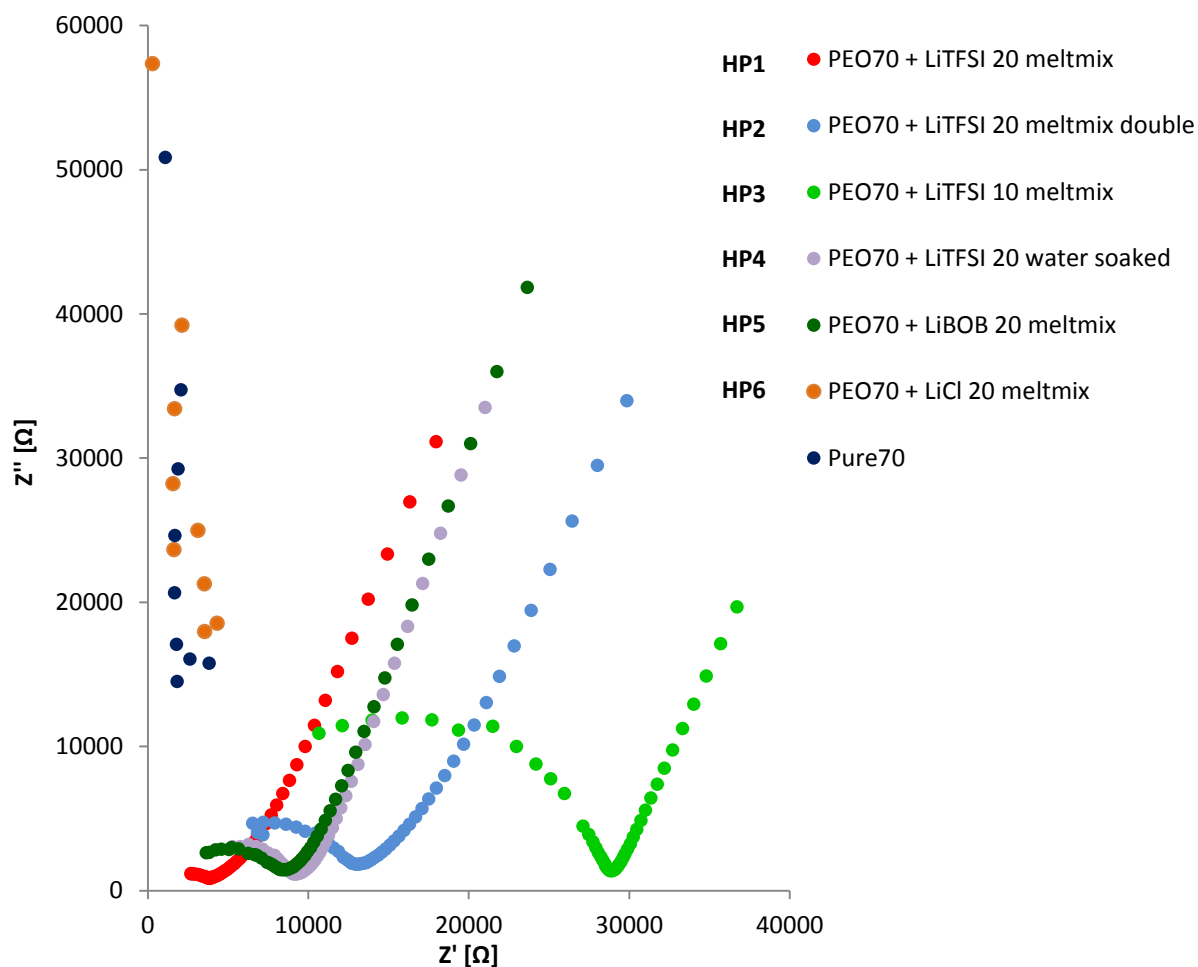


Figure 21 Comparison of Nyquist plots. Impedance measurements have been performed in the blocking cell.

A first general remark is that the impedance measurements revealed a very high fraction of the semicircle, although slightly depressed: this allows for easier fitting of the data and also indicates a good response of the system to high frequencies.

The samples that proved to be conductive were the ones containing LiTFSI and LiBOB. Conductivity values for these samples are shown in table 18. It is also important to remark that due to the uncertainty in the estimation of the sample thickness and active area, only the order of magnitude of the conductivity results is significant in this chapter.

The smallest semicircle (lowest resistance) is the red plot and represents the impedance measurement of sample HP1. Such sample contains LiTFSI in the EO:Li⁺ ratio of 20 and was prepared through melt-mixing. The calculated conductivity is in the order of 10^{-6} S/cm for this sample and can be considered a satisfactory result if compared with results available in literature for similar systems. Such first conductivity value was considered to be quite encouraging, especially considering that no optimization was done on the system. A similar result was obtained also for sample HP2 (in light blue in fig. 21), that is a thicker sample compared to HP1 but of the same material.

Sample name	Composition	Preparation method (prior to hot pressing)	Resistance [Ω]	Conductivity [S/cm]
HP1	PEO70 + LiTFSI EO:Li ⁺ =20	Melt-mixing	4315	$4,31 \cdot 10^{-6}$
HP2	PEO70 + LiTFSI EO:Li ⁺ =20	Melt-mixing	13244	$2,02 \cdot 10^{-6}$
HP3	PEO70 + LiTFSI EO:Li ⁺ =10	Melt-mixing	28042	$9,27 \cdot 10^{-7}$
HP4	PEO70 + LiTFSI EO:Li ⁺ =20	Water soaked	8845	$1,66 \cdot 10^{-6}$
HP5	PEO70 + LiBOB EO:Li ⁺ =20	Melt-mixing	8349	$1,64 \cdot 10^{-6}$
HP6	PEO70 + LiCl EO:Li ⁺ =20	Melt-mixing	Infinite	0

Table 18 Conductivities values calculated from the Nyquist plots in figure 21

A possible explanation for the lower conductivity of the thicker sample is the presence of an additional interface: HP2 sample was in fact produced by stacking two disks of material prior to hot pressing in order to achieve increased thickness. Since the hot pressing procedure does not reach the melting temperature of the material, an interface between the two pieces may have partially remained, thus hindering slightly the transportation of ions. The extrapolation of the resistance value was done as explained in Appendix E.

Sample HP3 (displayed in light green) also contains LiTFSI but the molar EO:Li⁺ ratio is 10, rather than 20 as in the previous two samples. This sample yielded a conductivity in the order of 10^{-7} S/cm (although the pre-factor brings the value almost one order of magnitude higher), therefore lower than the sample with a EO:Li⁺ ratio of 20. This result is surprising because, as explained in the first report, in the $6 < \text{EO:Li}^+ < 12$ range a crystallinity gap is expected according to the phase diagram. Conductivity is expected to increase with diminishing degree of crystallinity, but this is not what is encountered in the experiments here presented. Although the reasons for such discrepancy remain unclear, it has been decided to continue working on samples with a molar ratio of 20, as this seems to give the best conductivity results and because it is the standard molar ratio presented in literature for LiTFSI in PEO (more considerations on this topic at the end of this chapter).

Sample HP4 (showed in grey) has the same composition of sample HP1 and HP2, but differs in the processing: sample HP4 in fact was prepared through water soaking (see previous report). Such sample revealed a conductivity in the order of 10^{-6} S/cm, so just as high as the sample prepared via melt-mixing. This can be considered a very interesting result, as the two different methods of inserting the salt in the polymer appear to yield the same conductivity. The relevant doubt that

remains is whether such conductivity is ionic or electronic and whether the dissolution of the lithium salt in water leads to different chemical species. Further electrochemical testing will answer such questions. In the meantime such results can be considered very encouraging, especially considering the simplicity of using the polymer's high water uptake as means to insert the salt in the polymeric matrix.

Sample HP5 (in dark green in fig. 21) contains LiBOB and also shows a conductivity in the order of 10^{-6} S/cm, but due to the DSC data and to the darkening of the sample during melt-mixing (see chapters 3.1. and 3.2) it is possible that some unknown reaction between the polymer and the LiBOB had occurred at high temperature during melt-mixing and that such conductivity is electronic rather than ionic. Such high conductivity value thus does not at the moment represent any successful results.

The curve presented in dark blue refers to a pure PEO70 sample containing no lithium salt. This measurement was taken as a reference and in order to validate that the pure polymer has no conducting properties. It in fact can be seen that the blue data points form a vertical line that extends much more than what shown in the figure. Thus the system measured behaves as a capacitor and it may be concluded that indeed the pure polymer is an insulator.

The orange data points show a similar trend and refer to the PEO70 sample containing LiCl (sample HP6). It may be therefore concluded that this sample also behaves as an insulator even though it contains lithium salt. This was easily foreseeable for two reasons: the first is that after the melt-mixing process small crystals had been noticed in the sample. This already indicated that probably the salt had not been adequately dissolved during the procedure. Furthermore it must be recalled that in order to preserve the EO:Li⁺ ratio of 20, the mass ratio between the LiCl and the polymer was very low due to the very low molar weight of such simple salt. Such weight ratio could indeed be easily increased, but the visible small salt crystals seem to indicate that melt-mixing is not an adequate method to incorporate such salt in the polymer. For this reason no further experiments were conducted on the LiCl-containing sample prepared through such preparation route.

A comparison can be made between the results obtained in the work described up to here and internal DSM data: samples HP1, HP2 and HP5 have the same composition as Sample 02 of internal DSM data and the conductivities at room temperature differ by one order of magnitude, the latter exhibiting a conductivity of 10^{-5} S/cm while the former yield values in the order of 10^{-6} S/cm. Although an order of magnitude is a noticeable difference, it must also be kept in mind that the quality of the electrical contacts plays a fundamental role in such measurements. The system described above for impedance measurements is far from ideal and it is easy to imagine a drastic improvement in the conductivity values if better contact between the electrodes and the electrolyte could be guaranteed through applied pressure and smoother and cleaner interface surfaces. It is also for this purpose that the press-cells were designed, as to guarantee a smoother and more homogeneous electrolyte surface. As it will be shown in the next chapter, the improvement of such feature lead indeed to improvements in the conductivity, allowing for similar figures as the internal DSM data.

As a concluding remark, with the results presented up to this point, it was possible to affirm that both the melt-mixing procedure and the water soaking successfully achieve the goal of making the polymer conductive. Furthermore the most promising salt seems to be LiTFSI, as was already partially

anticipated after having prepared the different samples. In particular the EO:Li⁺ ratio of 20 seemed to yield the best conductivities values. For this reason it was decided to focus the experimental work on such salt for the following experiments.

Impedance in blocking cell – soaked thin films (TF series)

The impedance of the soaked thin films was measured in the blocking cell previously described. The complete system of thin film adherent to the copper foil was placed in the cell. The Nyquist plots obtained from these two experiments are shown below, while table 19 indicates the extrapolated resistance values together with the calculated conductivity values.

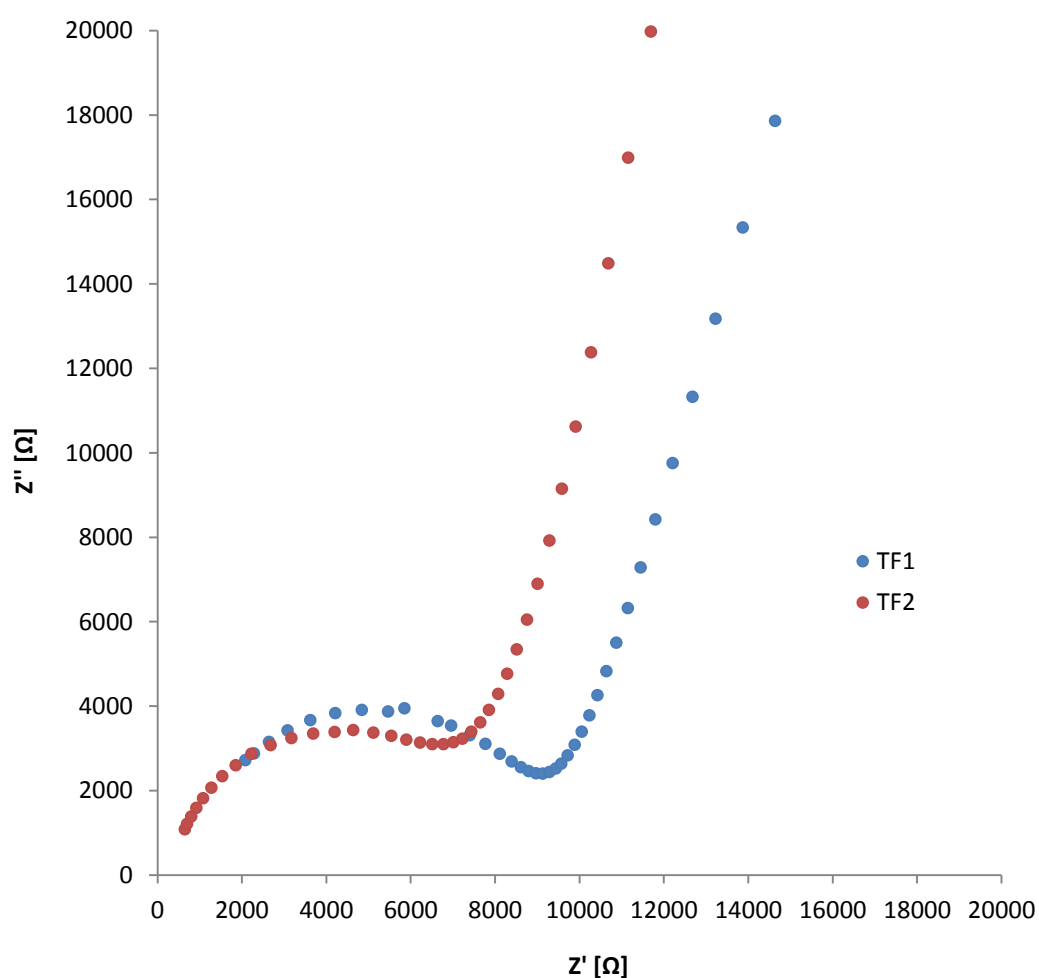


Figure 22 Nyquist plots of sample TF1 and TF2

The conductivity values are both in the order of 10^{-6} S/cm, although the proportion between salt and polymer is almost double in sample TF1 compared to TF2. This apparent independence of the measured conductivity from the EO:Li⁺ ratio may perhaps indicate there is a certain solubility limit for the LiTFSI in the PEO70 in aqueous environment, but the possibility of inhomogeneous salt concentration throughout the samples cannot be excluded, as explained in chapter 2.2.3. Because of such uncertainties it is difficult to draw conclusions.

What is though interesting to note is that these figures are an order of magnitude smaller than the equivalent hot pressed samples from the HP series, but it still proves that the sample is conductive. Reasons for lower conductivity may be ascribed to the unknown EO:Li⁺ ratio: as discussed in the dedicated chapter, it is currently not possible to precisely control the quantity of salt that is absorbed into the polymer. Furthermore the salt distribution through the thickness of the thin film may also be inhomogeneous as the diffusion coefficient of the ions in PEO and PBT structures is not known. Such disadvantages of this method of incorporating the lithium salt in the polymer could be overcome with further research and refinement of the procedure, but this was not considered the main goal of this project and these first trials can be considered a proof of concept.

Sample name	Composition	Preparation method	Resistance [Ω]	Conductivity [S/cm]
TF1	PEO70 + LiTFSI EO:Li ⁺ ≈12	Thin film soaking	8576	2,53·10 ⁻⁷
TF2	PEO70 + LiTFSI EO:Li ⁺ ≈20	Thin film soaking	9422	2,31·10 ⁻⁷

Table 19 Conductivities values of calculated from the Nyquist plots in figure 22

These results, together with the results of sample HP5, are sufficient to prove that there is potential in such a novel, simple, safe and cheap way of producing electrolyte material either from PEO70 thin films or pellets by taking advantage of the very high water uptake of the polymer.

Impedance in press cell – influence of pressure on contact quality (PC series)

The chapter is dedicated to the impedance measurements conducted directly on the press-cell introduced earlier in chapters 2.2.4 and 3.1.4. The most relevant feature that emerged during such measurements was the strong dependence between the measured resistance (and consequently the calculated conductivity) and the applied pressure on the press-cell while performing the measurement. As anticipated in chapter 2, two LiTFSI-containing samples, amongst others, were hot-pressed and measured in the press-cells: PC1 has a thickness of 200μm and surface area of 1cm², while PC2 has a thickness of 500μm and surface area of 2cm². Material and composition were instead the same for the two samples.

The Nyquist plots obtained for different applied pressures for sample PC2 are shown below. The relative conductivity values are instead shown in the table that follow. An analogous behaviour was observed for sample PC1, but the results are not shown for the sake of brevity.

Impedance measurements were initially performed on the press-cells without applying any pressure (referred to as 0 tons). The measurements that followed were repeated applying an increasing amount of pressure by means of a hand press in steps of half a ton at the time. As for the previous results, please refer to Appendix E for details regarding the extrapolation of the resistance value from the Nyquist plot.

The remarkable effect of the applied pressure on the measured conductivity can be visually noticed by the shift and shrinkage of the semicircles in the Nyquist plots as the applied pressure increases. The conductivity values presented in the table reveal in fact changes in terms of one order of magnitude, passing from 10^{-6} S/cm to 10^{-5} S/cm when the system is subjected to 1,5 tons of pressure.

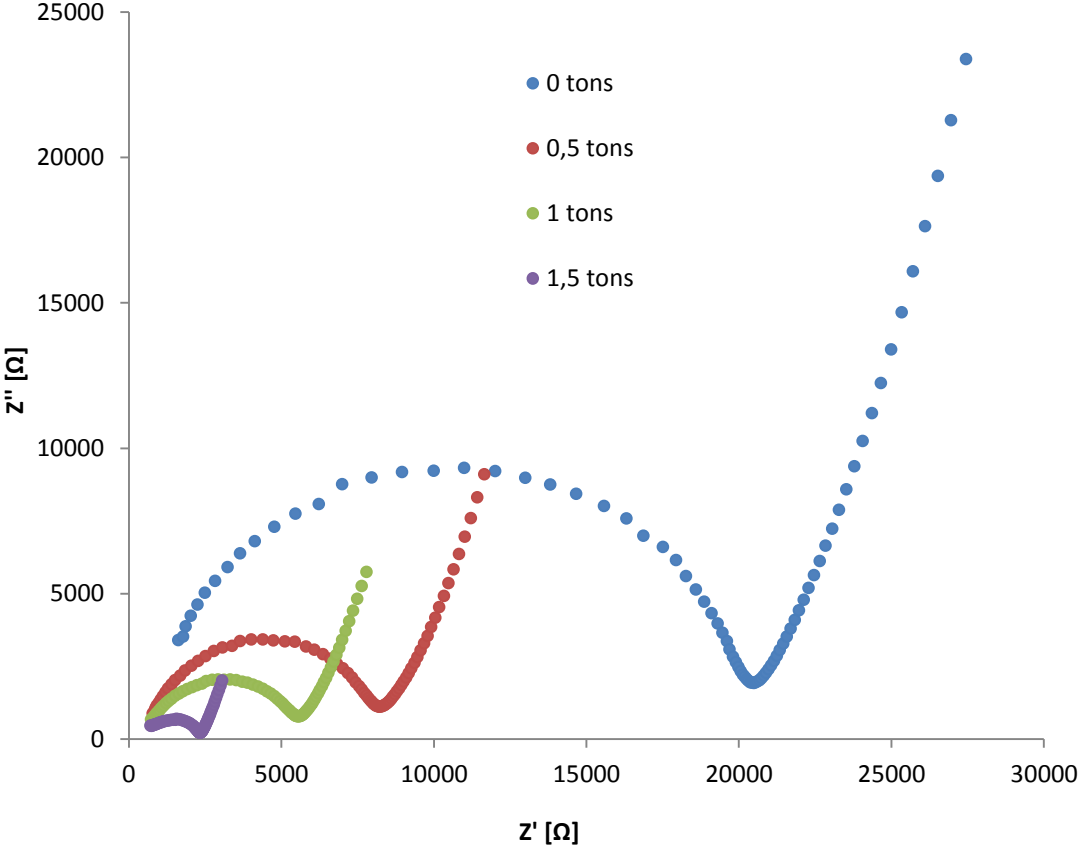


Figure 23 Nyquist plots of sample PC2 as a function of applied pressure

Applied pressure [tons]	R [Ω]	σ [S/cm]
0	20380	$1,23 \cdot 10^{-6}$
0,5	8235	$3,04 \cdot 10^{-6}$
1	5718	$4,37 \cdot 10^{-6}$
1,5	2418	$1,03 \cdot 10^{-5}$

Table 20 Conductivities values as function of applied pressure calculated from the Nyquist plots in figure 23

The results shown here clearly reconfirm the importance of good electrical contacts at the interfaces when performing conductivity measurements. By applying 1,5 tons on the system conductivity reaches 10^{-5} S/cm, in the same order of magnitude as the internal DSM results previously presented. Considering that the sample is of nominally the same composition as sample HP1 and HP2, the difference can only be ascribed to the measurement setup, i.e. the applied pressure, and not to

chemical differences. From the noticeable shrinkage of the semicircles in the figure above, the temptation of further increasing the applied pressure in order to improve the conductivity values may arise. Furthermore it would be interesting to reach a certain plateau for which a pressure increase does not yield improved conductivity: this would indicate that the best possible contact for the system has been achieved. The reason for not doing so is that the Peek separator in the press-cell should not deform as to not alter the predefined thickness of the sample. Peek has a Young modulus of 3,6 GPa, therefore applying a mass of 1,5 ton on its surface of approximately 1000 mm² leads to a deformation of only a fraction of a point percentage. Therefore such pressure has been considered a safe limit for performing the measurement.

It should though remain clear that such testing conditions are still not ideal and that conductivity values may further improve if an optimized system were to be employed. To this purpose it had been proposed to coat the sample with gold through sputtering in order to follow the standard sample preparation used by DSM for impedance measurements. Another option that was thought of was to paint the samples with a silver-containing epoxy resin. Because of organizational complications and time constraints this was not done, but should be definitely kept in mind as a further refinement step when trying to measure the most realistic conductivity value.

The experiments described above allowed to define a fixed procedure for impedance measurements in order to standardize experiments and allow for reproducible, consistent and comparable results. Please refer to chapter 2.4.1 for the description of such procedure that was used to obtain the results presented in the section that follows.

Impedance in press cell – Arrhenius plots of most relevant samples (PC series)

After the different impedance measurements presented above, the samples that proved to be most interesting were PC3, PC4, PC and PC6 (see composition in table below). The choice of these samples finds its grounds in the following facts:

- LiTFSI was the salt that yielded the highest conductivity according to the first sample overview presented in table 16. LiCl did not seem to dissolve properly as reported in 3.1.1 and in fact did not yield any conductivity. The sample containing LiBOB on the contrary showed very good conductivity but, due to the colour change during melt-mixing and to the irregular DSC plot at high processing temperatures, was discarded. For this reason only LiTFSI-containing samples were chosen.
- Both the melt-mixed sample and the water soaked sample were chosen because they both showed very encouraging results in terms of conductivity. Furthermore both production methods represent novel work and the procedures show potential deriving from the simplicity and the lack of solvent needed as examples of the many advantages.
- The LiTFSI containing sample with a molar EO:Li⁺ ratio was chosen although it shows a lower conductivity compared to the sample with a molar ratio of 20. This choice was taken as to allow for a complete comparison among samples with different compositions.
- The PEO35-containing sample was the least conductive out of the samples measured at room temperature (explainable with its lower “active material”, i.e. PEO, content), but it was considered still worth further investigation as the higher ratio of hard block in the polymer may

lead to other advantages such as increased resistance to higher operational temperatures and ability to hinder dendrite growth.

Sample name	Composition	Preparation method (prior to hot pressing)	Measured thickness [μm]
PC3	PEO 70 + LiTFSI E0:Li ⁺ =20	Melt-mixing	202 μm
PC4	PEO 70 + LiTFSI E0:Li ⁺ =20	Water soaking	195 μm
PC5	PEO 70 + LiTFSI E0:Li ⁺ =10	Melt-mixing	168 μm
PC6	PEO 35 + LiTFSI E0:Li ⁺ =20	Melt-mixing	155 μm

Table 21 Samples for which conductivity was measured as function of temperature in the press-cells. These are also the samples on which all remaining measurements were performed such as cyclic voltammetry and electroplating.

In this chapter only the Nyquist plots for PC5 is shown for brevity, the analogous plots for the three remaining samples are to be found in Appendix F. The obtained Arrhenius plots are instead reported here for all four samples in figure 25.

The Nyquist plots in the figure below nicely illustrate the effect of temperature on conductivity and the different response of the system for the range of frequencies. As expected the intersection with the horizontal axis, i.e. the resistance of the sample, shifts towards higher values as the temperature is progressively decreased. At the higher temperatures the conductivity is such that diffusion dominates even at the higher frequencies and therefore only a smooth diagonal plot is measured. In this case the intersection of the plot with the real axis is taken as the resistance value, without any kind of fitting as no further information is required.

As the temperature decreases an increasing portion of the semicircle due to kinetic processes is visible: for high frequencies (lower Z' values on the plot) polarization is the limiting factor as the ions are not able to polarize at such frequency as imposed by the measurement device. In this case the semicircle was fitted with a simple geometrical semicircle fit and the interception of such curve with the horizontal axis was taken as the resistance value (please refer to the appendixes for more detailed explanation on extrapolation).

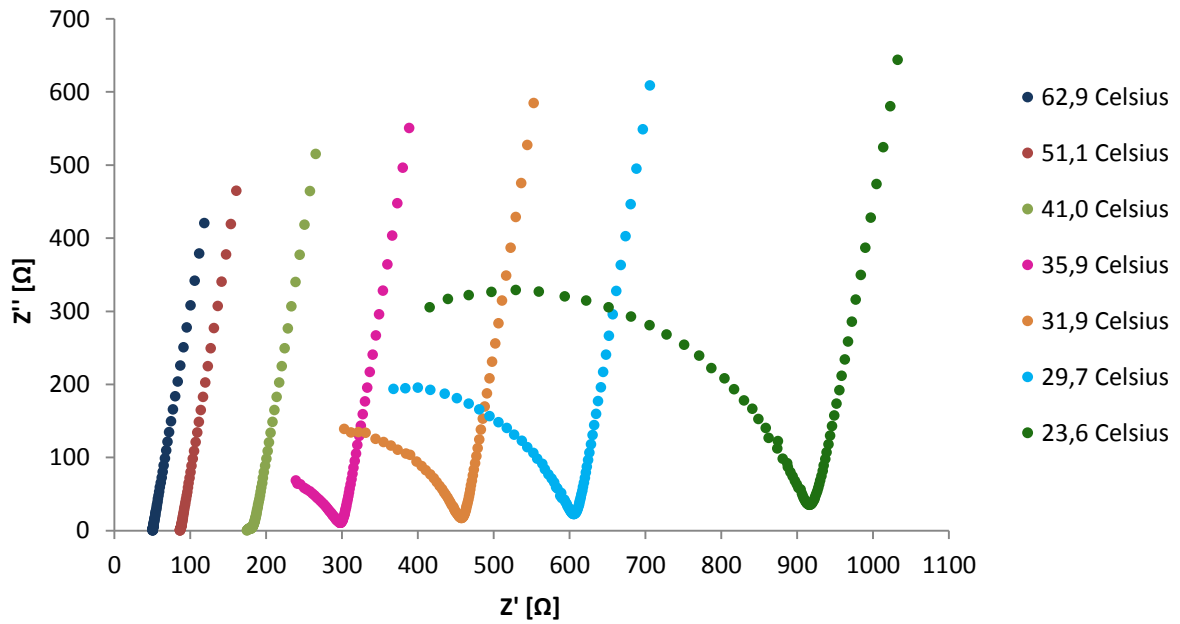


Figure 24 Nyquist plots at different temperatures of sample PC5

From the extrapolated resistance values for each temperature the conductivity of the sample was calculated and then plotted on a semi-logarithmic plot vs. the inverse of temperature. In this way it is possible to obtain the Arrhenius plots for all the samples as presented in the figure below.

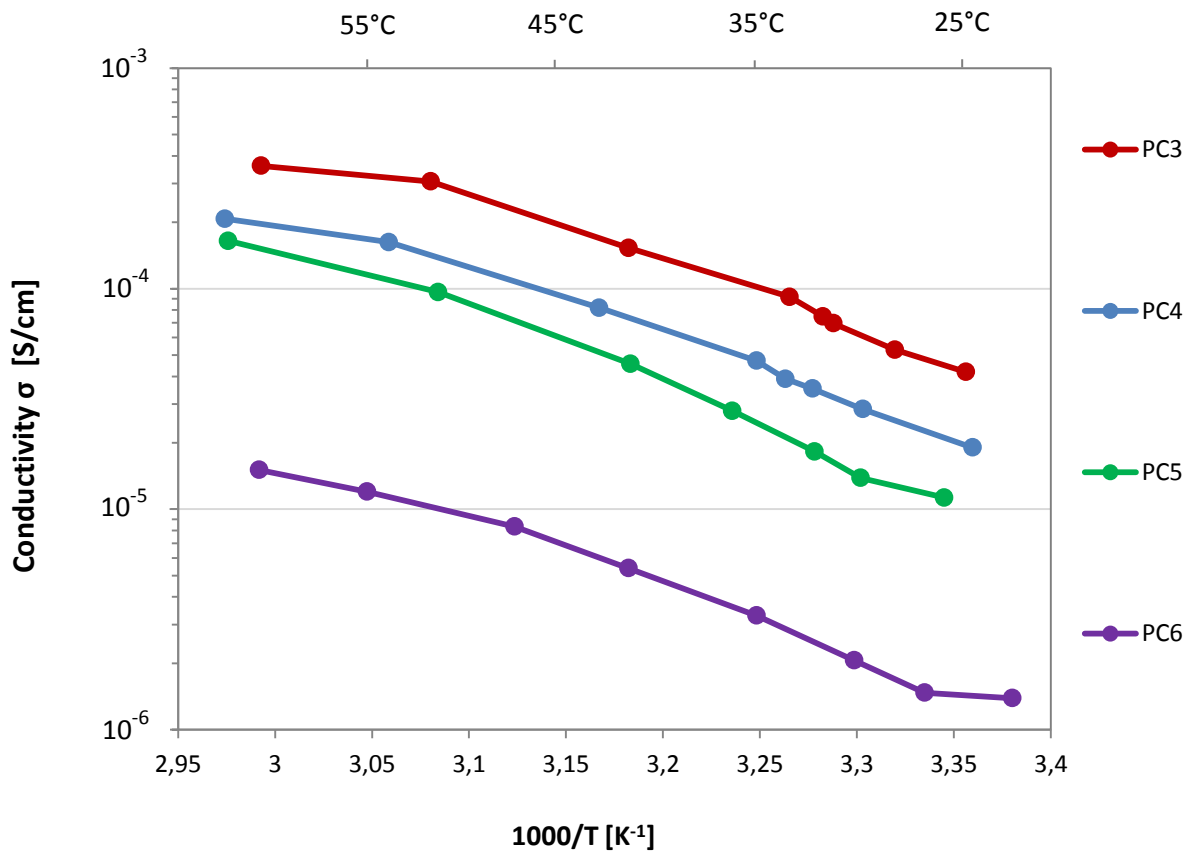


Figure 25 Arrhenius plots of most relevant samples (see table 17)

A first important consideration to be made is that conductivity increases with temperature and seems to follow a thermally activated process. Such conductivity behaviour is characteristic for ionic conductivity: electronic conductivity in fact shows an opposite temperature dependence, as it decreases for increasing temperature.

The Arrhenius plots of the four samples run almost parallel to each other in the considered temperature range, without crossings. It is therefore possible to state that the conductivity of sample PC3 (PEO70+LiTFSI 20 meltmix) is the best over the whole temperature window from room temperature to approximately 65°C. Samples PC4 (PEO70+LiTFSI 20 watersoaked), PC5 (PEO70+LiTFSI 10 meltmix) and PC6 (PEO35+LiTFSI 20 meltmix) follow in terms of decreased conductivity values. At room temperature all samples containing PEO70 (PC3, PC4 and PC5) show conductivity values in the order of 10^{-5} S/cm, while the sample containing PEO35 (sample PC6) yields one order of magnitude less in terms of conductivity. This is to be expected, as the PEO35 contains less PEO and therefore an overall lower charge carrier concentration.

What instead is counterintuitive is the lower conductivity of sample PC5: from the literature review presented in chapter 1.3 a conductivity improvement was expected for the EO:Li⁺ ratio of 10 compared to the ratio of 20 due to the crystallinity gap that forms in the phase diagram of PEO and LiTFSI. Decreased crystallinity of the PEO70+LiTFSI 10 meltmix compared to PEO70+LiTFSI 20 meltmix was indeed confirmed by the DSC results presented in chapter 3.2. The reason why the sample PC5 yielded lower conductivity can perhaps be explained by phase segregation: Marzantowicz *et al.* (31) in fact report coexistence of crystalline phases of pure PEO and amorphous PEO₆:LiTFSI in the eutectic region. This would explain the decrease in conductivity in compositions close to the eutectic system. Indeed the EO:Li⁺ ratio of 20 seems to be common practice in literature.

Another very important feature that emerges from fig. 25 is that the sample produced by watersoaking (sample PC4) is highly conductive and comparable to the equivalent melt-mixed sample PC3. As discussed in chapter 3.1.2, the water soaked sample actually has a slightly lower salt content than the melt-mixed, so slight variations in the measured conductivity may also be ascribed to this. Such comparable conductivity values indicate that both the methods of salt insertion in the polymer matrix lead to equivalent results. This is a very important finding, especially considering their potential for eventual industrial up-scale. A comparison with internal DSM data shows in fact that samples produced through the traditional solvent route (involving HFIP) yield the same conductivity results as the sample produced during this graduation project by alternative routes such as melt-mixing and watersoaking. The negative consequences of using HFIP have already been pointed out in chapter 1.3 and make the alternative routes proposed in this work very attractive. As will be discussed in the remaining subchapters, the samples prepared through melt-mixing and water soaking show very similar results to internal DSM data. The different preparation methods therefore seem to give equivalent results from the aspects considered in this work.

From a comparison with results available in literature on PEO+LiTFSI sample with EO:Li⁺=20, a net superiority of the conductivity values obtained from DSM Arnitel material appears evident. While conductivity values are reported both in this work and in internal DSM data as values in the order of 10^{-5} S/cm at room temperature, conductivity in the order of 10^{-7} - 10^{-6} S/cm is reported in literature for equivalent systems that do not involve the use of plasticizers, inorganic nanoparticles or any type of conductivity enhancer (26) (27) (32) (33). Apparently the hard block of the Arnitel materials, i.e.

the PBT, has a drastic positive influence on the conductivity, although “inactive” from a ion transport perspective. This positive influence may be due to a decrease in crystallinity in the “active” PEO.

From the Arrhenius plots presented in fig. 25 some considerations on fitting are also presented. Fitting the experimental data in fact enables the calculation of the activation energy for the conduction process and therefore allows a quantification of the ease with which the ions move through the electrolyte. The ionic conduction can be analysed in terms of the Arrhenius law for thermally activated processes:

$$\sigma = \sigma_0 \cdot e^{-\frac{E}{kT}} \quad \text{Equation 5}$$

where σ is the conductivity, σ_0 is an ideal conductivity at infinite temperature, E is the conduction process activation energy, k is Boltzmann’s constant and T is the absolute temperature.

The table that follows summarizes the activation energy obtained for the four samples (complete results, calculations and comparison with another fitting model are presented in Appendix G).

Sample	Activation energy for ionic conduction [eV]
PC3	0,62
PC4	0,55
PC5	0,66
PC6	0,57

Table 22 Calculated activation energies for ionic conduction

The activation energy values found are in the expected order of magnitude. An activation energy of 0,37 eV is reported by Shin *et al.* (34) on a system of PEO and LiTFSI with a molar ratio EO:Li⁺ of 20: the difference between this value and the one reported in table 22 can be ascribed to the presence of the PBT in the Arnitel copolymers. A direct comparison is not made with the equivalent internal DSM data as the reported activation energies appear too low to be realistic: a value of 0,06eV is reported, but this would entail even superior conductivity than crystalline electrolytes that are in general known to pose a lower energy barrier to the motion of lithium ions. Therefore no comparison is made with this data.

It must be also noted that the activation energies summarized in table 22 do not follow the trend of conductivity values: sample PC3 for example had the highest conductivity over the entire temperature range, but does not yield the lowest activation energy. It must, however, be noted that the error in the calculation of the activation energies may also be the reason for such discrepancies (for details on the precision of the fit and on the calculations please refer to Appendix G).

3.3.2 Stability window

The cyclic voltammetry scans of samples PC3, PC4, PC5 and PC6 at room temperature are presented in figure 26 (individual plots are to be found in Appendix H). A reminder of the composition and preparation procedure for each sample is also given in the figure. The CV scans took place over two cycles and it must be noted that in all cases the second cycle shows the same trend as the first one, but with less intense currents. This may be ascribed to the formation of passivating layers that slightly increase the resistance at the interfaces. The four plots of the four samples vary quite significantly in terms of peak intensity, but overall show many features in common. All samples seem to be fairly stable in the higher voltage region, revealing weak oxidative peaks only above 4-4,5V. For lower voltages instead all samples show a more marked negative peak starting between 1 and 1,5V. These current peaks probably indicate reductive processes and reactions between the polymer electrolyte and the lithium metal and most likely cannot be ascribed to lithium plating. If lithium plating were taking place the peaks should be located around 0V (or slightly lower considering possible over potentials) and would be much sharper. Furthermore, if lithium were being plated, lithium stripping would necessarily take place on the return scan at approximately voltages just above 0V (again some over potential would be expected as stripping of lithium is more hindered than the plating process). No such peak on the return scan can instead be seen. It may be concluded therefore that no lithium plating and stripping is taking place at room temperature, but there are definitely ongoing reactions leading to the conclusion that the electrolyte and the lithium metal are involved in degradation processes. The lack of evidence of lithium plating and stripping cannot be ascribed to low conductivity as the conductivity measurements proved on the contrary very good conductivity even at room temperature (please see previous chapter). It must be noted however that the interface contact between the electrodes and the electrolyte in the setup used for CV experiments was not nearly as good as in the press-cell used for impedance measurements (please refer to chapter 2.4.1 and 2.4.2).

Very similar CV results are reported in internal DSM data for which samples were prepared with the same salt and polymers, in the same concentration but with a different preparation method. For the internal DSM experiments the salts were in fact introduced in the Arnitel material by using HFIP solvent. Therefore such electrochemically instable behaviour is not to be ascribed to the solvent-free routes proposed in this graduation work but to the inherent characteristics of the materials. The stability issues between PEO electrolytes and lithium metal turns out to be a known problem in literature: Croce et al. (35) state for example that PEO-LiX electrolytes are not stable in contact with a lithium electrode and report about the “interfacial stabilizing” effect of inorganic fillers that has also been reported by other groups. It appears therefore reasonable that the CV measurements performed during the course of this project indicate instability at the interface.

Further experiments were carried out to verify whether any lithium plating is taking place, perhaps covered by dominating degradation processes. These results are presented and discussed in the following chapter and suggested that there may be a kinetic barrier for the lithium ion swapping from one electrode to other. For this reason another set of CV scans were performed at 45°C. The reason for choosing this temperature will be appear clear in the following chapter. Such results are shown in fig. 27. As may be expected, the peak currents are higher than those found at room temperature and this is related to the improved conductivity. Overall samples PC3, PC5 and PC6 do

not reveal any novel feature compared to the room temperature measurements. Sample PC4, produced by water soaking and plotted in red, instead shows a distinct peak at approximately 0,2 V. This peak could strongly suggest that lithium is actually being stripped from the cathode, but no evidence of this is shown by the discharge curves on this sample shown in the next chapter. This peak therefore may not be considered as proof of successful lithium stripping.

As a concluding note it is important to remark that all these measurements, as the impedance measurements, were performed only on one sample per type due to lack of time and experimental complications. Therefore no statistics in such results is available and this implies that differentiation between an actual characteristic behaviour of the sample and random errors is nearly impossible.

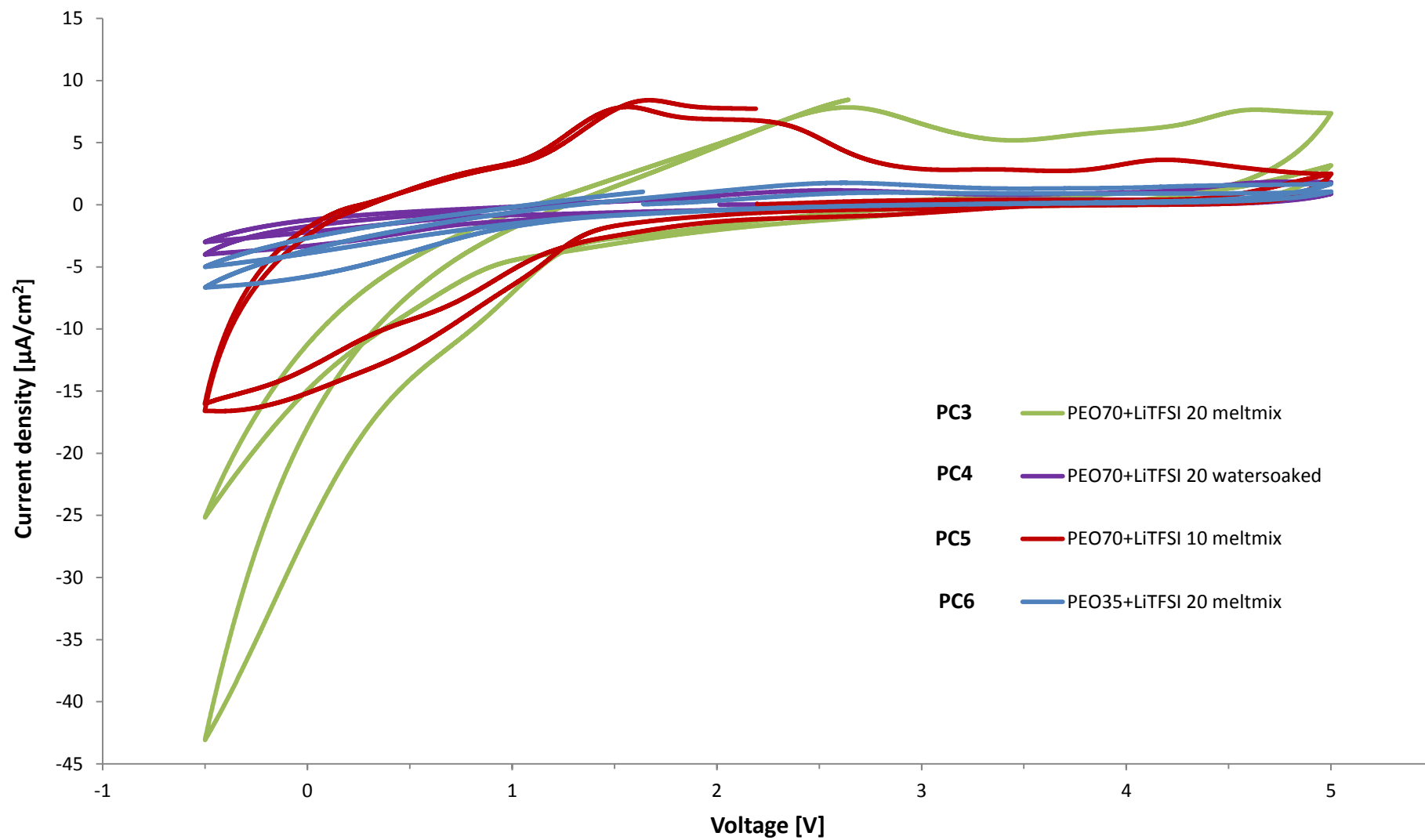


Figure 26 Cyclic voltammetry (CV) scans performed at room temperature. Each sample has been scanned twice in the same voltage range.

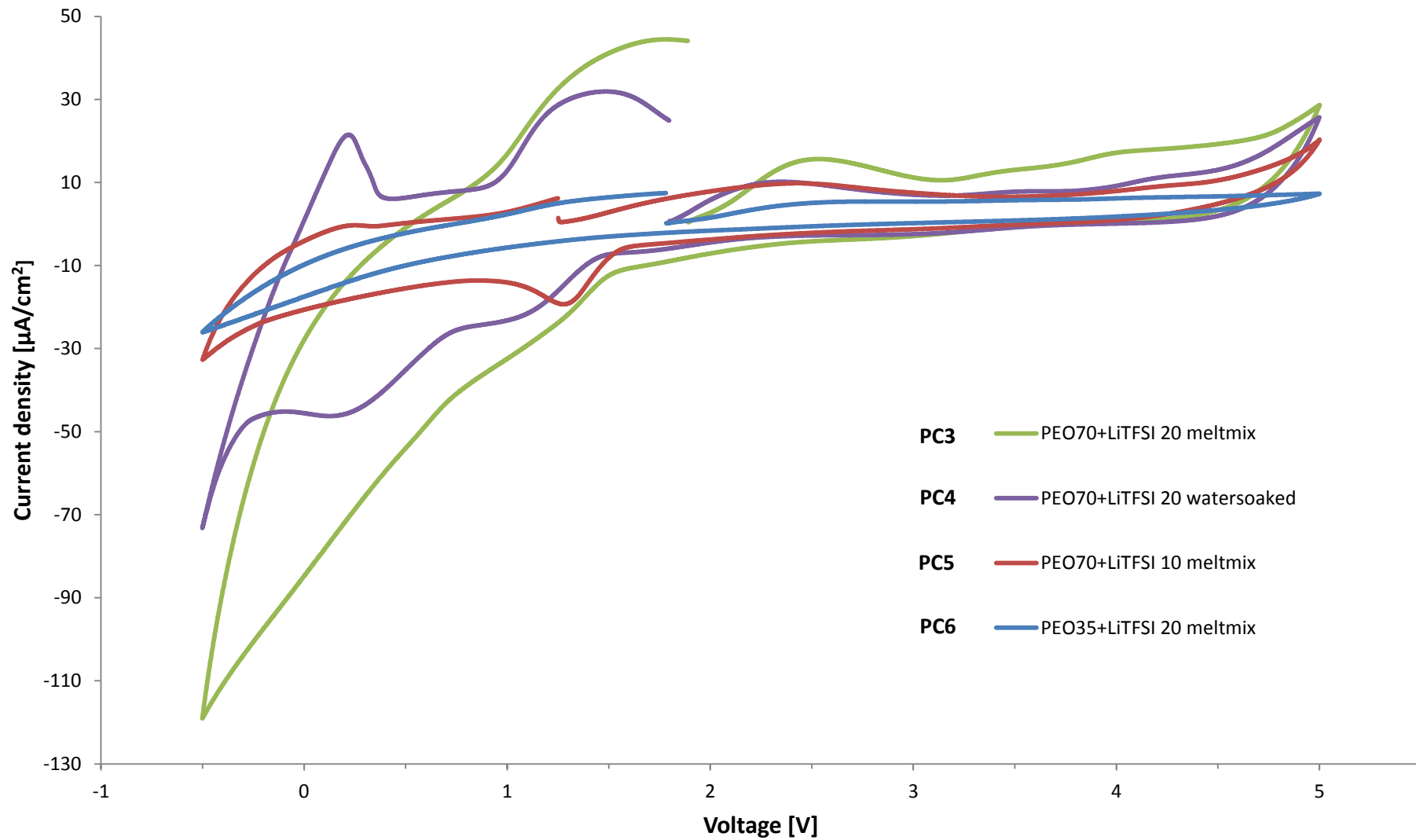


Figure 27 Cyclic voltammetry (CV) scans performed at room temperature

3.3.3 Discharge experiments

Discharge experiments were performed in order to further verify whether any of the samples was able to effectively prove lithium plating and stripping. If this occurs a characteristic plot can be expected. While galvanostatically discharging the lithium vs. stainless steel system, a quick drop of the potential to negative values is expected. The voltage should then stabilize to a flat plateau at 0V or slightly negative voltages; the latter case proves that a certain over potential is needed for lithium plating, but this can be expected in a relatively thick solid-state polymeric electrolyte. When the cell is put at rest, i.e. no current is forced through the system, the potential should briefly rise and establish a plateau at 0V or slightly positive values (again due to over potentials, this time caused by lithium stripping from the working electrode). During the plating, in fact, lithium has nucleated and grown on the working electrode creating thus a Li/Li cell. The potential therefore should be null when at rest. This process is shown in the figure below. During discharge the lithium ions (full blue dots) move from the lithium source (in blue) through the electrolyte; at the working electrode (in green) the positive lithium ions and the electrons (empty blue dot) from the external circuit meet and thus lithium metal starts plating on the interface between the stainless steel and the electrolyte. At this point lithium metal is present on both sides of the cell and therefore the measured potential should be null when the cell is at rest.

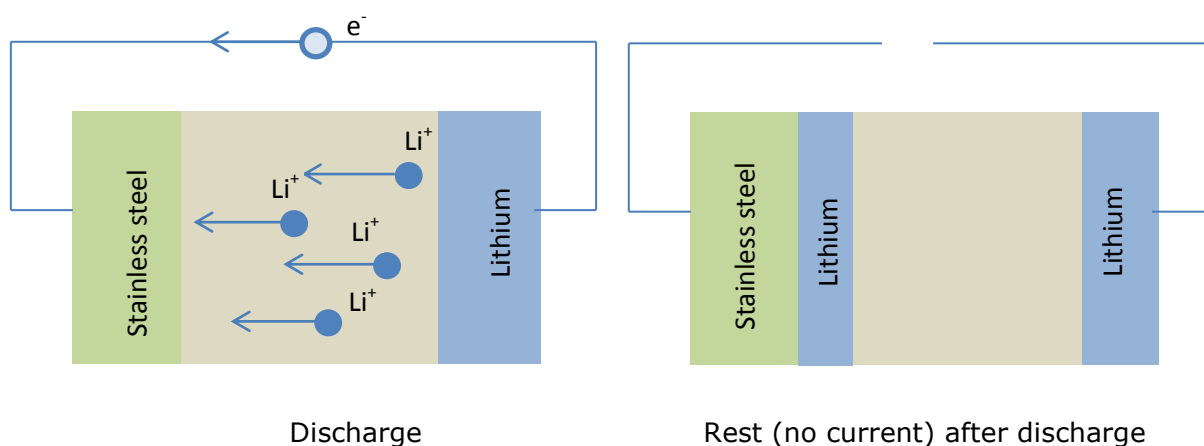


Fig. 28 Schematic representation of the discharging process and the consequent situation when the cell is at rest

The results from the discharge experiments are hereby presented. Figures 29 to 32 show the discharge and rest curves per each sample (PC3, PC4, PC5 and PC6) at increasing temperatures. In some cases some curves can be almost entirely covered by other ones, therefore the graphs require a careful observation. The plots consist of a first curve that corresponds to the discharge process, while the second curve shows the voltage change over time during the rest period (5 minutes as the discharge process). The discharge and the rest process at the same temperature are shown in the same colour. The voltage difference between the end of the discharge curve and the beginning of the rest curve represents the IR drop and, as may be expected, such voltage drop decreases with increasing temperature. The current is in fact constant but the resistance decreases in accordance to the Arrhenius behaviour of thermally activated processes such as ionic conduction.

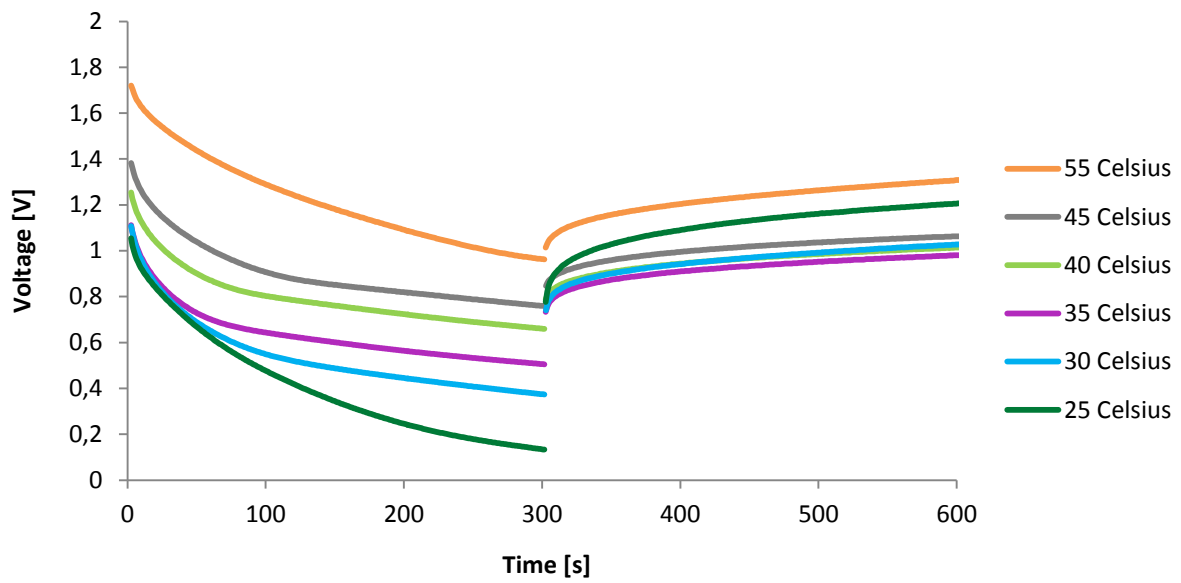


Figure 29 Sample PC3 (PEO70+LiTFSI 20 meltmix): discharge and rest curves at different temperatures.

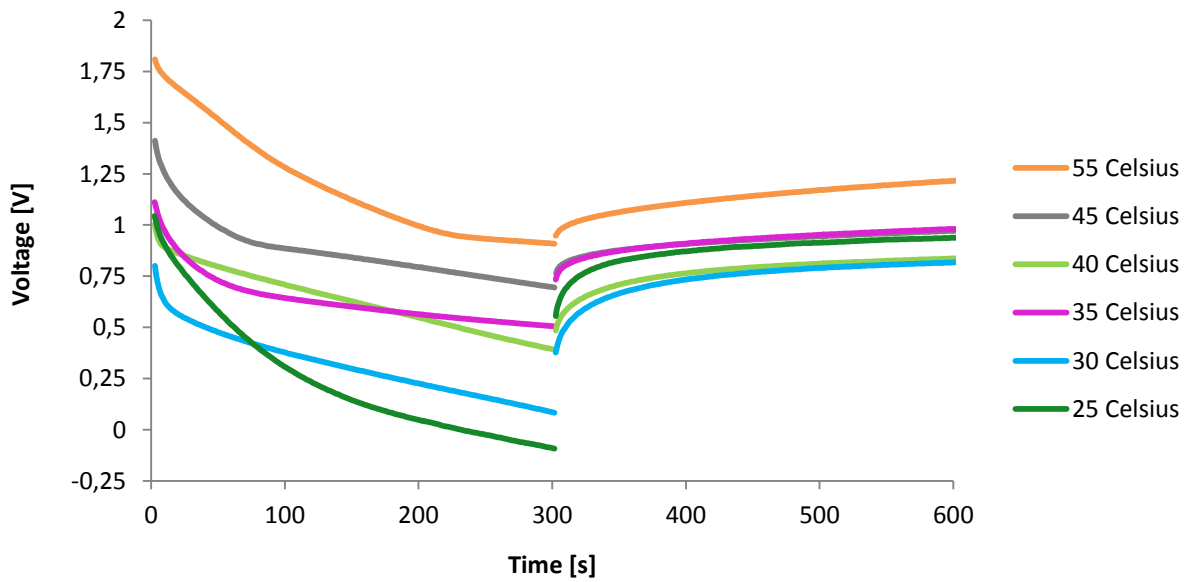


Figure 30 Sample PC4 (PEO70+LiTFSI 20 watersoaked): discharge and rest curves at different temperatures.

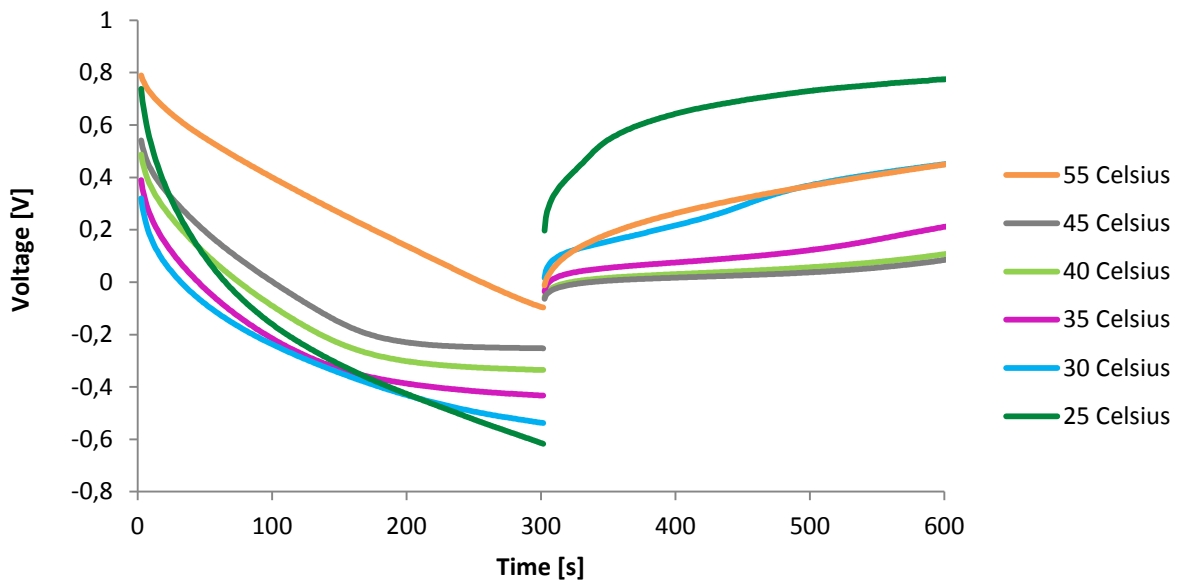


Figure 31 Sample PC5 (PEO70+LiTFSI 10 meltmix): discharge and rest curves at different temperatures.

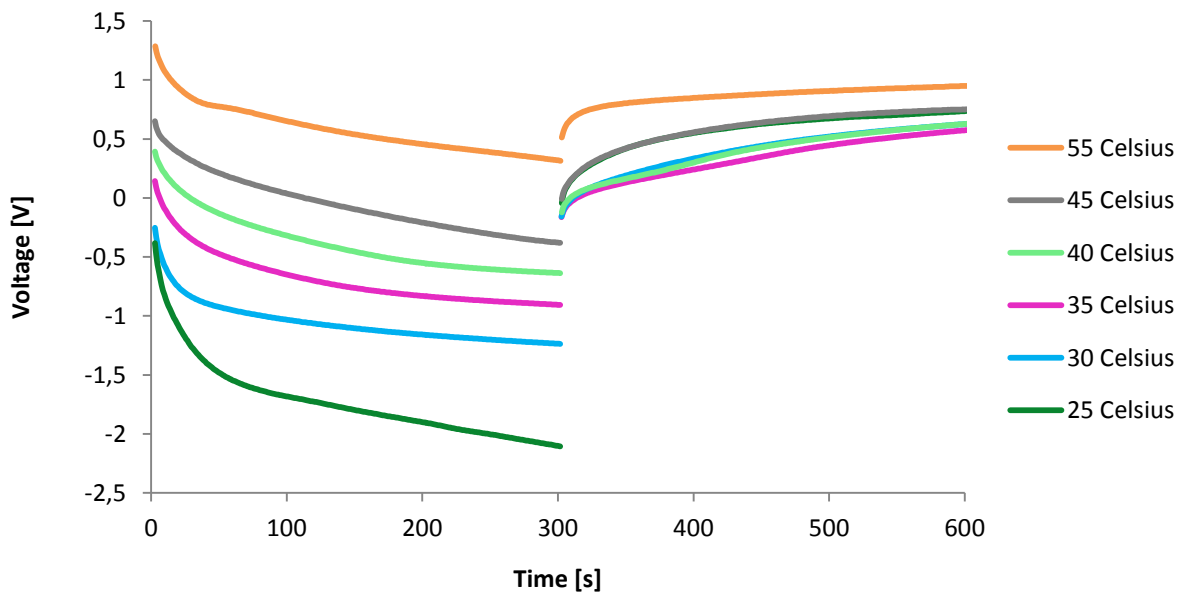


Figure 32 Sample PC6 (PEO35+LiTFSI 20 meltmix): discharge and rest curves at different temperatures.

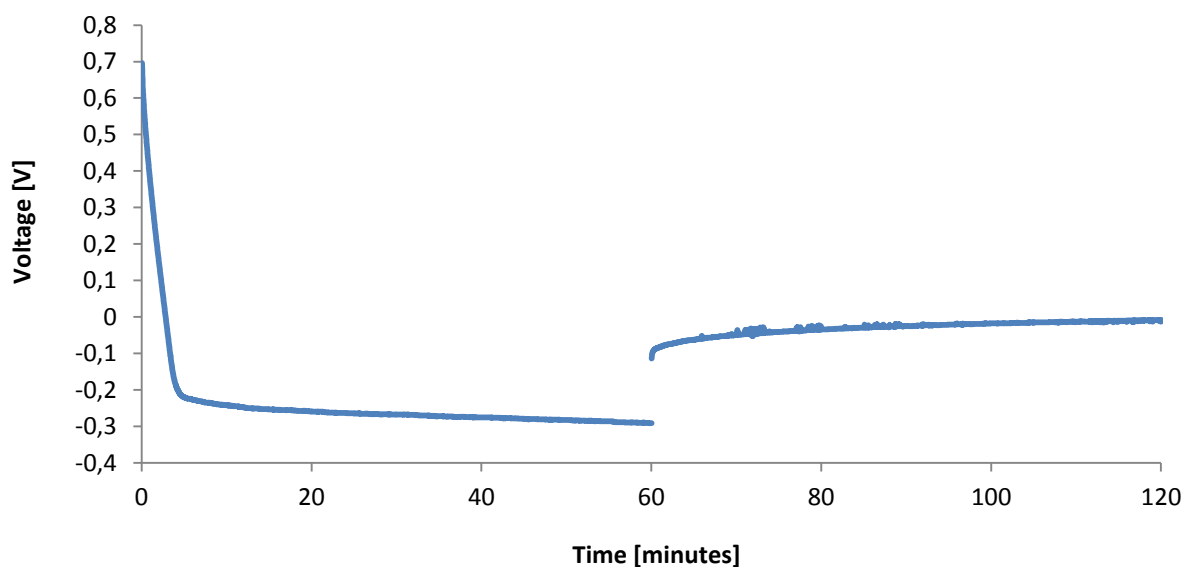


Figure 33 Sample PC5 (PEO70+LiTFSI 10 meltmix): 1 hour discharge and rest curves at 45°C.

Samples PC3 and PC4 do not exhibit a negative or null plateau as lithium plating would show. Therefore it may be concluded that such process is not taking place as it would be expected to. The CV scans at room temperature and at 45°C (previous chapter) of sample PC3 confirm this fact, although due to its very high conductivity this was deemed to be the most promising sample. The lack of evident plating for sample PC4 also indicates that the peak at approximately 0,2V visible in the CV scan at 45°C (fig. 27) is not due to lithium stripping: the discharge and rest curves at 45°C (in grey in fig. 30) in fact indicate no such proof of lithium plating.

Sample PC5 shows a series of discharge/rest curves that are more promising in terms of lithium plating and stripping: the discharge curves seem to reach an increasingly flat negative plateau as temperature is increased up to 45°C. At this temperature the over potential is approximately 0,2V: this is a fairly high over potential, but is reasonable for a polymeric solid-state electrolyte. The rest curves are also just above 0V. The behaviour of this sample was deemed promising and therefore the experiment was repeated for longer time: in fig. 33 the result for a discharge/ rest experiment of 1 hour each is shown. These results seem to confirm that no side reaction is taking place. The measurement taken at 55°C (fig. 33) instead seems to show a completely different trend and cannot be clearly explained. Perhaps at such temperatures other degradation processes are kinetically preferred. What remains also unclear, though, is that the CV scans of sample PC5 indicate no evidence of lithium plating or stripping. Therefore there seems to be an incongruence between what is revealed by the results in this chapter and the CV results.

Sample PC6 shows improved discharge/rest curves only as the temperature is increased up to 40°C. As the previous sample, though, no evidence of lithium plating/stripping is revealed by the CV results and therefore no conclusive proof is given.

Again it is important to remark the lack of statistical data as the measurements were performed only on one sample per type, as previously discussed. In general the discharge experiments yield no proof of lithium plating or stripping for any sample, with the exception of sample PC5. Overall there is a strong disagreement between the discharge experiments and the CV measurements regarding the lithium plating and stripping, but both types of measurement seem to confirm that in any case other degradation processes are taking place. It is difficult to speculate what other reactions are taking place, especially considering the very high conductivity of the samples. In any case the conduction must be ionic because it shows an Arrhenius temperature dependence that would not apply for electronic conduction. Out of the two ions that certainly are present in the electrolyte (Li^+ and TFSI^-) it is reasonable to affirm that the lithium ion is moving the most because of its small size compared to the bulky anion grants it much higher mobility. Such incoherent results on the ability of the produced electrolytes to plate and strip lithium definitely will require further investigation in the future. The results presented in this chapter cannot be compared with analogous internal DSM data as, to the knowledge of the student, no similar investigation has been performed on these Arnitel materials. However the apparent side reactions between the electrolyte and the lithium metal confirm what is already known in literature regarding such electrochemical instability as briefly discussed at the end of the previous chapter.

4 Conclusions

In this work three solvent-free methods to produce solid-state polymeric electrolytes for lithium ion batteries are presented, based on di-block PEO/PBT copolymers produced by DSM. Meltmixing and watersoaking are the methods that have been developed in more detail, while thin film soaking requires further development, although it already reveals to be promising. Out of the three initially proposed salts LiTFSI, LiBOB and LiCl, LiTFSI yielded immediately better results in terms of sample production and electrochemical behaviour. Therefore research efforts were focused on samples containing this salt. The meltmixed and water soaked samples have been hot pressed in specifically designed press-cells and thus smooth free-standing electrolyte membranes have been produced that exhibit conductivity values in the order of 10^{-5} S/cm at room temperature when containing PEO70 and LiTFSI in a molar EO:Li⁺ ratio of 20. Ionically conducting systems were therefore obtained. Overall the PEO35 polymer yielded conductivity values ten times lower due to the lower content of active PEO. This polymer therefore may seem less attractive in electrochemical terms, but may still reveal to be very promising if future work will prove that its higher content of hard block PBT hinders effectively dendrite growth while cycling the cell. Samples containing an eutectic concentration of LiTFSI (EO:Li⁺ =10) revealed an unexpected lower conductivity compared to the EO:Li⁺ ratio of 20: such incongruence was attributed to the phase separation and coexistence of crystalline and amorphous phases even at the eutectic composition. Temperature dependent impedance measurement were performed between approx. 25°C and 65°C. The conductivity values have been fitted with an Arrhenius curve and the activation energy for ionic conductivity has been thus calculated to be approximately 0,5 - 0,6eV. None of the samples produced proved to be stable at low voltages when in contact with lithium metal and degradation processes seem to be strongly competing with lithium plating and stripping. Such interfacial instability has been ascribed to the inherent instability between lithium metal and PEO. Such results, together with the high conductivities obtained, are comparable to samples prepared via the HFIP solvent route in internal DSM investigation. Thus the solvent-free methods proposed in this work proved be potential candidate routes for preparing electrolytes based on DSM material through safer, cheaper and more environmentally friendly routes.

5 Synopsis and outlook of the project

This concluding chapter includes a short synopsis of the work performed during the graduation project and completes the report with future prospects, thus setting the basis for recommended further research.

5.1 Summary

The research work here presented has dealt with innovative production methods and electrochemical characterization of solid-state polymeric electrolytes for lithium ion batteries based on Arnitel® materials from DSM. The Arnitel material produced and provided by DSM is a di-block copolymer of PEO (polyethylene oxide) and PBT (polybutylene terephthalate), the PEO being the soft phase and the PBT being the hard block. Two versions of such material were used for the research, the difference lying in the relative quantity of the two components: the one containing 35wt% of PEO was named PEO35 and the other version, with 70wt% of PEO, is referred to as PEO70. The advantages deriving from such copolymer compared to pure PEO are the higher melting temperature (thus allowing for a wider operating temperature range) and the potential higher blocking resistance to lithium dendrites.

Adequate lithium salts must be added to the polymer in order to obtain a system able to conduct lithium ions (the charge carriers) and hinder the movement of electrons, while simultaneously avoiding physical contact between the electrodes. A membrane that functions as an electrolyte and separator can thus be obtained. The graduation project focused on proposing and implementing solvent-free routes of incorporating lithium ion salts in the DSM polymers in order to obtain a free-standing electrolyte without the use of hazardous solvents such as HFiP (hexafluoroisopropanol) previously used in internal DSM research. After initial literature study, three different lithium salts were proposed to be tested in combination with the two DSM polymers, namely bis(trifluoromethanesulfonyl)imide (LiTFSI), bis(oxalato)borate (LiBOB) and lithium chloride (LiCl). Three different solvent-free methods of inserting the lithium salts in the polymer were proposed: melt-mixing, water soaking and thin film soaking. Melt-mixing requires melting the polymer ($T_m=210^\circ\text{C}$ approximately) and mixing in the salt until complete dispersion. The two latter methods instead take advantage of the very high water uptake of the Arnitel materials: water is used as a means of carrying the salt into the polymer chains by soaking the polymer in a aqueous solution of the desired lithium salt. The water can then be removed by complete drying. This was performed on PEO70 material in form of pellets (water soaking method) and directly on thin films of the PEO70 (thin film soaking method). Samples produced through melt-mixing and water soaking were then hot pressed in order to achieve thin electrolyte membranes. All such procedures constitute pioneering work and the necessary setups have needed to be devised, designed, produced and tested, as nothing similar had been previously done to the knowledge of the student. Therefore much time and effort has been dedicated to the actual production of the electrolyte membranes. One of the most important achievements in terms of setups was the press-cell, a device that allows for hot pressing

and consequent impedance measurements in the same system, while allowing to apply temperature and pressure on the system and thus obtain improved interface contact between the electrodes and the electrolyte during testing.

Once the samples were produced, they were characterized by means of DSC (differential scanning calorimetry) and in terms of electrochemical properties such as conductivity and voltage stability. LiBOB and LiCl were processed by meltmixing and water soaking but were soon disregarded due to inferior results compared to LiTFSI: LiBOB in fact showed unwanted and unknown reactions with the polymer at the processing temperatures, while LiCl did not prove to adequately dissolve in the polymer matrix. Therefore most experiments were finally performed on LiTFSI-containing samples, that was also the salt used in internal DSM experiments and is the most commonly found in literature. Samples containing LiTFSI were prepared in all of the three proposed methods and were used in combination with PEO70 and PEO35 polymer matrixes. Four final very satisfactory samples were prepared once improved setups were designed and tested. PEO70-containing samples with LiTFSI in a molar EO:Li⁺ ratio of 20 prepared by meltmixing or watersoaking (and consequent hot pressing) yielded conductivity values in the order of 10⁻⁵ S/cm at room temperature. This is a remarkably high value if compared to equivalent results available in literature. The meltmixed sample of PEO70 and LiTFSI in a EO:Li⁺ ratio of 10 gave slightly lower conductivity results but in the same order of magnitude. This sample was actually expected to yield higher conductivity because the ratio between salt and polymer was at the eutectic point, where a crystallinity gap is found and an improved conductivity is foreseen due to the better ion mobility in the amorphous phase. The discrepancy between the theory and the experimental result was ascribed to coexistence of crystalline and amorphous phases even at the eutectic composition. In accordance to theory, instead, the PEO35-containing sample showed lower conductivity (10⁻⁶ S/cm at room temperature). This is due to the lower content of active phase, i.e. the PEO, compared to the PEO70 polymer and is also compatible with the previous internal DSM data. Conductivity measurements for the four samples here summarized were taken also in a temperature range between room temperature and approximately 65°C. Arrhenius plots were therefore obtained and the activation energy for ionic conduction was also calculated.

Overall the conductivity results proved to be extremely satisfactory from two perspectives: firstly, conductivity values at room temperature are orders of magnitude higher compared to analogous PEO-based systems (without conductivity enhancers such as fluidizers, inorganic nanoparticles, room temperature ionic liquids) found in literature. On the other side the conductivity of the samples produced in this research through new and solvent-free methods such as melt-mixing or water soaking was in the same order of magnitude as the samples produced with use of HFIP in previous internal DSM investigation.

The samples produced revealed some evident stability issues at lower voltages starting from approximately 1,5V, while in the higher voltage range they proved to be quite stable. While performing discharge experiments and cyclic voltammetry (CV), no actual coherent proof of lithium plating and discharging was found, but the instability between PEO-based electrolytes in contact with lithium metal turned out to be a recurrent and established problem in literature. Furthermore internal DSM experiments gave the same stability issues on the equivalent samples produced with the use of solvent. For this reason the encountered electrochemical instability has not been ascribed

to the new proposed production methods, but to the inherent behaviour of the Arnitel materials in contact with lithium metal.

The third proposed production method, namely the thin film soaking film, proved to be an extremely simple and straightforward method for obtaining thin electrolytes in a one-step procedure. On the other side, tuning the salt concentration in the polymer proved to be very challenging and therefore much lower room temperature conductivity values were obtained (10^{-7} S/cm). Considerations on future work to improve such a simple and promising method follow in the last chapter.

Overall the work performed during the graduation project has been very practically oriented and aimed at finding experimental workable solutions, setups and testing protocols to answer the research questions that were initially posed. Concisely it may be said that LiTFSI proved to be the best out of the three salts proposed, while melt-mixing and water soaking (followed by hot pressing) seemed to be equally successful solvent-free routes to produce solid state polymeric electrolytes based on Arnitel materials. Concentration of salt in the polymer matrix respecting the molar ratio of EO:Li⁺=20 proved to be the most common in literature and the most satisfactory in this work.

It was possible overall to propose different alternatives to the solvent route previously investigated by DSM and obtain comparable electrolytes in terms of conductivity and stability, but my means of cheaper, safe, more environmentally friendly and possibly industrially viable methods.

5.2 Future work and recommendations

Fine tuning and optimization has not been the goal of this work, but some ideas for further improvement are given in this final chapter of this work. Ideas and reflections are given regarding the sample preparation methods, the measurement techniques and options to obtain better electrochemical properties and are arranged as bullet points for clarity.

- **Gold sputtering:** At this stage it is possible to obtain smooth and well defined electrolytes by hot pressing in the custom-made press-cells. Therefore it would be now possible to prepare more samples and to sputter them with gold in order to have ideal interface contact for conductivity measurements, thus eliminating the need to perform impedance measurements under high applied pressure.
- **Electrochemical stability:** The inherent electrochemical instability between the PEO-based electrolyte and the lithium metal is an issue that needs to be solved to bring research to actual implementation of electrolytes based on Arnitel materials. Much work is already done in literature and is mainly based on the use of small size inorganic powders as additives. An important line of future work should be dedicated to explaining why lithium plating and stripping is not taking place in discharge experiments and solving interfacial instability. Discharge experiments could be performed using an anode such as LTO (lithium titanium oxide) in order to avoid drastically low voltages and avoid instability that derives from the contact of the electrolyte with lithium metal.

- **Conductivity enhancers:** Now that a proof of concept has been given for the proposed solvent-free routes, it is possible to start optimizing the obtained electrolytes. Much work is presented in literature about the use of conductivity enhancers such as inorganic nanoparticles, fluidizers (to reduce the degree of crystallinity of the system) or combining different lithium salts together. Fine tuning of the conductivity therefore could be another line of future research.
- **Thin film soaking:** Such production technique has been proposed in this work but not sufficiently developed in the course of this project due to time restraints, but it remains a very promising technique especially bearing in mind industrial implementation. A way to control and measure the salt concentration in the polymeric matrix must be investigated. Furthermore it would be very interesting to perform such experiments also with LiBOB and LiCl. These salts were in fact soon discarded from this work due to chemical reactions at higher temperature with the polymer matrix (in the case of LiBOB) or bad dissolution of the salt in the polymer during meltmixing (in the case of LiCl). Both these limitation may be completely avoided with the thin film soaking method. No high temperature would be needed and such a polar salt as LiCl may easily dissociate in aqueous solution allowing for good distribution of the ions in the polymer chains. Different concentrations between polymer and salt should also be tested, particularly in the case of the chloride that with its low molecular weight would allow for much higher molar concentrations than what was tried throughout this work.
- **Dendrite formation and NDP:** Once the electrochemical stability issues have been understood and solved, an important line of work could be opened, this being the investigation on the ability of the Arnitel materials to hinder or impede the growth of lithium dendrites. This is a very well-known problem with polymeric solid-state electrolytes based on pure PEO, but the presence of the hard phase PBT in the Arnitel material leaves room for optimism regarding its ability to stop dendrites. This could be, together with the higher operating temperature allowed by the DSM polymers, the feature that would distinguish the Arnitel electrolytes from any other solid-state polymer electrolyte available up to now. Neutron depth profiling (NDP) is most likely a very effective technique to “see” the lithium inside the electrolyte and establish whether it accumulates after or during cycling of the cell. To prove that the PBT is actually responsible for the hindrance of dendrite formation (and therefore improve cyclability), it would be advisable to prepare equivalent electrolytes based on pure PEO, PEO70 and PEO35 and test whether the increasing content of PBT corresponds to lower dendrite formation after performing the same cycling procedure. NDP analysis could be performed ex-situ on electrolytes prior to cycling (as already reported in the appendixes) and after having cycled: a comparison between the two states would therefore be possible. In-situ NDP could be also performed as to track the lithium movement while cycling. This would yield some elegant and sophisticated insights, but will require the development of adequate air-tight laminate cells. Electrolyte samples for NDP may be prepared through meltmixing or water soaking and consequent hot-pressing. Relatively thick samples would be obtained and therefore it would be possible to obtain information on only the first few decade of microns, as the depth resolution of the neutron beam is limited. For this reason developing and improving the thin film soaking methods seems to be the most straightforward route: in this way extremely thin samples can be

obtained and these would be ideal for cycling in a laminate cell while performing in-situ NDP measurements.

- **Full battery:** Up to this point any kind of electrochemical test has taken place in lithium vs. stainless steel cells. The next step is to make a full battery using standard electrodes such as LTO (lithium titanium oxide) and LFP (lithium iron phosphate). Such a system could be prepared by hot pressing the electrolyte (previously produced by hot pressing on its own as done in this work) between the two electrodes. This could be performed in the press-cells and should be a quite straightforward procedure. Hot pressing should allow for very good interfacial contact as the polymer would be able to partially enter the pores of the electrodes. A complete system could be therefore prepared and tested.
- **Long term vision:** When developing an actual complete cell that includes a solid-state Arnitel electrolyte, a longer term vision can be thought of. The adequate electrodes should be prepared by using Arnitel material as a binder in order to optimize the interfacial contact between the electrodes and the electrolyte and obtain the lowest internal resistance to ionic movement.

Bibliography

1. *Solid polymer electrolytes: materials designing and all-solid-state battery applications: an overview.* **Agrawal R.C., Pandey G.P.** 22, s.l. : Journal of Physycs D: Applied Physics, 2008, Vol. 41.
2. *Issues and challenges facing rechargeable lithium batteries.* **Tarascon J.M., Armand M.** s.l. : Nature, 2001, Vol. 414.
3. *Lithium-ion conducting electrolyte salts for lithium batteries.* **Aravindan V., Gnanaraj J., Madhavi S., Liu H.K.** s.l. : European Journal of Chemistry, 2011, Vol. 17.
4. *Ceramic and polymeric solid electrolytes for lithium-ion batteries.* **J.W., Fergus.** s.l. : Journal of Power Sources, 2010, Vol. 195.
5. *A review on PEO based solid polymer electrolytes (SPEs) complexed with LIX (X=Tf, BOB) for rechargeable lithium ion batteries.* **Karuppasamy K., Anony R., Alwin S. Balakumar S., Sahaya Shajan X.** s.l. : MAterial Science Forum, 2015, Vol. 807.
6. *Mechanism of ion transport in PEO/LITFSI complexes: effect of temperature, molecular weight and end groups.* **Devaux D., Bouchet R., Glé D., Denoyel R.** s.l. : Soild State Ionics, 2012, Vol. 227.
7. **Sequeira C.A.C, Santos D.M.F.** Introduction to polymer electrolyte materials. [book auth.] Diogo Santos César Sequeira. *Polymer electrolytes - Fundamentals and applications.* s.l. : Woodhead Publishing, 2010.
8. **Ye F., Feng Z.** Polymer electrolytes as solid solvents and their applications. [book auth.] César Sequeira Diogo Santos. *Polymer electrolytes - Fundamentals and applications.* 2010 : Woodhead Publishing.
9. *Solid polymer electrolytes based on ethylene oxide polymers.* **Florjanczyk Z., Zygadlo-Monikowska E., Ostrowska J., Frydrych A.** 1, s.l. : Polimery, 2014, Vol. 59.
10. *Block copolymer solid battery electrolyte with high Li-ion trasnference number.* **Ghosh A., Wang C., Kofinas P.** 7, s.l. : Journal of the Electrochemical Society, 2010, Vol. 157.
11. *Block Copolymer Electrolytes for Rechargeable Lithium Batteries.* **Young W.S., Kuan W.F., Epps T.H.** s.l. : Journal of Polymer Physics, 2013, Vol. 52.
12. *Electrical conductivity in ionic complexes of poly(ethylene oxide).* **P.V., Wright.** s.l. : British Polymer Journal, 1975, Vol. 7.
13. *Nanocomposite PEO-LiBOB polymer electrolytes for low temperature lithium rechargeable batteries.* **Croce F., Settimi L., Scrosati B., Zane D.** s.l. : Journal of New Materials for Electrochemical Systems, 2005, Vol. 9.

14. *Phase diagrams and conductivity mehaviour of poly(ethylene oxide) - molten salt rubbery electrolytes.* **Armand M., Lasaud S., Perrier M., Vallée A., Besner S., Prud'homme J.** s.l. : Macromolecules, 1994, Vol. 27.
15. *Synthesis and electrochemical characterization of PEO-based polymer electrolytes with room temperature ionic liquids.* **Chenh H., Zhu C., Huang B., Lu M., Yang Y.** s.l. : Electrochimica Acta, 2007, Vol. 57.
16. *LiBOB: Is it an alternative salt for lithium ion chemistry?* **Xu K., Zhang S.S., Lee U., Allen J.L., Richard Jow T.** s.l. : Journal of Power Sources, 2005, Vol. 146.
17. *LiBOB as salt for lithium ion batteries: A possible solution for high temperature operations.* **Xu K., Zhang S., Richard Jow T., Xu W., Austen Angell C.** 1, s.l. : Electrochemical and Solid-State Letters, 2002, Vol. 5.
18. *Preparation, thermal stability and electrochemical properties of LiODFB.* **Zhou H., Liu F., Li J.** 8, s.l. : Journal of Material Science and Technology, 2012, Vol. 28.
19. *Lithium Oxalyldifluoroborate as a salt for the improved electrolyts of Li-ion batteries.* **Zhang, Sheng Shui.** 27, s.l. : ECS Transactions (The Electrochemical Society), 2007, Vol. 3.
20. *On the use of LiPF₃(CF₂CF₃)₃ (LiFAP) solutions for Li-ion batteries. Eletrochemical and thermal studies.* **Gnanaraj J.S., Zinigrad E. Asraf L., Sprecher M., Gottlieb H.E., Geissler W. et al.** s.l. : Electrochemistry Communications, 2003, Vol. 5.
21. *Thermal behavior of new polymer electrolytes.* **Fauteux D., McCabe P.** s.l. : Polymers for Advances Technologies, 1994, Vol. 6.
22. *Characterization of solvent-free polymer electrytes consisting of ternary PEO-LiTFSI-PYR14 TFSI.* **Shin J. H., Henderson W.A., Tizzani C., Passerini S., Jeong S.S., Jim K.W.** 9, s.l. : Journal of The Electrochemical Society, 2006, Vol. 153.
23. *High performance PEO-based polymer electrolytes and their application in rechargeable lithium polymer batteries.* **Sumathipala H.H., Hassoun J., Panero S., Scrosati B.** s.l. : Ionics, 2007, Vol. 13.
24. *Carrier transport and generation processes inpolymer electrolyts based on poly(ethylene oxide) networks.* **Watanabe M., Itoh M., Sanui K., Ogata N.** s.l. : Macromolecules, 1986, Vol. 20.
25. *Poly(ethylene oxide) - LiCF₃SO₃ - polystyrene electrolyte systems.* **Gray F.M., MacCallum J.R., Vincent C.A.** s.l. : Solid State Ionics, 1986, Vol. 18.
26. *Hot-pressed, dry, composite, PEO-based electrolyte membranes I. Ionic conductivity characterization.* **Appetecchi G.B., Croce F., Hassoun J., Scrosati B., Salomon M., Cassel F.** s.l. : Journal of Power Sources, 2002, Vol. 114.

27. *Dual-composite polymer electrolytes with enhanced transport properties.* **Paner S., Scrosati B., Sumathipala H.H., Wieczorek W.** s.l. : Journal of Power Sources, 2007, Vol. 167.
28. *Structure and properties of poly(ethylene oxide)-organo clay composite prepared via melt mixing.* **Abraham T.N., Ratna D., Siengchin S., Karger-Kocsis J.** s.l. : Polymer Engineering and Science, 2009.
29. *Effect of hot pressing on the ionic conductivity of the PEO/LiCF₃SO₃ based.* **Zhou X., Yin Y., Mansour A.N., Balizer E. et al.** s.l. : Solid State Ionics, 2011, Vol. 196.
30. *Salt-concentration dependance of the polymer glass transition temperature in PEO-NaI and PEO-LiTFSI polymer electrolytes.* **Stolwijk N.A., Heddier C., Reschke M., Wiencierz M., Bokeloh J., Wilde G.** s.l. : Macromolecules, 2013, Vol. 46.
31. *Crystalline phases, morphology and conductivity of PEO:LiTFSI electrolytes in the eutectic region.* **Marzanatowicz M., Dygas J.R., Frok F., Nowinski J.L., Tomaszewska A., Florjanczyk Z., Zygadlo-Monikowska E.** s.l. : Journal of Power Sources, 2006, Vol. 159.
32. *Ionic liquids to the rescue? Overcoming the ionic conductivity limitations of polymer electrolytes.* **Shin J.H., Henderson W.A., Passerini S.** s.l. : Electrochemistry Communications, 2003, Vol. 5.
33. *Synthesis and electrochemical characterization of PEO-based electrolytes with room temperature ionic liquids.* **Cheng H., Zhu C., Huang B., Lu M., Yang Y.** s.l. : Electrochimica Acta, 2007, Vol. 52.
34. *PEO-based polymer electrolytes with ionic liquids and their use in lithium metal-polymer electrolyte batteries.* **Shin J.H., Henderson W.A., Passerini S.** 5, s.l. : Journal of The Electrochemical Society, 2005, Vol. 152.
35. *Nanocomposite polymer electrolytes and their impact on the lithium battery technology.* **F. Croce, L. Persi, F. Ronci, B. Scrosati.** s.l. : Solid State Ionics, 2000, Vol. 135.

Appendixes

Appendix A

Lithium salts: molar and mass calculations

Appendix B

EO:Li⁺ ratio estimation for soaked thin films

Appendix C

Sample series HP: thickness estimation

Appendix D

Individually presented DSC results

Appendix E

Extrapolation of resistance (R value) from Nyquist plots

Appendix F

Complete Nyquist plots of samples PC3, PC4, PC5 and PC6 as function of temperature

Appendix G

Arrhenius plot fittings

Appendix H

CV scans of samples PC3, PC4, PC5 and PC6 displayed individually

Appendix I

Neutron Depth Profiling (NDP)

Appendix A

Lithium salts: molar and mass calculations

The masses shown in Table 9 (chapter 2.2.1) have been calculated as shown below. For the mass calculations the following data is necessary.

	Chemical formula	Molar weight [g mol⁻¹]
PEO (unit)	H-(O-CH ₂ - CH ₂) _n -OH	44,05
LiTFSI	CF ₃ SO ₂ NLiSO ₂ CF ₃	287,09
LiBOB	LiB(C ₂ O ₄) ₂	193,79
LiCl	LiCl	6,94

Table A1 Molar weights of the used polymer and lithium salts

The calculation is shown as an example only in the case of LiTFSI. For LiBOB and LiCl the same algorithm is clearly valid, remembering to use the correct molar mass.

Similarly the calculations for a EO:Li⁺=10 are done by multiplying the number of moles of salt by ten (rather than 20) to obtain the necessary number of moles of PEO.

$$0,250g / 287,09g\text{mol}^{-1} = 8,71\text{mol}$$

Mass to mole conversion of 250g of LiTFSI

$$8,71e^{-4}\text{mol} \cdot 20 = 1,74e^{-2}\text{mol}$$

Number of PEO moles observing a EO:Li⁺=20 ratio

$$1,74e^{-2}\text{mol} \cdot 44,05g \cdot \text{mol}^{-1} = 0,767g$$

Mole to mass conversion of the required amount of PEO

$$0,767g / 0,35 = 2,19g$$

Necessary quantity of PEO35 considering it contains 35wt% PEO

Appendix B

EO:Li⁺ ratio estimation for soaked thin films

The estimation is shown only for sample TF1 and is equivalent to the one for TF2.

The container has a flat bottom area of 5,2 x 5,2cm, as do the copper foil and the thin PEO70 film. The area measures 27,04 cm². The active area is the area of the smallest electrode in the blocking cell is 0,69 cm², therefore this area is considered for the calculations.

Assuming uniform deposition of the salt, the following relation can be written

$$21\text{mg} : 27,04\text{cm}^2 = x : 0,69\text{cm}^2$$

Therefore x = 0,54 mg are deposited on the active area.

The mass of active polymer, i.e. the PEO present in the 0,69 cm² of active area, can be calculated knowing the thickness of the thin film:

$$\begin{aligned}\text{Volume of PEO70} &= \text{thickness} \cdot \text{area} \\ &= 15 \cdot 10^{-4}\text{cm} \cdot 0,69\text{cm}^2 = 1,04 \cdot 10^{-3}\text{cm}^3\end{aligned}$$

$$\begin{aligned}\text{Mass of PEO} &= 0,7 \cdot \text{density of PEO70} \cdot \text{volume of PEO70} \\ &= 0,7 \cdot 1,22\text{g/cm}^3 \cdot 1,04 \cdot 10^{-3}\text{cm}^3 = 8,88 \cdot 10^{-4}\text{g}\end{aligned}$$

To determine the molar ratio between PEO and LiTFSI it first necessary to calculate the numbers of moles of the two compounds:

$$\text{mol}_{PEO} = \frac{8,88 \cdot 10^{-4}\text{g}}{44,05\text{g/mol}} = 2,02 \cdot 10^{-5}\text{mol}$$

$$\text{mol}_{LiTFSI} = \frac{5,4 \cdot 10^{-4}\text{g}}{287,09\text{g/mol}} = 1,88 \cdot 10^{-6}\text{mol}$$

Therefore the estimated molar ratio is

$$EO:Li^+ = \frac{2,02 \cdot 10^{-5}\text{mol}}{1,88 \cdot 10^{-6}\text{mol}} = 11,7$$

Appendix C

Sample series HP: thickness estimation

The thickness of the samples belonging to the HP series (chapter 3.1.4) was estimated according to the following calculations.

$$\rho_{electrolyte} = \frac{mass}{volume}$$

$$volume = l \cdot \pi \cdot \left(\frac{d}{2}\right)^2$$

$$l = \frac{4 \cdot volume}{\pi \cdot d^2}$$

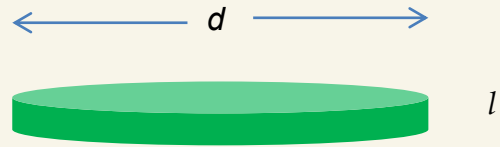


Figure C1 Dimensions of a disk of electrolyte

The density of the electrolyte is calculated as a weighted average of the density of the PEO70 and the salt

$$\rho_{electrolyte} = \frac{(mass_{salt} \cdot \rho_{salt}) + (mass_{polymer} \cdot \rho_{polymer})}{mass_{salt} + \rho_{polymer}}$$

The obtained density values are shown below.

Sample	Density PEO70 [g/cm ³]	Density salt [g/cm ³]	PEO70 [g]	Salt [g]	Density electrolyte [g/cm ³]
PEO70+LiTFSI EO:Li+=20	1,220	1,406	2,19	0,500	1,255
PEO70+LiTFSI EO:Li+=10	1,220	1,406	2,19	1,000	1,278
PEO70+LiBOB EO:Li+=20	1,220	1	2,16	0,333	1,191
PEO70+LiCl EO:Li+=20	1,220	2,07	2,38	0,08	1,248

Table C1 Density calculation for the different combinations of lithium and polymer

Thus, the estimation of sample thickness for the HP sample series according to the formulas above is shown below.

Sample	Membrane mass [g]	Density [g/cm³]	Estimated electrolyte diameter [cm]	Estimated electrolyte thickness [cm]
HP1	0,0182	1,255	1,2	0,0128
HP3	0,0180	1,278	1,0	0,0179
HP2	0,0307	1,255	1,3	0,0184
HP4	0,0121	1,255	1,1	0,0101
HP5	0,0111	1,191	1,2	0,0082
HP6	0,0260	1,248	1,2	0,0184

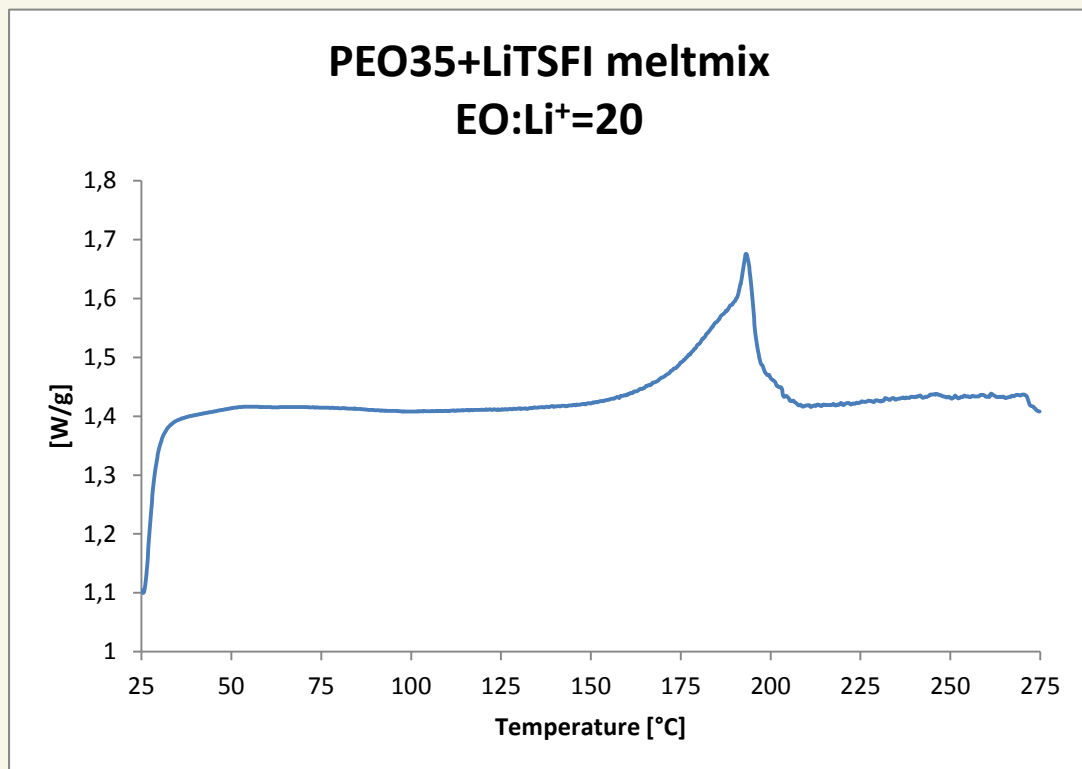
Table C2 Estimation of the thickness of the electrolyte sample prepared by hot pressing in the conventional cylindrical die set

Appendix D

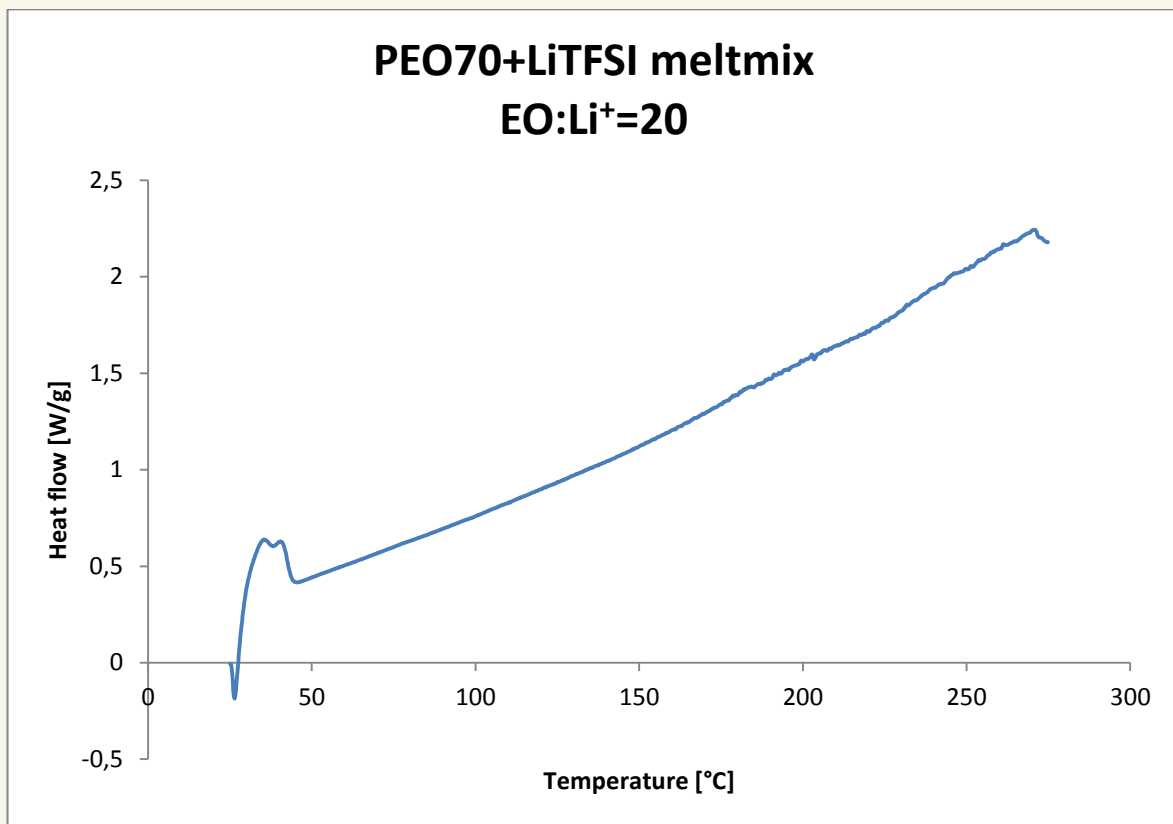
Individually presented DSC results

Sample 1

Sample ID:	150401 S1		
Results:			
Area	X1	119,91	°C
	Y1	1,4105	W/g
	X2	209,25	°C
	Y2	1,4169	W/g
	Peak	193,2	°C
	Peak Area	27,192	J/g
	Delta H	27,192	J/g



Sample 2

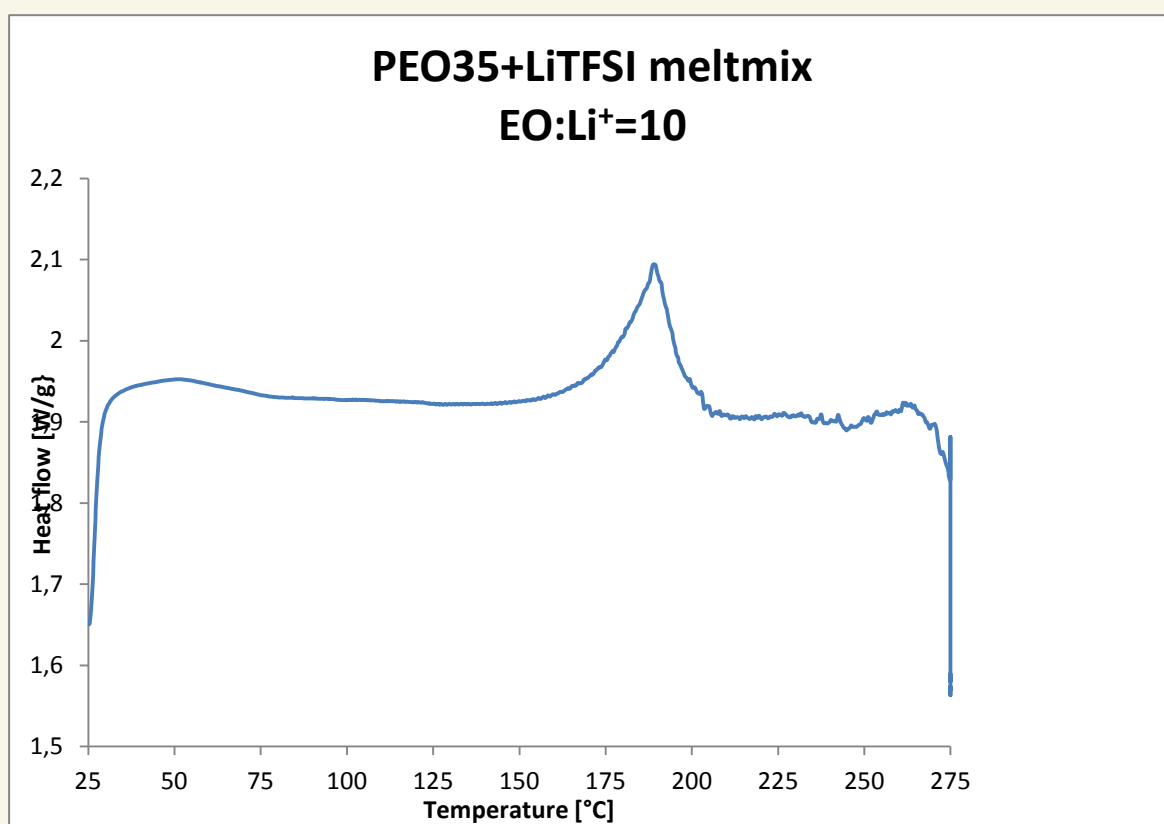


Sample 3

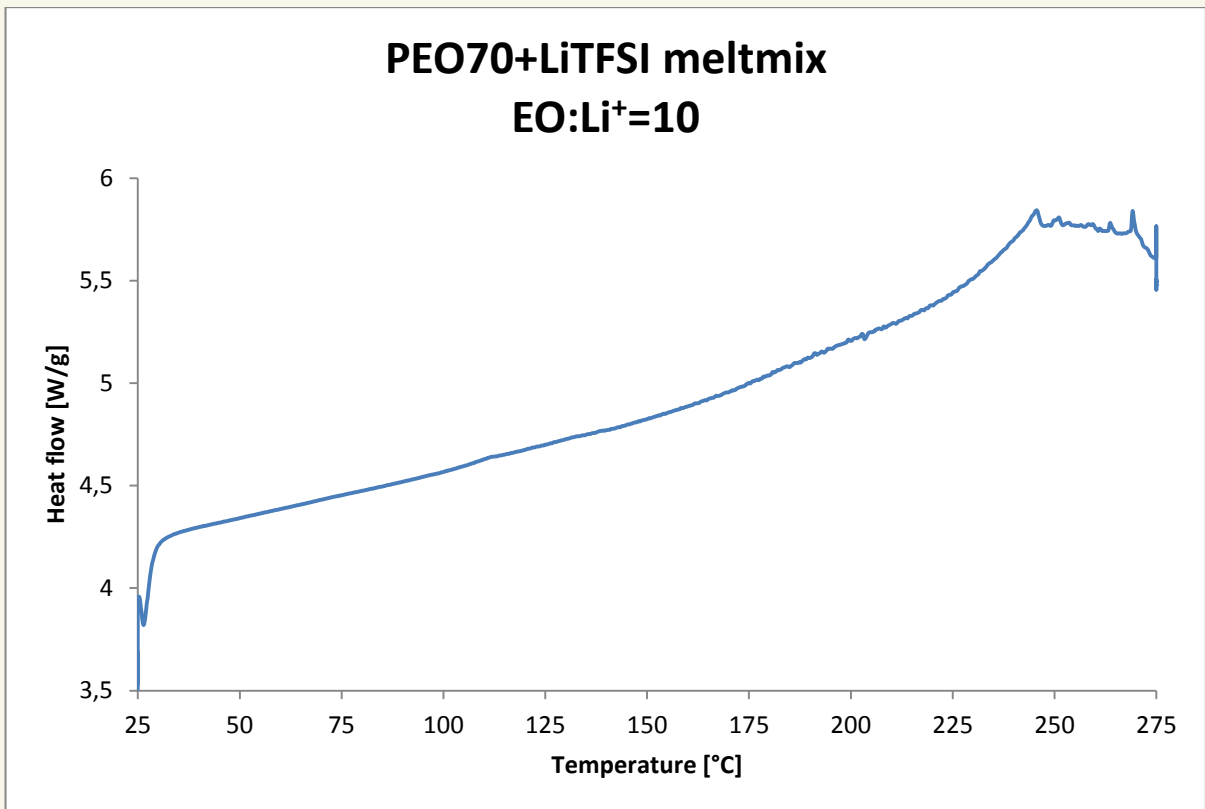
Sample ID: 150401 S3

Results:

Area	X1	138,92	°C
	Y1	1,9223	W/g
	X2	207,75	°C
	Y2	1,9105	W/g
	Peak	189,2	°C
	Peak Area	19,976	J/g
	Delta H	19,976	J/g

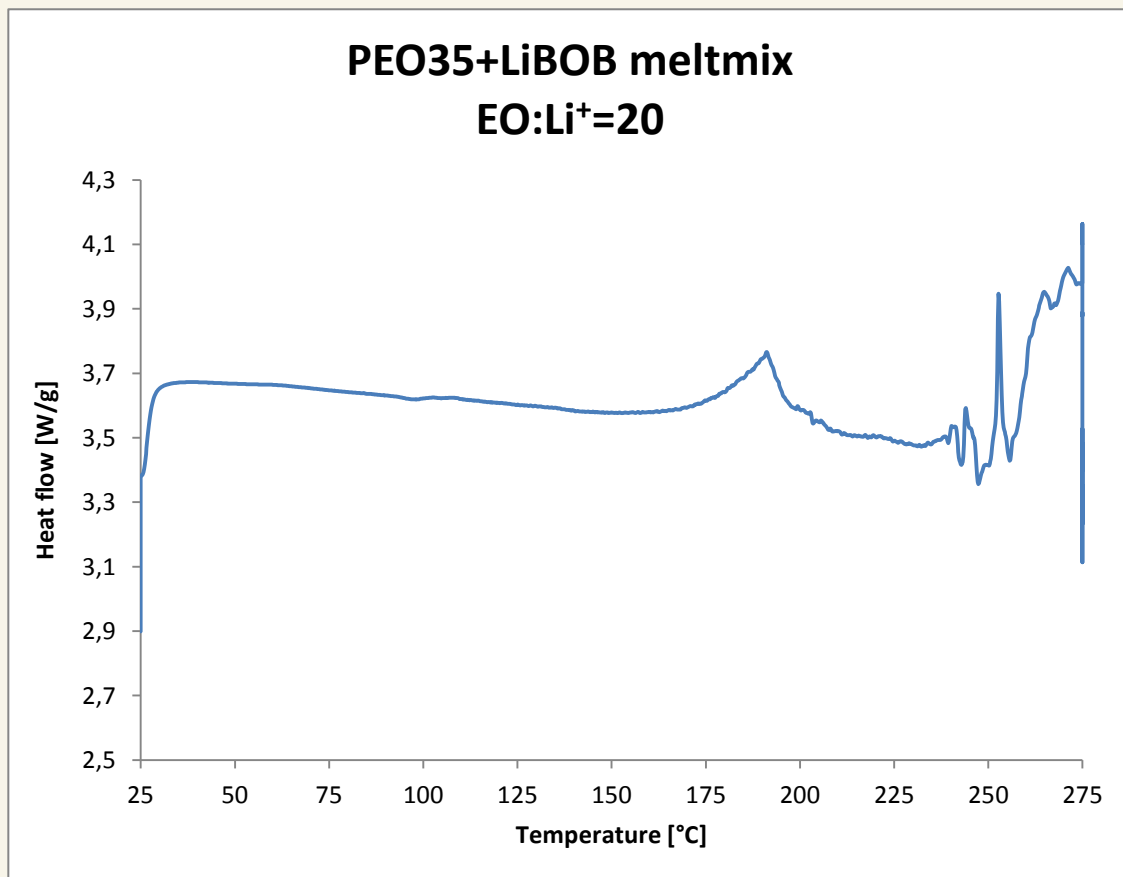


Sample 4



Sample 5

Sample ID:	150401 S5	
Results:		
Area	X1	146,37 °C
	Y1	3,5792 W/g
	X2	205,31 °C
	Y2	3,5498 W/g
	Peak	191,2 °C
	Peak Area	18,958 J/g
	Delta H	18,958 J/g

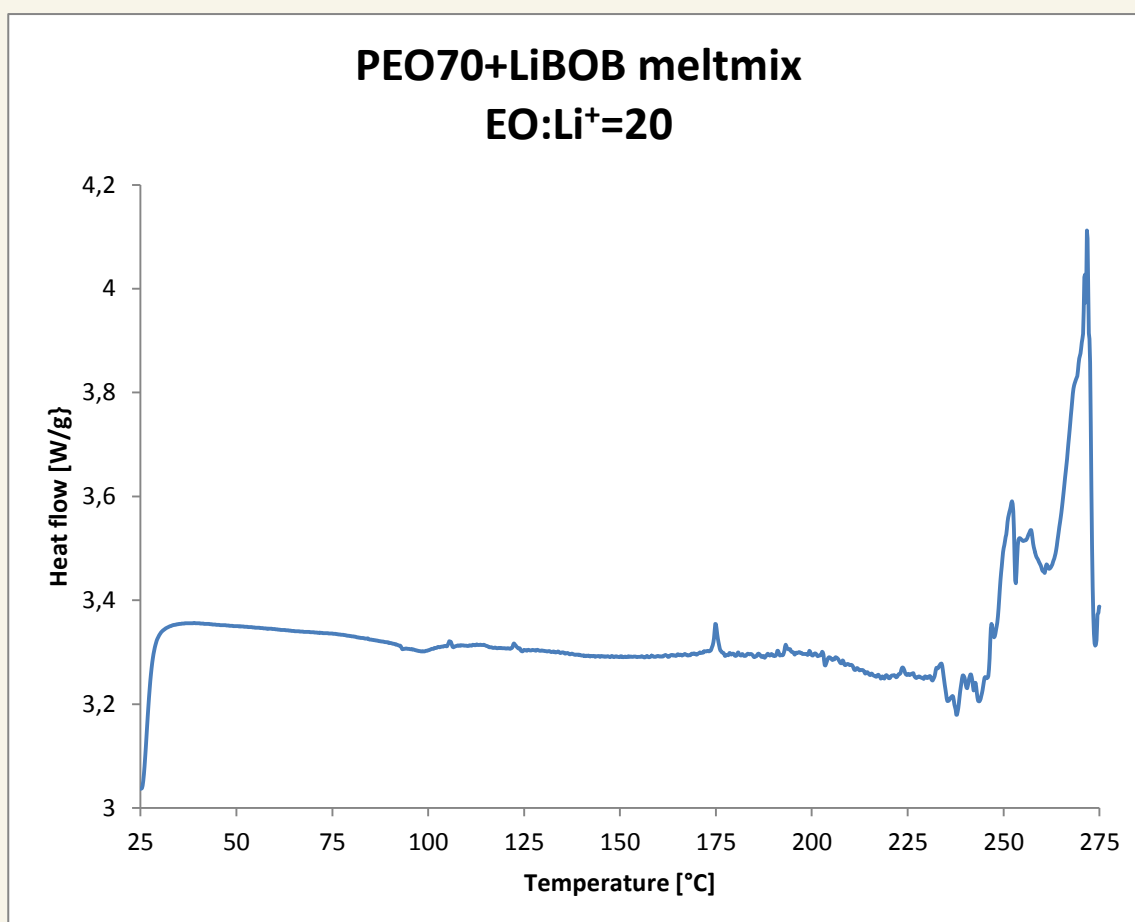


Sample 6

Sample ID: 150401 S6

Results:

Area	X1	169,77	°C
	Y1	3,2959	W/g
	X2	179,79	°C
	Y2	3,2951	W/g
	Peak	174,87	°C
	Peak Area	0,57	J/g
	Delta H	0,57	J/g



Sample 7

Sample ID: 150401 S7

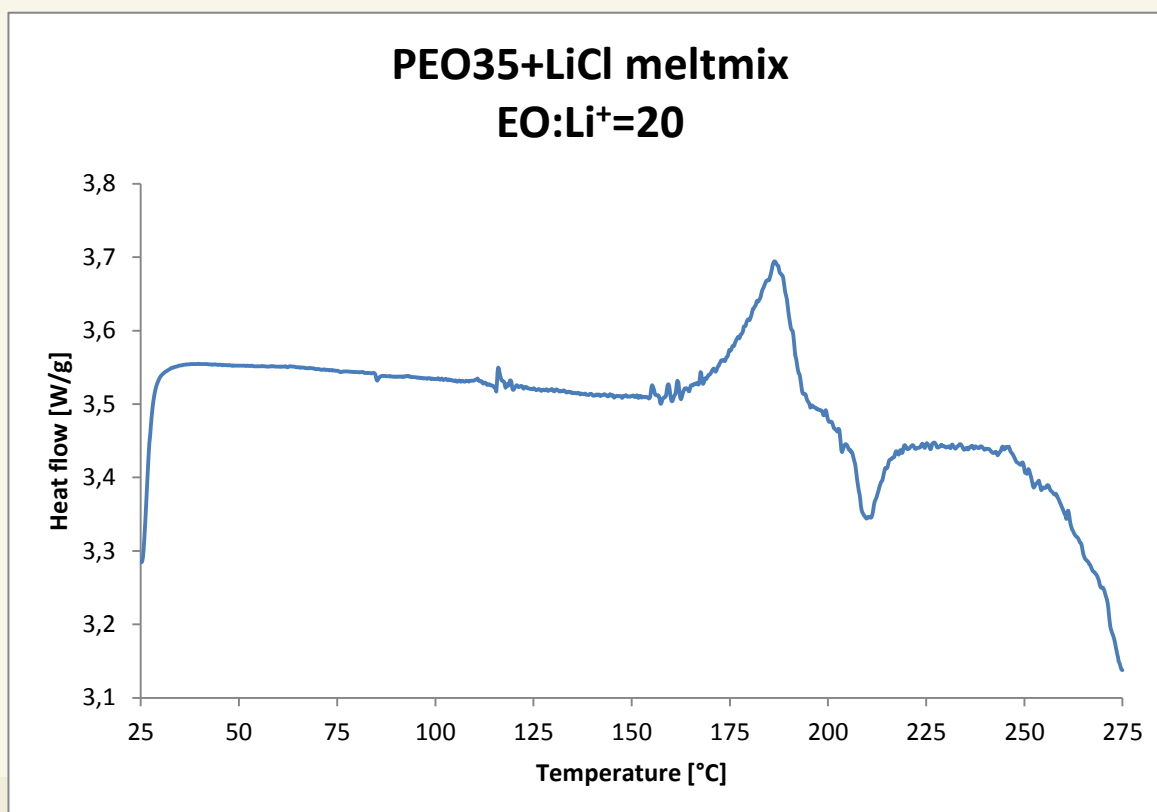
Results:

Area	X1	147,12	°C
	Y1	3,5107	W/g
	X2	196,65	°C
	Y2	3,4955	W/g
	Peak	186,37	°C
	Peak Area	16,952	J/g
	Delta H	16,952	J/g

Sample ID: 150401 S7

Results:

Area	X1	198,22	°C
	Y1	3,4914	W/g
	X2	220,23	°C
	Y2	3,4388	W/g
	Peak	209,87	°C
	Peak Area	-5,825	J/g
	Delta H	-5,825	J/g



Sample 8

Sample ID: 150401 S8

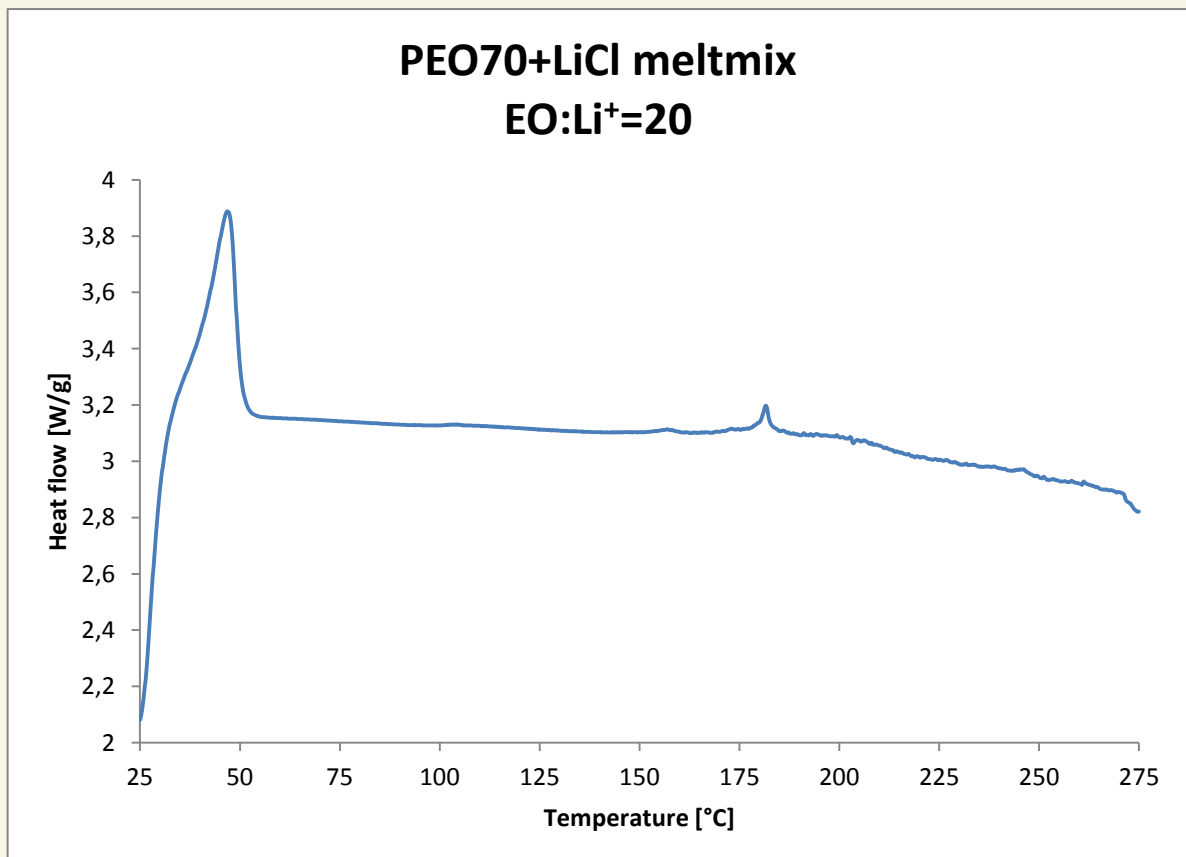
Results:

Area	X1	28,49	°C
	Y1	2,6517	W/g
	X2	56,14	°C
	Y2	3,1564	W/g
	Peak	46,7	°C
	Peak Area	75,365	J/g
	Delta H	75,365	J/g

Sample ID: 150401 S8

Results:

Area	X1	168,55	°C
	Y1	3,1029	W/g
	X2	188,6	°C
	Y2	3,0991	W/g
	Peak	181,7	°C
	Peak Area	2,29	J/g
	Delta H	2,29	J/g



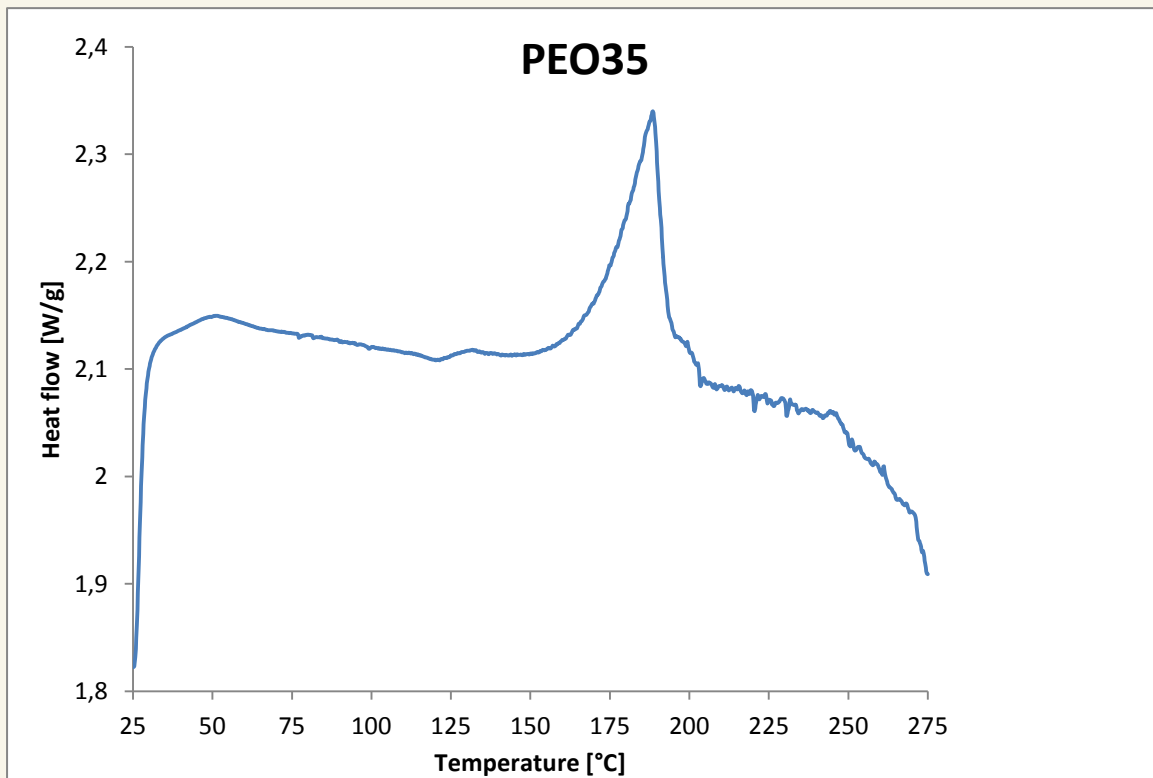
Sample 9

Sample

ID: 150401 S9

Results:

Area	X1	138,78	°C
	Y1	2,1147	W/g
	X2	203,49	°C
	Y2	2,0841	W/g
	Peak	188,53	°C
	Peak Area	26	J/g
	Delta H	26	J/g

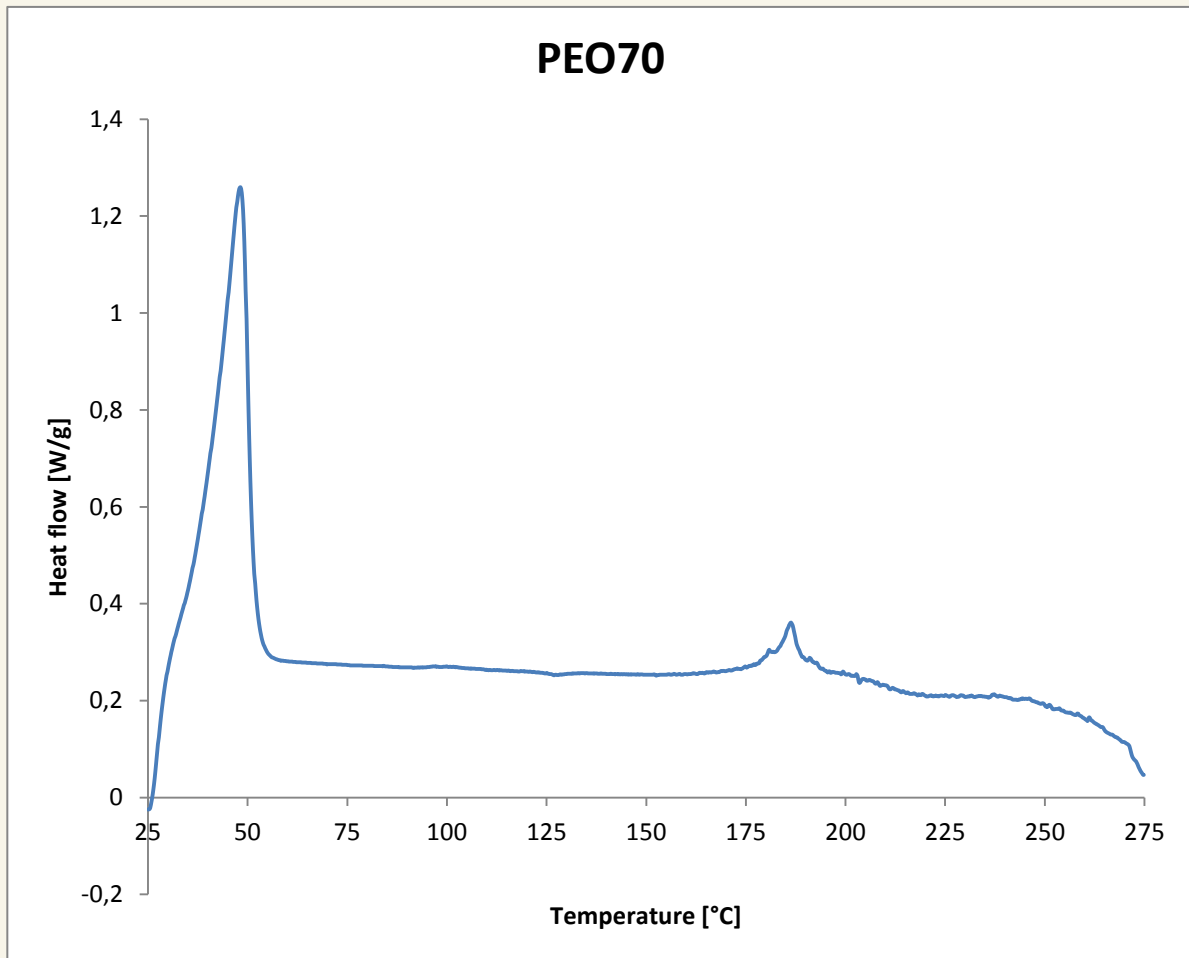


Sample 10

Sample ID: 150401 S10

Results:

Area	X1	145,48
	Y1	0,2539
	X2	217,27
	Y2	0,2153
	Peak	186,37
	Peak Area	11,961
	Delta H	11,961

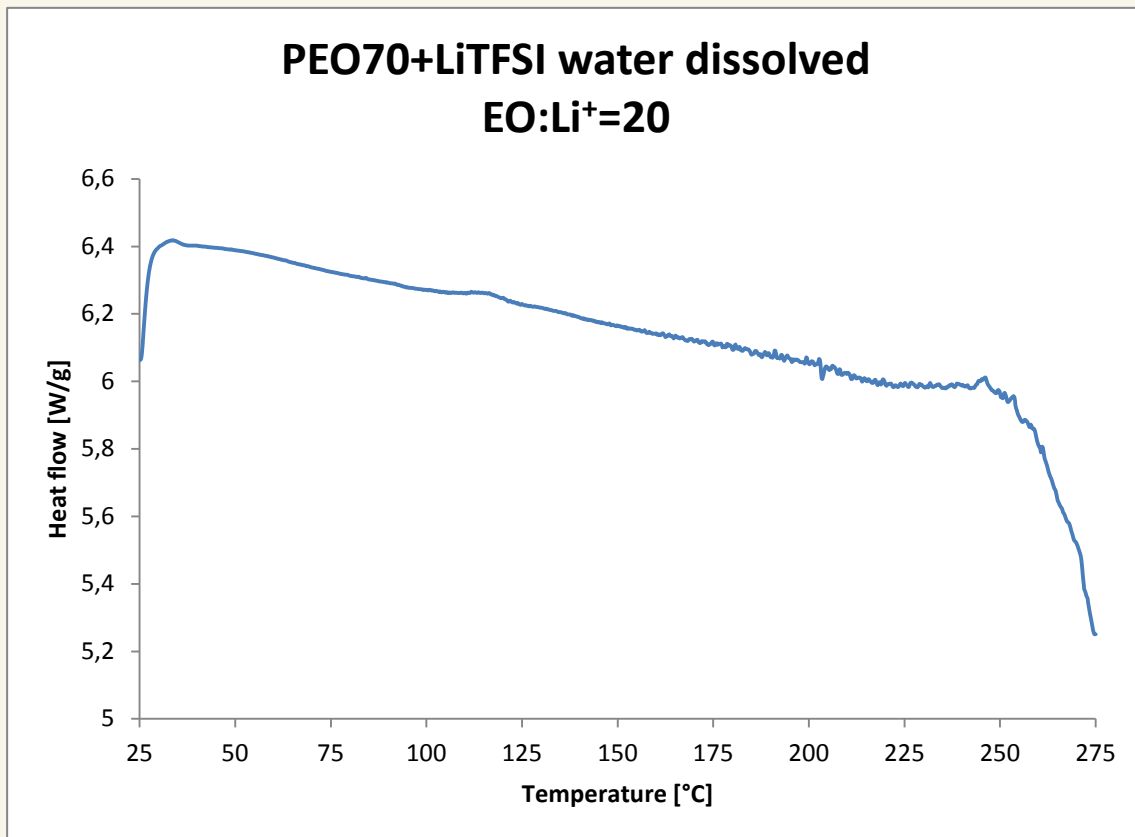


Sample 11

Sample ID: 150401 S11

Results:

Area	X1	104,14	°C
	Y1	6,2655	W/g
	X2	124,8	°C
	Y2	6,2281	W/g
	Peak	116,37	°C
	Peak Area	0,983	J/g
	Delta H	0,983	J/g

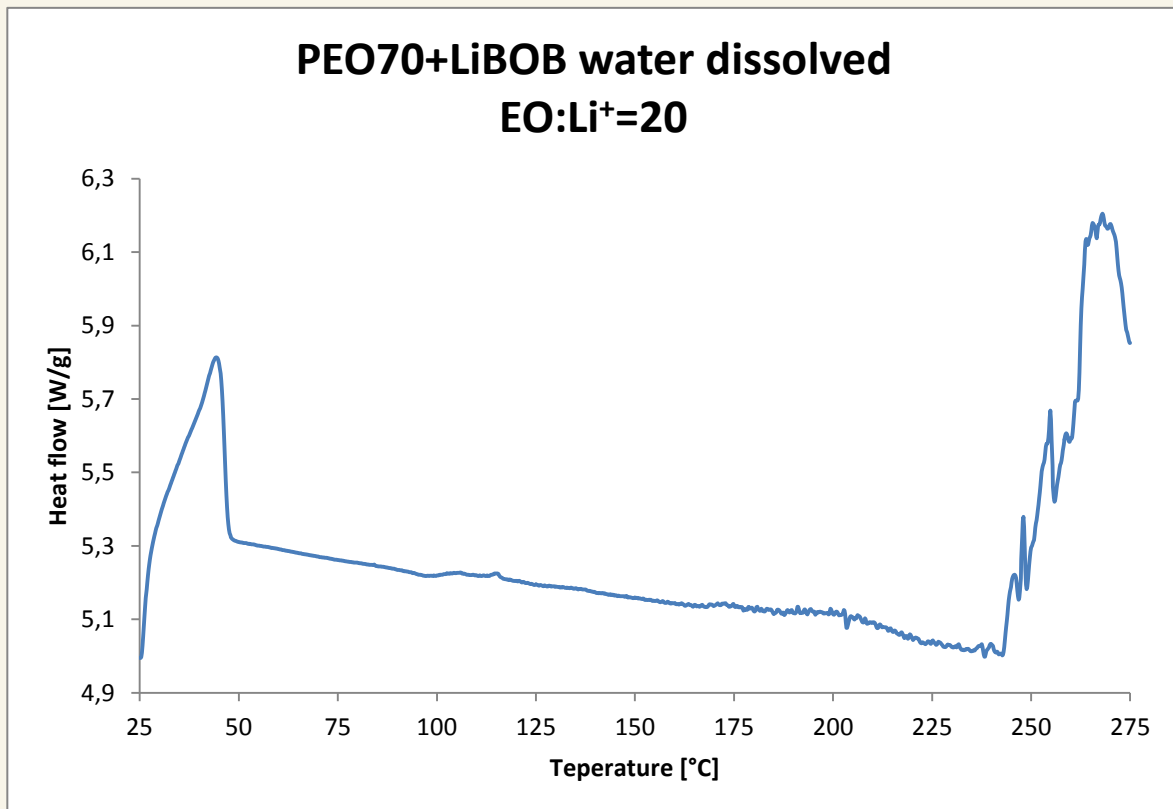


Sample 12

Sample ID: 150401 S12

Results:

Area	X1	26,37	°C
	Y1	5,1345	W/g
	X2	50,98	°C
	Y2	5,3086	W/g
	Peak	44,2	°C
	Peak Area	43,448	J/g
	Delta H	43,448	J/g



Sample 13

Sample ID: 150401 S13

Results:

Area	X1	30,1	°C
	Y1	9,6702	W/g
	X2	51,08	°C
	Y2	9,613	W/g
	Peak	44,7	°C
	Peak Area	47,875	J/g
	Delta H	47,875	J/g

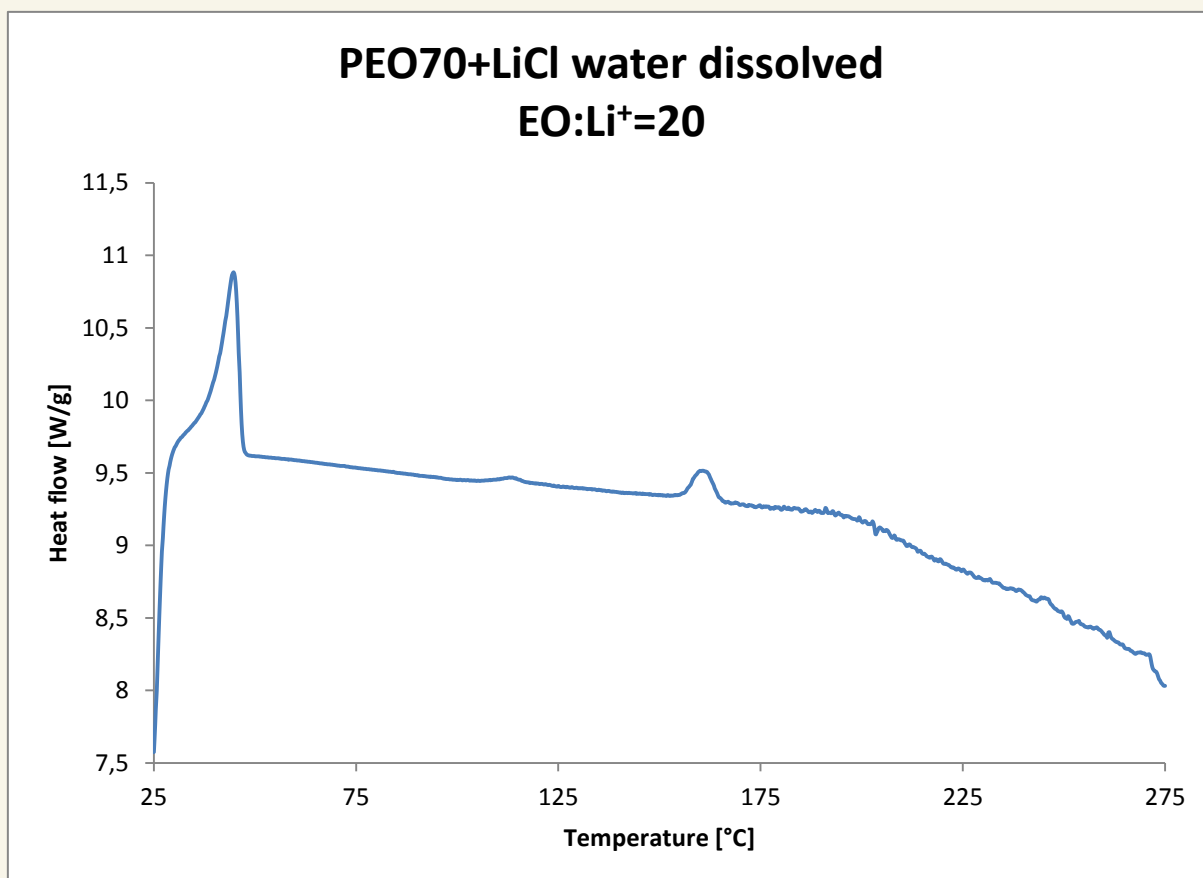
Method

Filename: D:\DSC\Data\Frans ooms\150401 S13.dsd

Sample ID: 150401 S13

Results:

Area	X1	151,05	°C
	Y1	9,3451	W/g
	X2	168,83	°C
	Y2	9,296	W/g
	Peak	160,7	°C
	Peak Area	6,955	J/g
	Delta H	6,955	J/g



Appendix E

Extrapolation of resistance (R value) from Nyquist plots

The intersection of the semicircle with the horizontal axis in the Nyquist plots determines the resistance value.

In the plots obtained the sum of two effects is visible: a semicircle attributed to a simplified Randles cell and a diagonal slope due to diffusion control. This requires extrapolation of the intersection of the semicircle with the horizontal axis. This can be done by simulating the circuit or by doing a geometrical fitting of the semicircle by choosing at least three points of the semicircle. Since the purpose in this case is purely to obtain the R value, performing the circuit simulation yields no additional useful information. Therefore the simple geometrical fitting has been used. The two routes in fact yielded equivalent results as is shown in the example below.

Both methods have been performed using the Nova software provided with the Autolab.

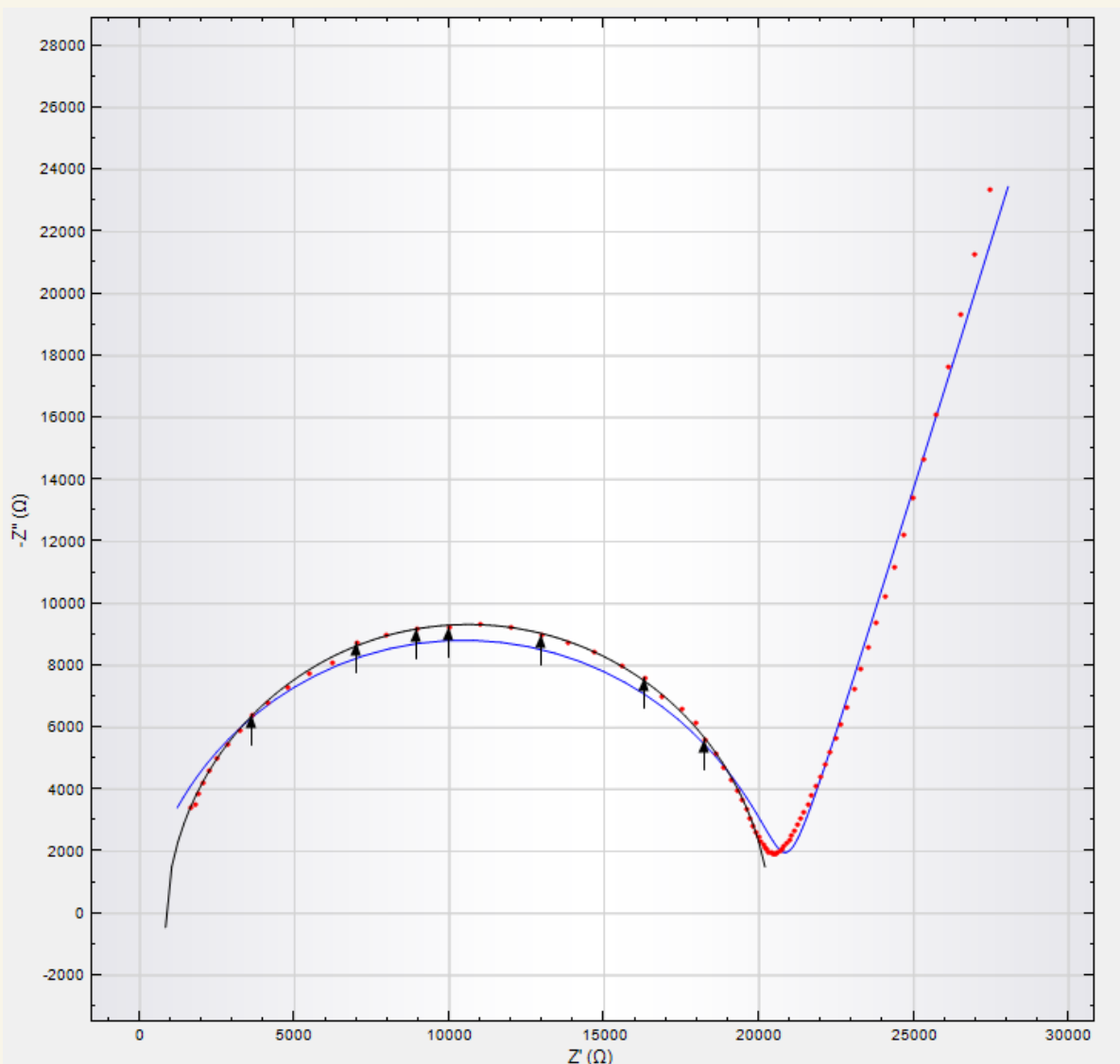


Figure E1 Comparison between data points (in red), equivalent circuit fit (in blue) and electrochemical circle fit (in black)

In the figure above one of the measurement previously shown in chapter 3.3.1 is reported as an example. The red dots represent the data points, the black semicircle is the electrochemical circle fit and the blue graph is the fitting done through the equivalent circuit shown below in fig. E2 In fig. E3 the values of the electrochemical circle fit are instead shown. The $R_p.R$ value represents the diameter of the semicircles, while $R_s.R$ indicates the intersection of the semicircle with the horizontal axis closest to the origin. The sum of the two values yields the resistivity value, i.e. the second intersection with the Z'' axis.

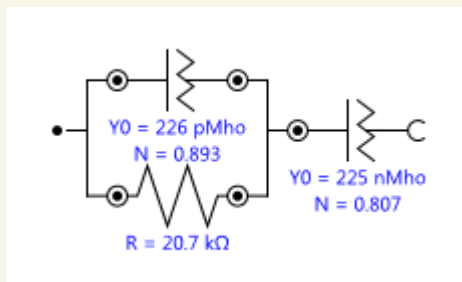


Figure E2 Equivalent circuit fit shown in blue in fig. E1

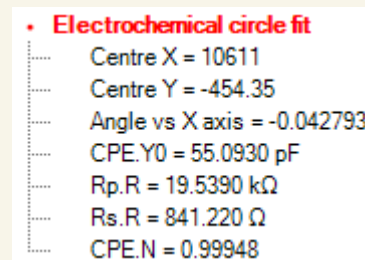


Figure E3 Numerical values for the electrochemical circle fit shown in black in fig. E1

Indeed the converging fitting with the equivalent circuit yields much more detailed information, but the purpose being solely the one of extrapolating the intersection of the semicircle with the horizontal axis, the two methods can be considered equally adequate. A comparison of the extrapolated resistance values is shown below.

Equivalent circuit fitting $\rightarrow R=20,7k\Omega$
 Electrochemical circle fit $\rightarrow R=19.539k\Omega + 841\Omega=20,480k\Omega$
 Percent error: 1%

It may occur that more than one semicircle should appear from the measurement indicating more complex processes. But even in this case only the total resistance is required for calculating conductivity of the sample.

Appendix F

Complete Nyquist plots of samples PC3, PC4, PC5 and PC6 as function of temperature

The Nyquist plots from samples PC3, PC4, PC5 and PC6 taken in a range of temperatures between room temperature and approximately 65°C are here presented for completeness. Only the plots for sample PC5 were presented in chapter 3.3.1 for the sake of conciseness. Extrapolation of the resistance values from the plots below was done according to what described in Appendix E and the conductivity value was then calculated as explained in chapter 2.4.1. In this way the Arrhenius plots presented in chapter 3.3.1 were obtained.

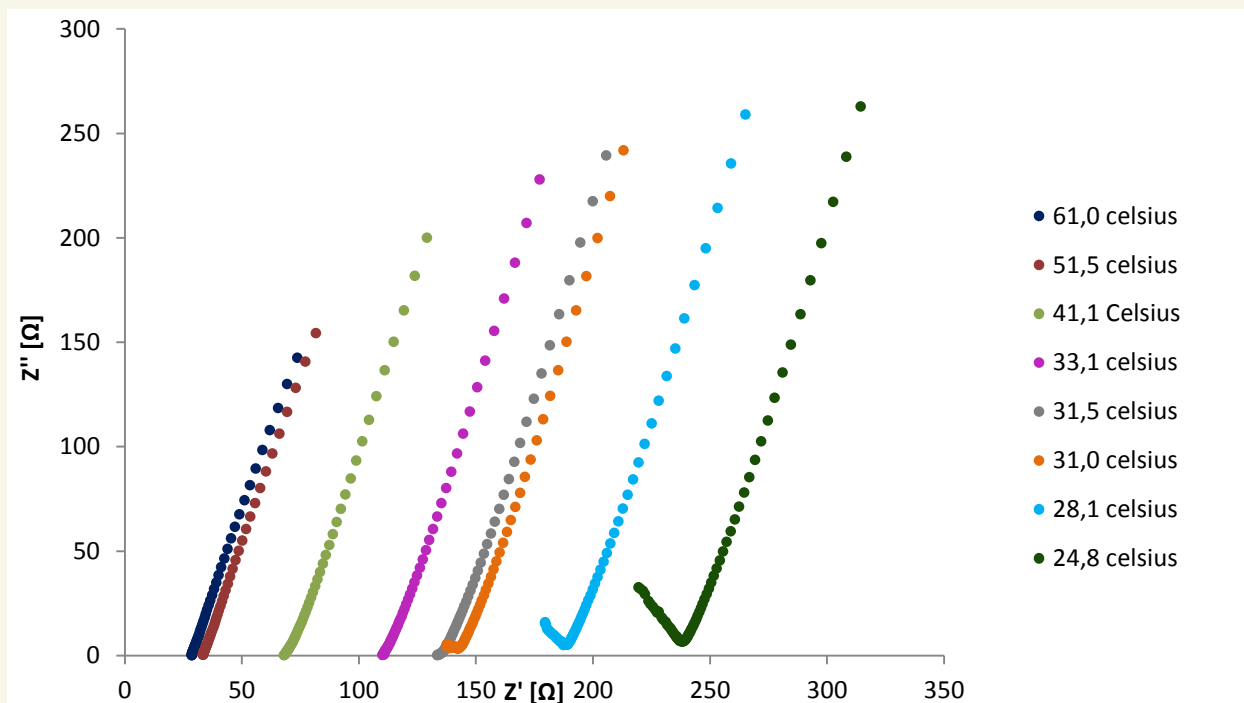


Fig. F1 Sample PC3 (PEO70+LiTFSI 20 meltmix): Nyquist plots at different temperatures

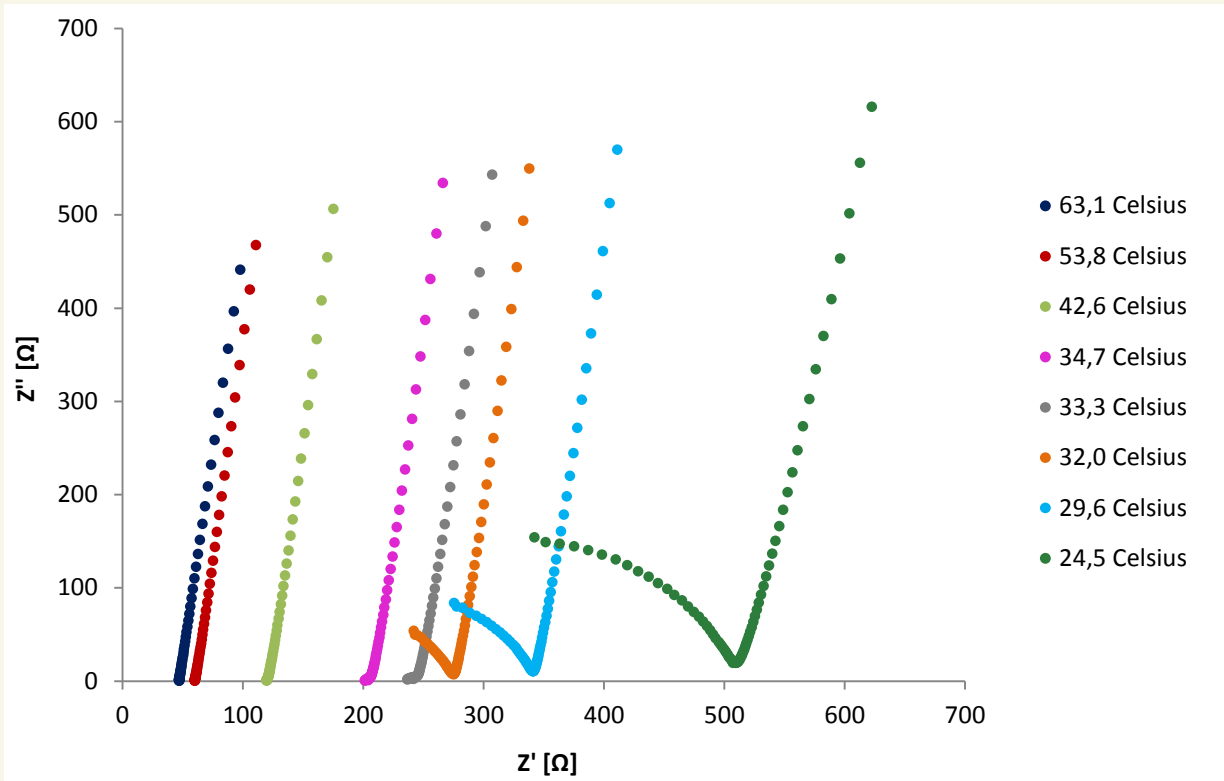


Fig. F2 Sample PC4 (PEO70+LiTFSI 20 watersoaked): Nyquist plots at different temperatures

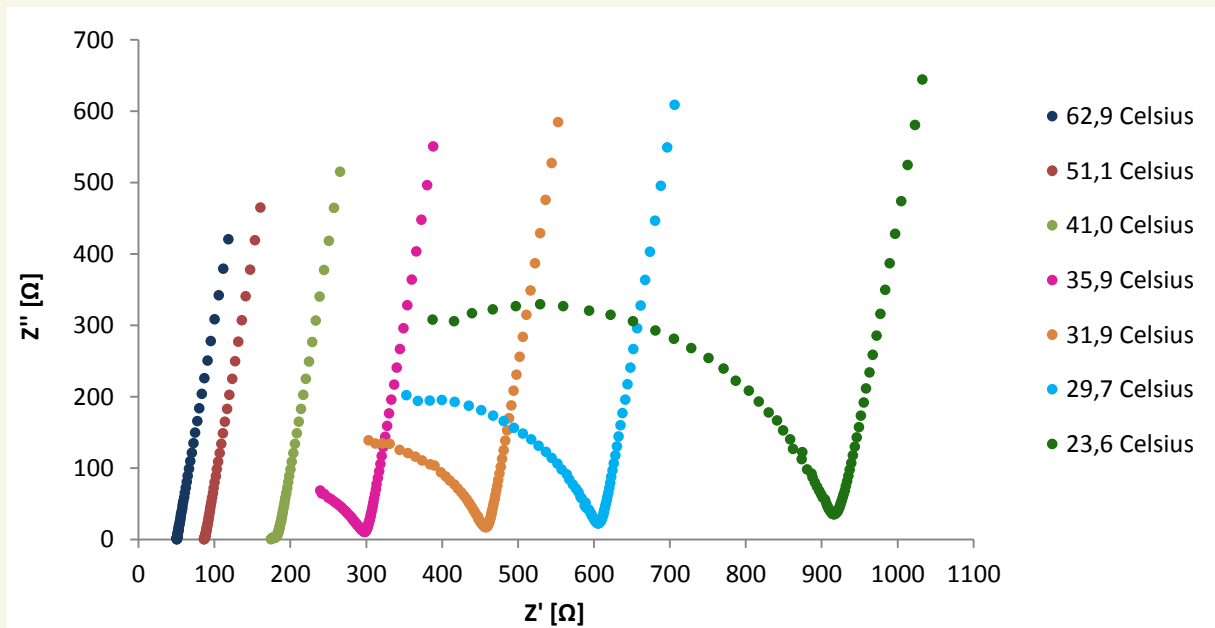


Fig. F3 Sample PC5 (PEO70+LiTFSI 10 meltmix): Nyquist plots at different temperatures

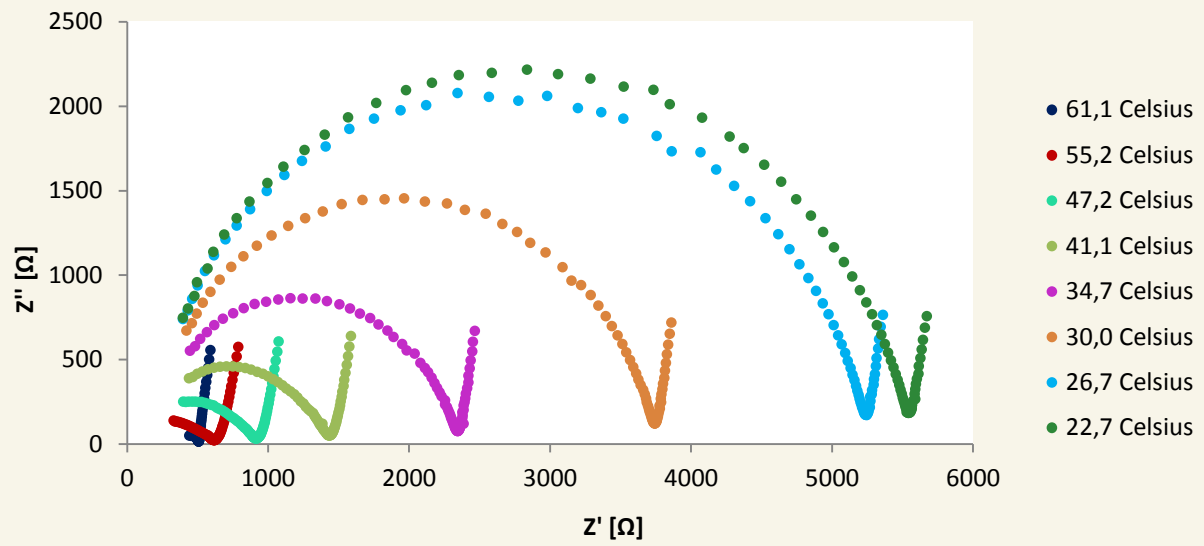


Fig. F4 Sample PC6 (PEO35+LiTFSI 10 meltmix): Nyquist plots at different temperatures

Appendix G

Arrhenius plot fittings

The Arrhenius plots presented in fig. 25 of sample PC3, PC4, PC5 and PC6 have been fitted in order to obtain the activation energy for ionic conductivity presented and discussed at the end of chapter 3.3.1.

Two types of fitting have been tried in order to find the closest one. The empiric Vogel-Tammann-Fulcher (VTF) temperature dependence is expressed as

$$\sigma = A \cdot e^{-\frac{B}{R \cdot (T - T_0)}} \quad \text{VTF}$$

where A is an ideal conductivity at infinite temperature, B is the activation energy for conduction, R is the universal gas constant, T is the absolute temperature and T_0 is related to the glass transition temperature T_g of the polymer by the empirical relationship $T_0 \approx T_g - T_0$. This type of dependency is typical of polymer electrolytes, where charge transport is influenced by the dynamics of the polymer chains and is therefore related to the glass transition temperature

The other type of fitting employed is the Arrhenius dependency already presented in chapter 3.3.1 in equation 5.

$$\sigma = \sigma_0 \cdot e^{-\frac{E}{kT}} \quad \text{Arrhenius}$$

In all cases the Arrhenius fitting gave a closer fit and was therefore chosen. The reason for which the VTF gives a less accurate fitting may be ascribed to the reduced temperature range for which the data points were taken. If conductivity were to be measured for a wider temperature range (including for example measurements below 0°C), it may be expected that the VTF fit would yield a better fit.

The fittings were performed using CurvExpert. The actual fitting models are reported hereunder:

VTF: $y = a \cdot \exp(-b/(8,31446 \cdot (x - c)))$ on a semi-logarithmic plot that displays the absolute temperature on the x-axis. The activation energy expressed in eV is therefore $E = b / (1,6 \cdot 10^{-19} \cdot 6,02 \cdot 10^{23})$

Arrhenius: $y = a \cdot \exp(-b/x)$ on a semi-logarithmic plot that displays $1000/T$ as the inverse of the absolute temperature on the x-axis. The activation energy expressed in eV is therefore $E = b \cdot 1000 / (1,6 \cdot 10^{-19} \cdot 6,02 \cdot 10^{23})$.

In some cases one data point was purposely taken out in order to obtain a better fit and compare results. The activation energy was taken for each plot from the best fit and is presented in chapter 3.3.1. All the fits are shown below for completeness.

Sample PC3

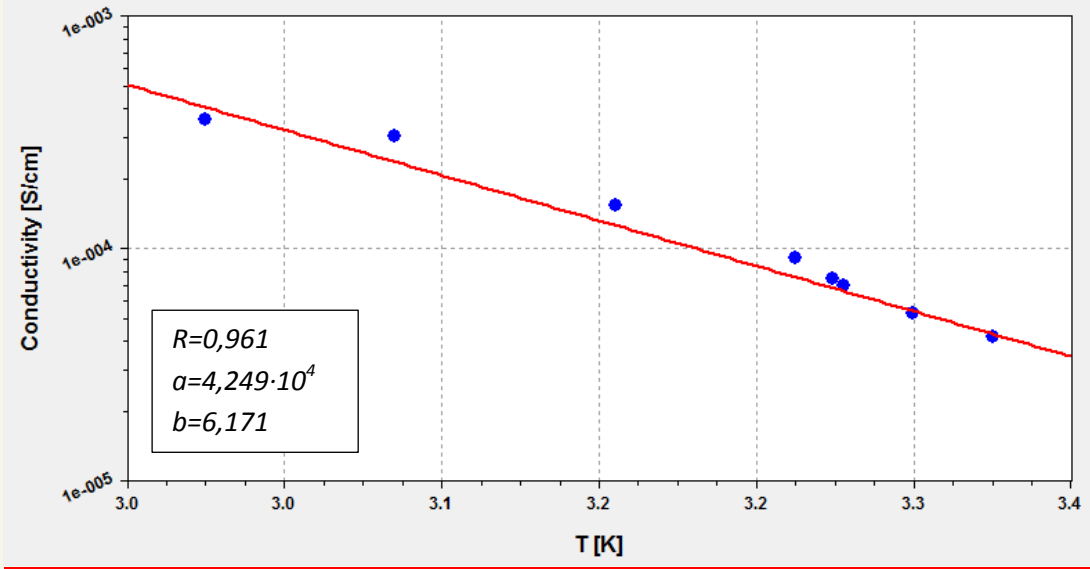


Figure G1: Sample PC3; Arrhenius fit on complete data set

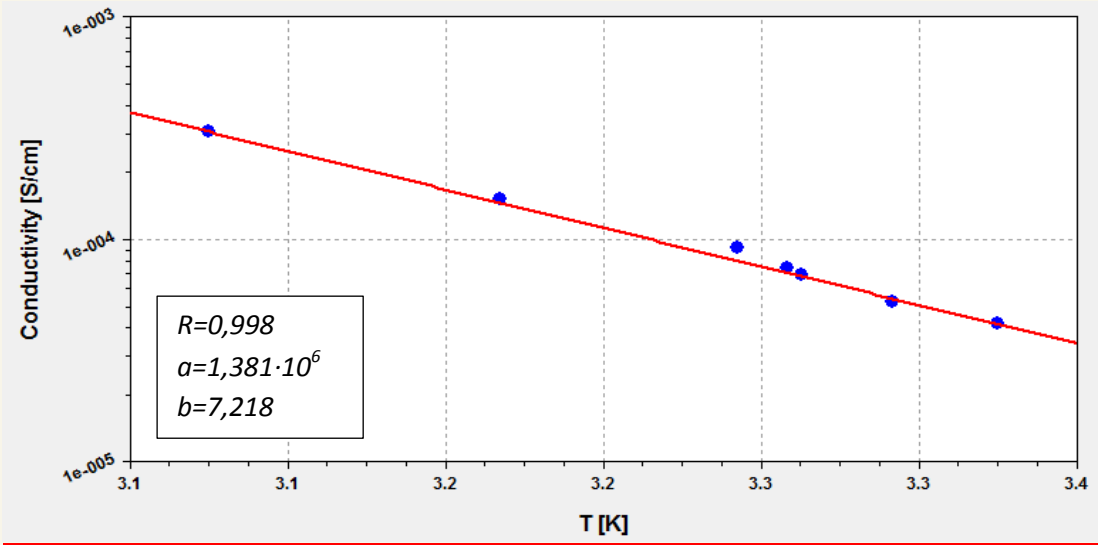


Figure G2: Sample PC3; Arrhenius fit with one deleted data point

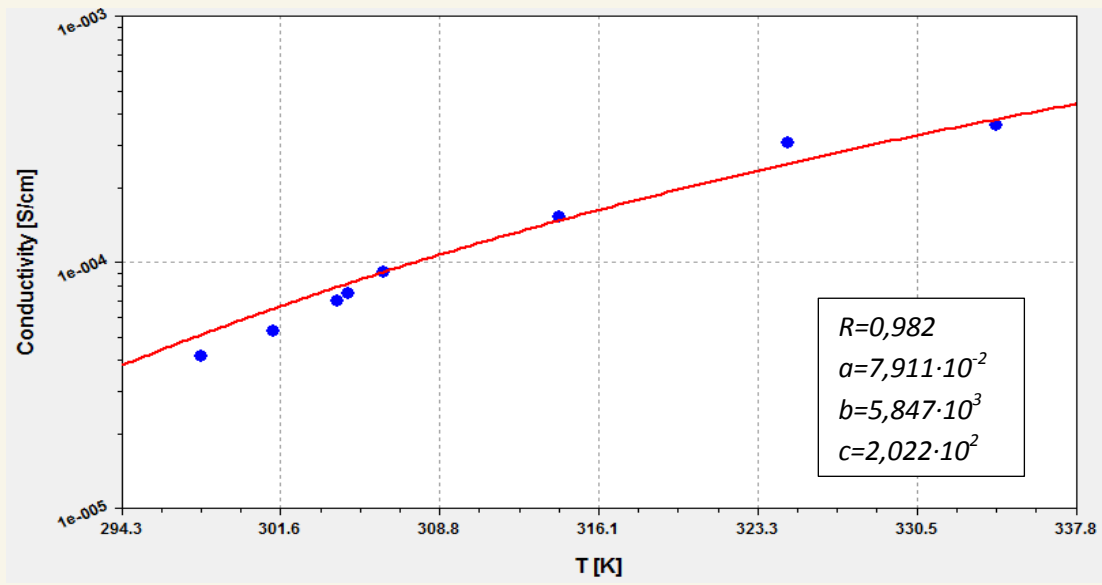


Figure G3: Sample PC3; VTF fit with one complete data set

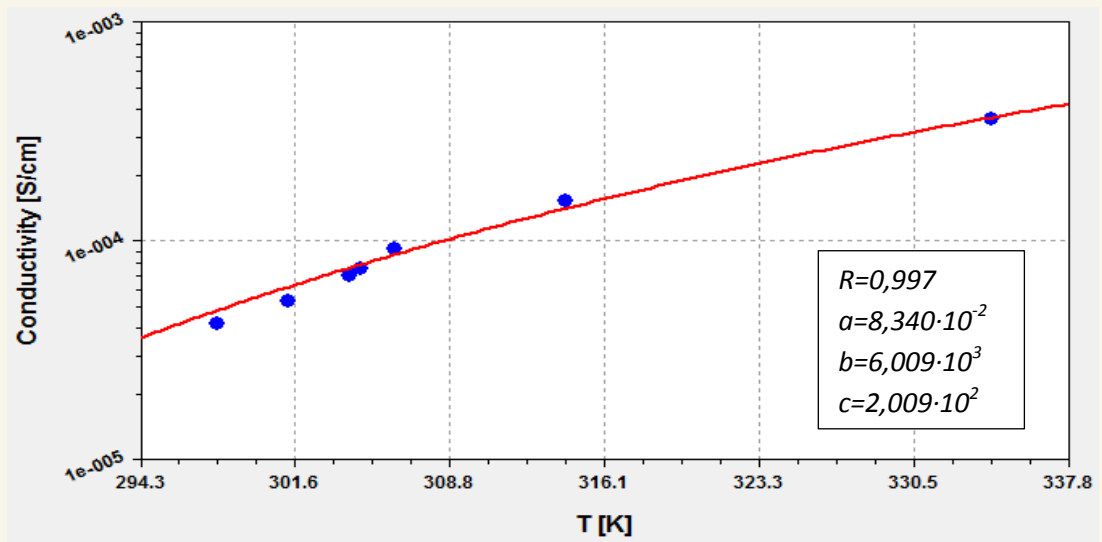


Figure G4: Sample PC3; Arrhenius fit with one deleted data point

Sample PC4

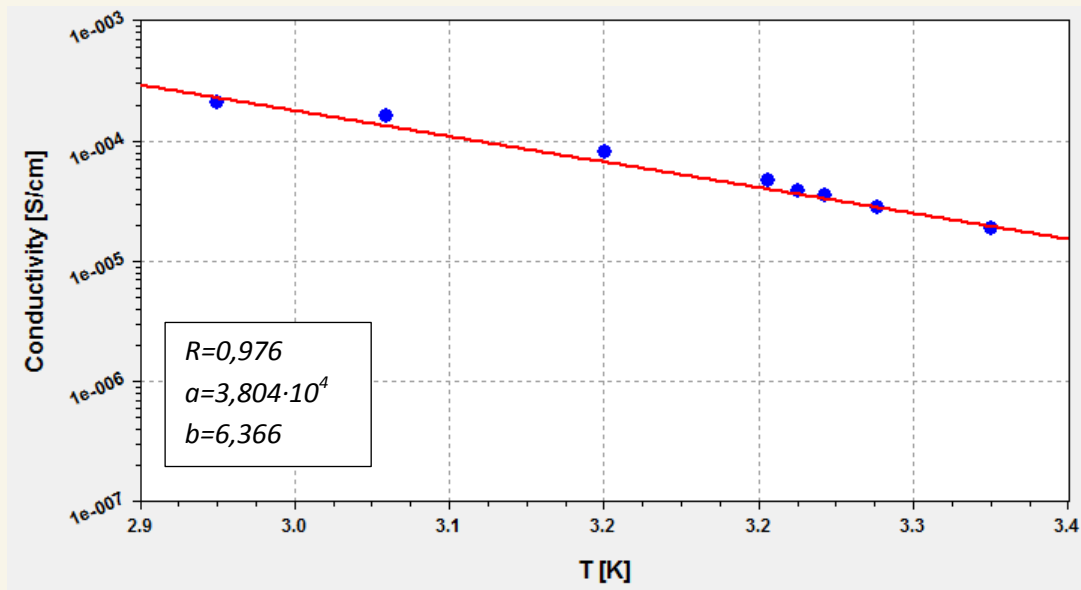


Figure G5: Sample PC4; Arrhenius fit on complete data set

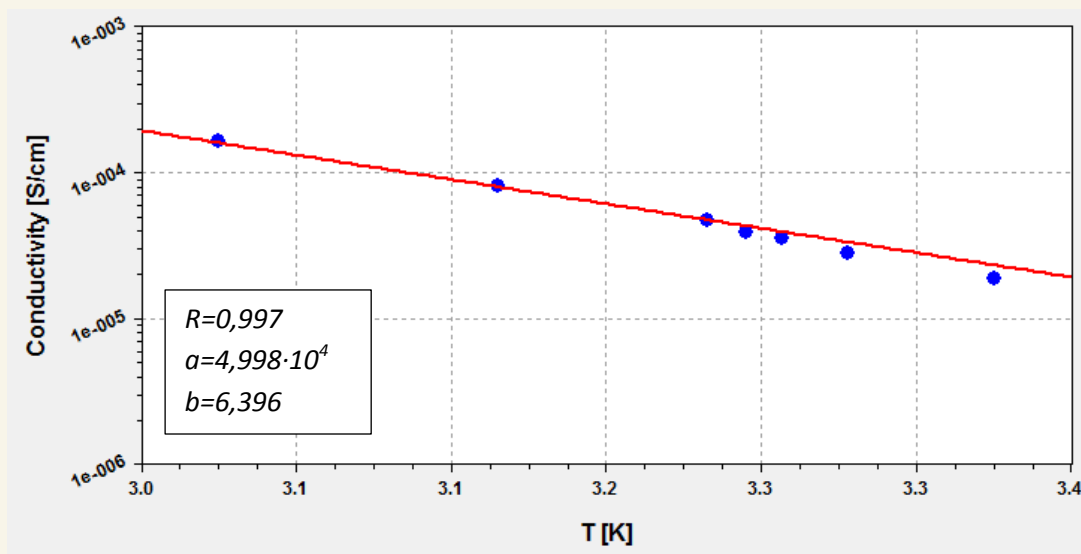


Figure G6: Sample PC4; Arrhenius fit with one deleted data point

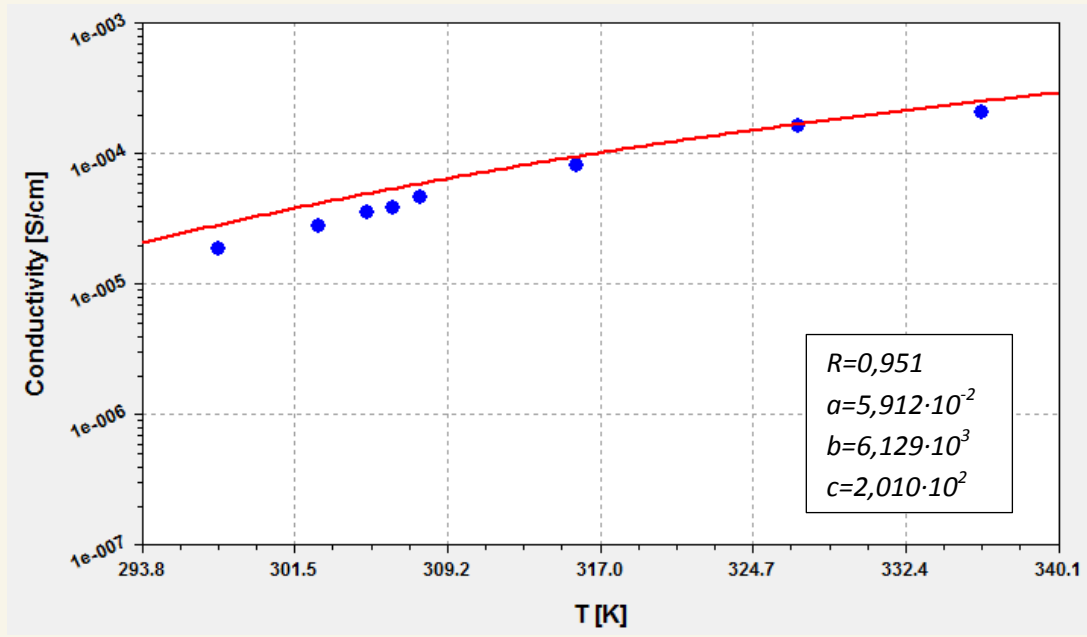


Figure G7: Sample PC4; VTF fit on complete data set

Sample PC5

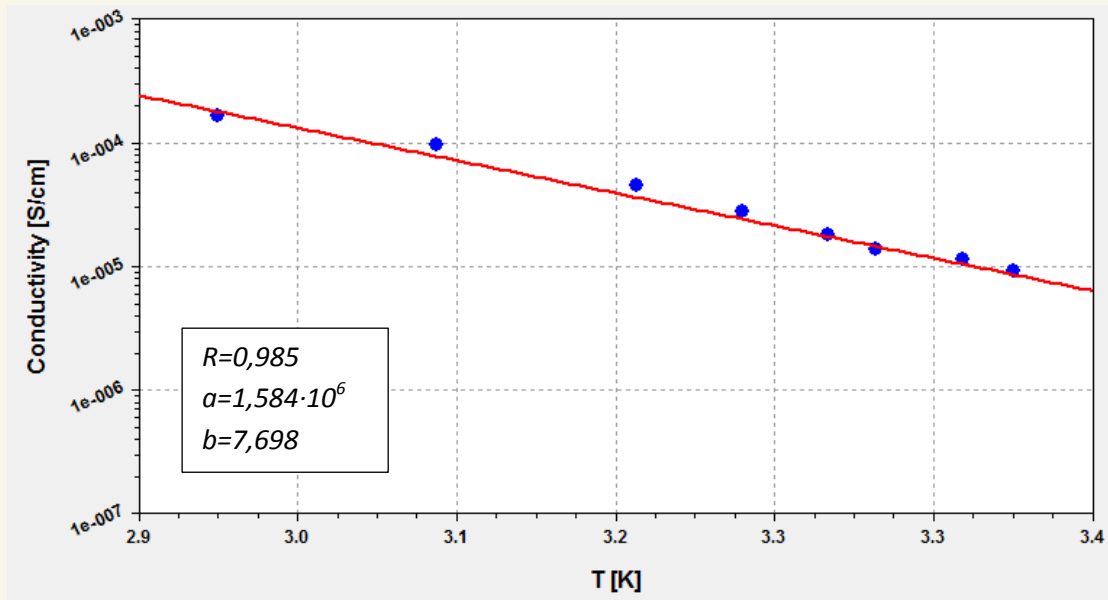


Figure G8: Sample PC5; Arrhenius fit on complete data set

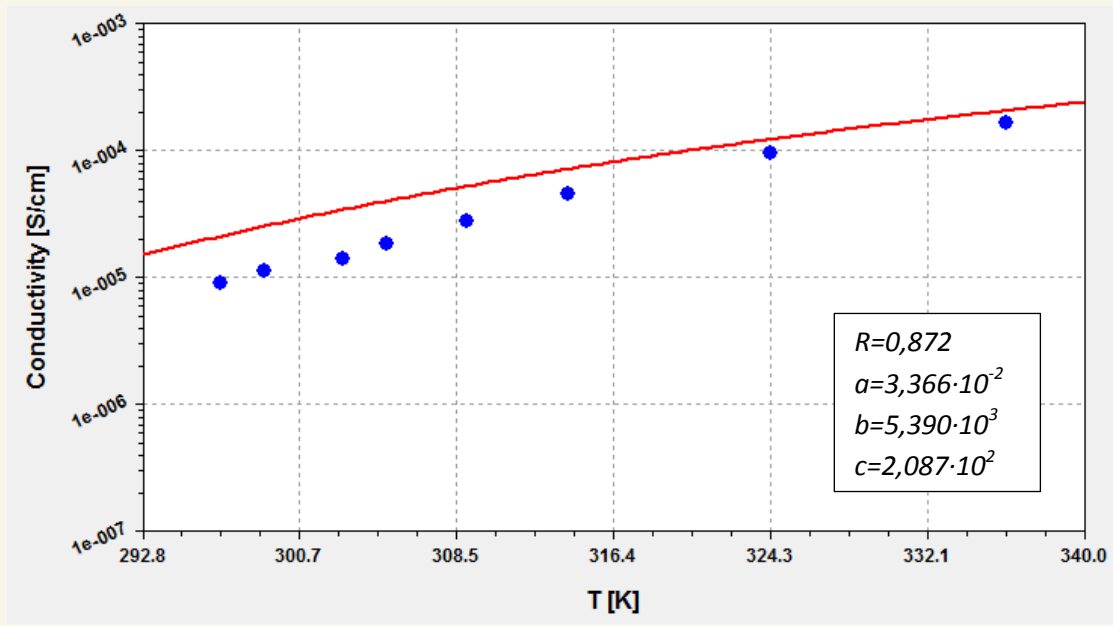


Figure G9: Sample PC5; VTF fit on complete data set

Sample PC6

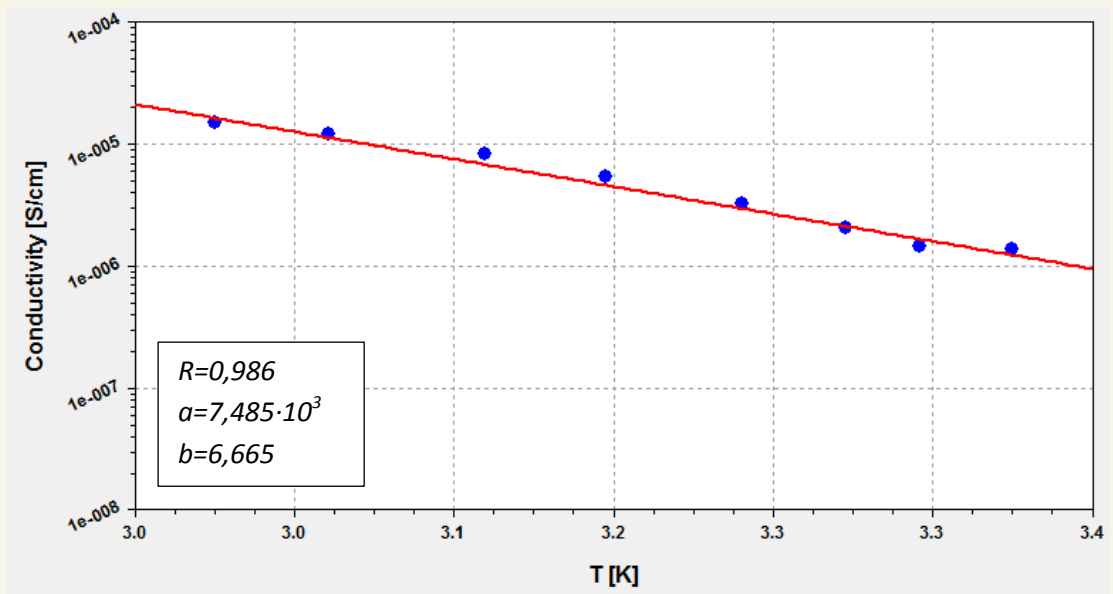


Figure G10: Sample PC4; VTF fit on complete data set

Appendix H

CV scans of samples PC3, PC4, PC5 and PC6 displayed individually

The CV scans of sample PC3, PC4, PC5 and PC6 were presented in chapter 3.3.2 in one graph as to allow for comparability. The plots are here instead individually displayed, both for the measurements performed at room temperature and for the measurements at 45°C.

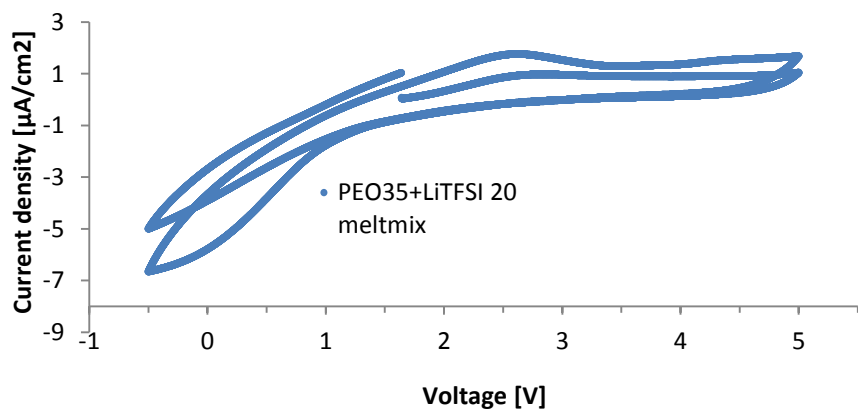
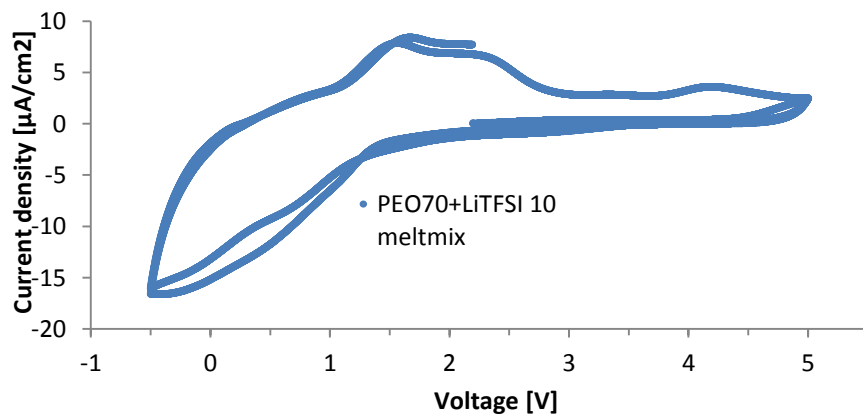
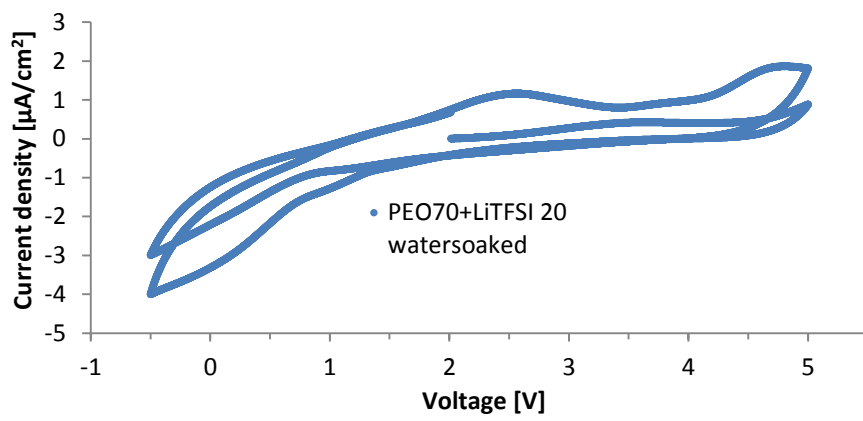
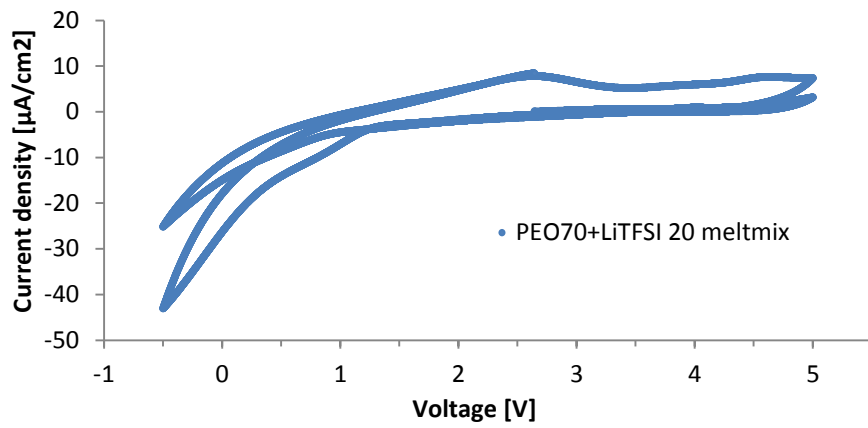


Figure H1: Double scan CV at room temperature

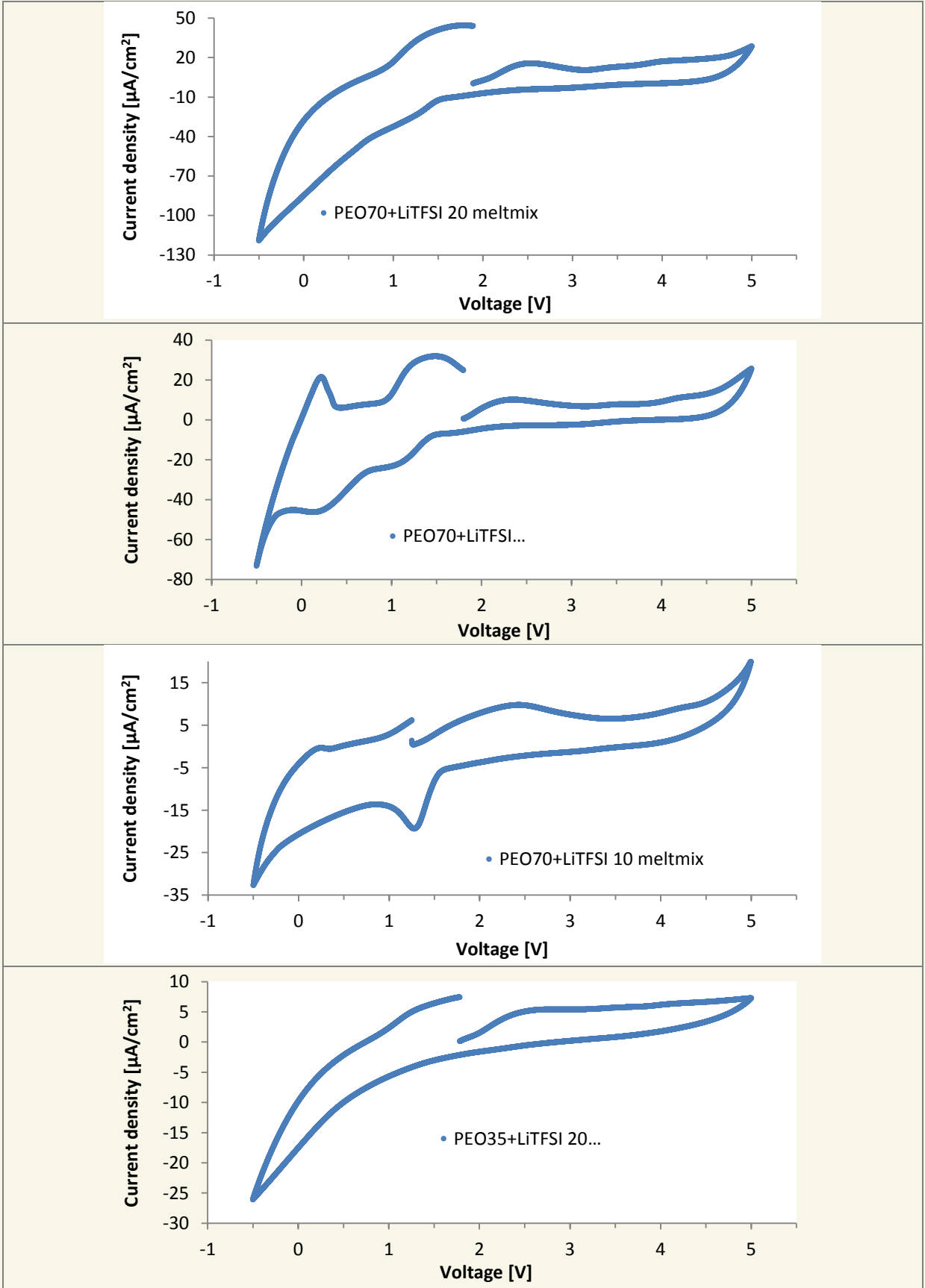


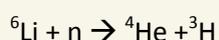
Figure H1: Single scan CV at 45°C

Appendix I

Neutron Depth Profiling (NDP)

Neutron Depth Profiling (NDP) is a near-surface analysis technique that allows to obtain profiles of concentration as a function of depth for light elements within a substrate. When detecting Li in a Li-ion battery, NDP can be used ex-situ, in-situ or in-operando, thus yielding spatial and temporal measurement of the lithium within the material. This allows for direct tracking and counting of Li atoms without any interference to the Li transport phenomena that may occur from indirect measurements.

The NDP technique is based on a beam of low energy neutrons that interact with the isotope ${}^6\text{Li}$ to form an α -particle (${}^4\text{He}$) and triton (${}^3\text{H}$) according to the following reaction



Such particles have well defined energy upon formation; by measuring the energy loss of the particles that reach the detector, the depth at which these particles were formed (and therefore the location of the lithium) can be calculated.

Such analysis tool is employed in a wide range of applications and has a very relevant role specifically in the Li-ion battery field of research. For the purposes of this project, NDP has been chosen as a tool to evaluate the homogeneity of the lithium concentration throughout the thickness of the electrolyte membrane and to try to detect possible dendrites that may form in the polymeric film upon cycling.

Because of the stopping power deriving from the environment surrounding the lithium, there is a limit to depth resolution. In the case of the polymeric samples produced during this research project it would not be possible to detect the lithium throughout the entire thickness of a few hundreds of microns, but already the information deriving from the first few decades of microns yields very useful information.

The purpose of such investigation was to determine ex-situ the Li distribution on an electrolytic sample prior to cycling. This will allow to understand whether the lithium concentration in the depth direction of the sample is homogeneous. Furthermore it would have been interesting to repeat such an experiment on an electrolyte after it has been cycled in a “0 Volt” battery where the anode is lithium metal and therefore an infinite source of lithium ions. If dendrites were to form during cycling it should be possible to visualize them through an increased lithium concentration in the electrolyte compared to the state prior to cycling. If this were to prove possible, it would represent a major success of such analysis technique, enabling the direct “visualization” of dendrites.

As a first trial, a PEO70 sample containing LiTFSI (with EO:Li⁺ ratio equal to 20 produced through melt-mixing and hot pressed in the press-cells) underwent NDP. The measurement was carried out for 17 hours on the free-standing membrane placed in the vacuum chamber of the instrument. The result of this first experiment is displayed in the figure below where the vertical axis displays the counts and the horizontal axis displays the energy of the detected particles. The slope in the graph is ascribed to background, while the two barely noticeable bumps in the flat area of the graph are ascribed to the triton and α -particles (the former at higher energies and the latter at lower energies).

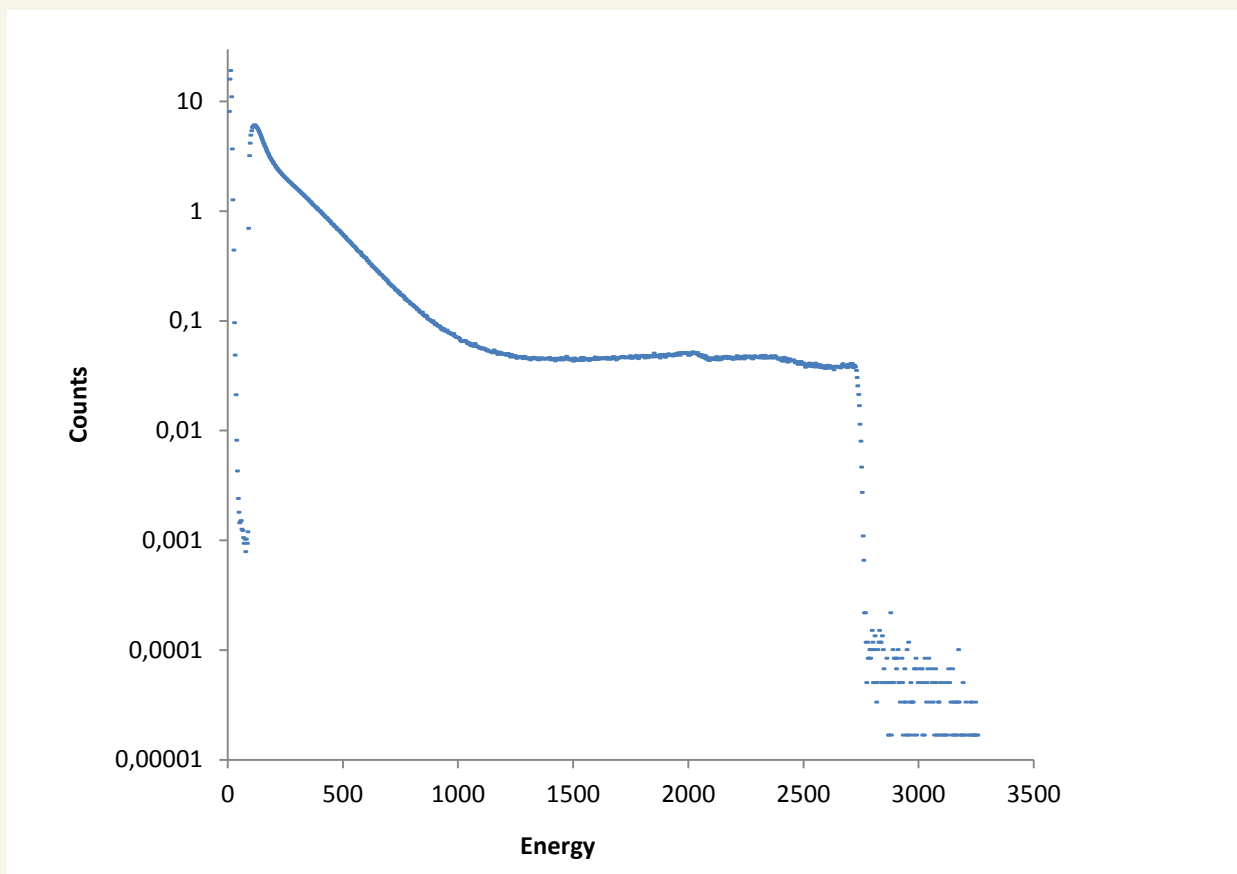


Figure I1 First NDP analyses on samples PEO+LiTFSI produced by melt-mixing and hot press in press-cell.

The signal obtained is indeed very mild and barely detectable above background, but it is still possible to track the lithium inside the sample. It must be also considered that such samples have a very low lithium concentration and are therefore very hard to analyse. In future experiments, if lithium will have formed dendrites in the electrolyte after cycling, the stronger signal will reveal such higher concentration of lithium. Therefore the first trial presented above is promising enough as it proves to be a valid starting point for comparison of spectra before and after cycling.

In order to maximize the signal and obtain readable results, the lithium metal that should be used as an anode for cycling is be a ^6Li isotope metal.

NDP could add a scientifically elegant counterpart to the more standard electrochemical investigations such as determination of Arrhenius plots, stability window and proof of ionic conductivity but it is first necessary to be able to successfully run a cell to compare a post-cycling sample with the one presented above. This will be possible only when the stability issues between PEO and lithium metal will be solved or when a stable anode will be employed. With the CVs and electroplating results obtained during this project there was no reason to continue NDP measurements, but should be kept in mind as a valid tool for future investigation.

